

Fundamentals of positron annihilation spectroscopy and its application in semiconductors

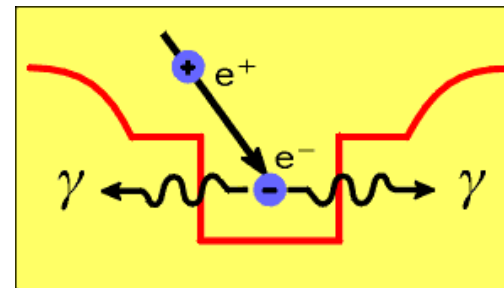
Reinhard Krause-Rehberg

Martin-Luther-University Halle-Wittenberg, Germany

mail@krauserehberg.de

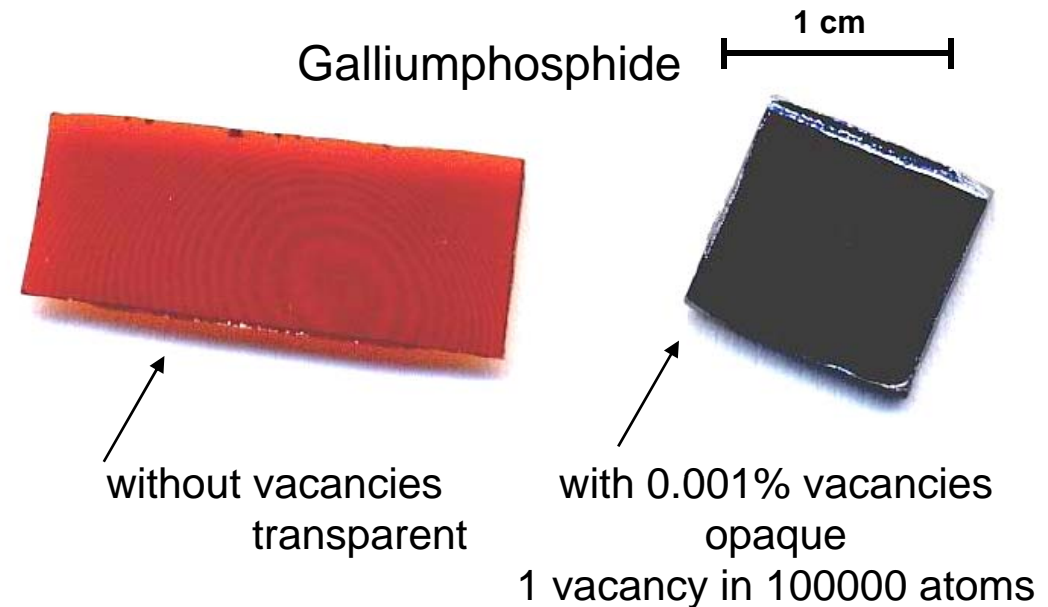


Martin-Luther-Universität
Halle-Wittenberg



Point defects determine properties of materials

- Point defects determine electronic and optical properties
- electric conductivity strongly influenced



- Point defects are generated by irradiation (e.g. cosmic rays), by plastic deformation or by diffusion, ...
- Metals in high radiation environment - formation of voids - embrittlement
- Properties of vacancies and other point defects must be known
- Analytical tools are needed to characterize point defects
- Positron Annihilation is a unique tool for nano-sized open-volume defects

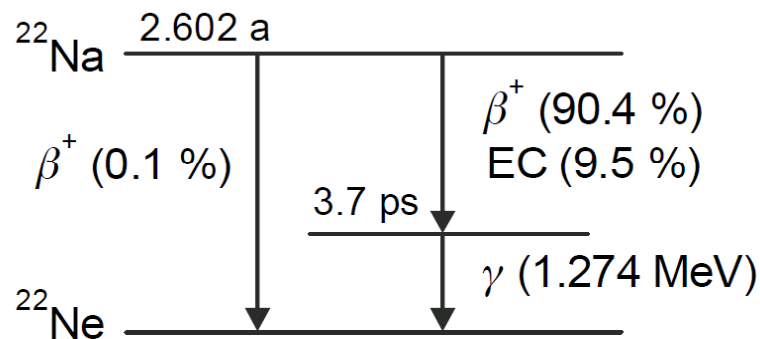
Content

1. Positron production
 - isotope sources (22-Na, 64-Cu, 58-Co)
 - pair production (Bremsstrahlung from accelerators, reactor-based positron sources)
2. Methods of Positron Annihilation Spectroscopy
 - Positron lifetime spectroscopy
 - Angular correlation of annihilation radiation - ACAR
 - Doppler broadening spectroscopy
 - Age-momentum correlation (AMOC)
3. Possible setups
 - Sandwich geometry with isotope sources
 - Gamma-induced Positron Spectroscopy (GiPS at EPOS)
 - Positron beam setups (continuous and bunched beams, focused systems)
4. Large-scale user-dedicated positron facilities
5. Defect spectroscopy by Positrons
 - Trapping model
 - Determination of trapping coefficient
6. Peculiarities of Positron Annihilation in semiconductors
7. Defect studies in semiconductors – 11 Examples
8. Conclusions
9. Literature

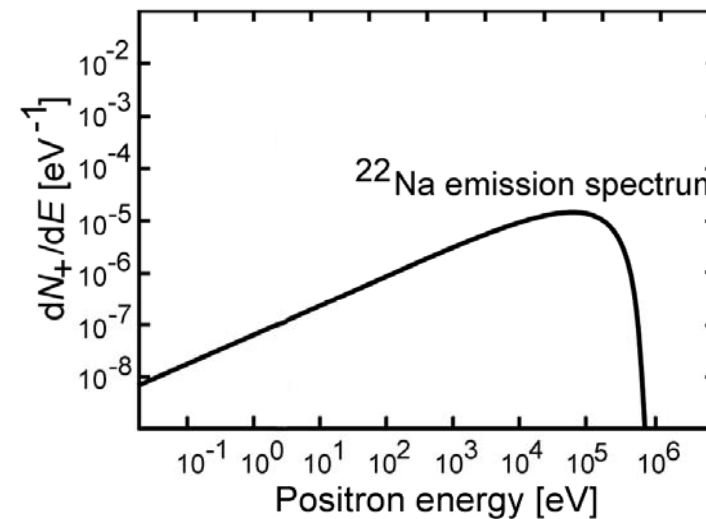
1. Positron generation: isotope sources

Positrons are obtained for laboratory setups usually by the β^+ decay of isotopes

- Most popular isotopes: ^{22}Na , ^{64}Cu , ^{58}Co and ^{68}Ge
- ^{22}Na has many advantages: long half life (2.6 a); short biological half life (3 d); relatively cheap; effective (>90% in β decay); easy to handle in water solution as $^{22}\text{NaCl}$ or $^{22}\text{Na}_2\text{CO}_3$
- β^+ decay: $^{22}\text{Na} \rightarrow ^{22}\text{Ne} + \beta^+ + \nu_e + \gamma_{(1.27\text{MeV})}$
- 1.27 MeV γ appears almost simultaneously with positron - can be used as start event for lifetime spectroscopy



Decay scheme of ^{22}Na

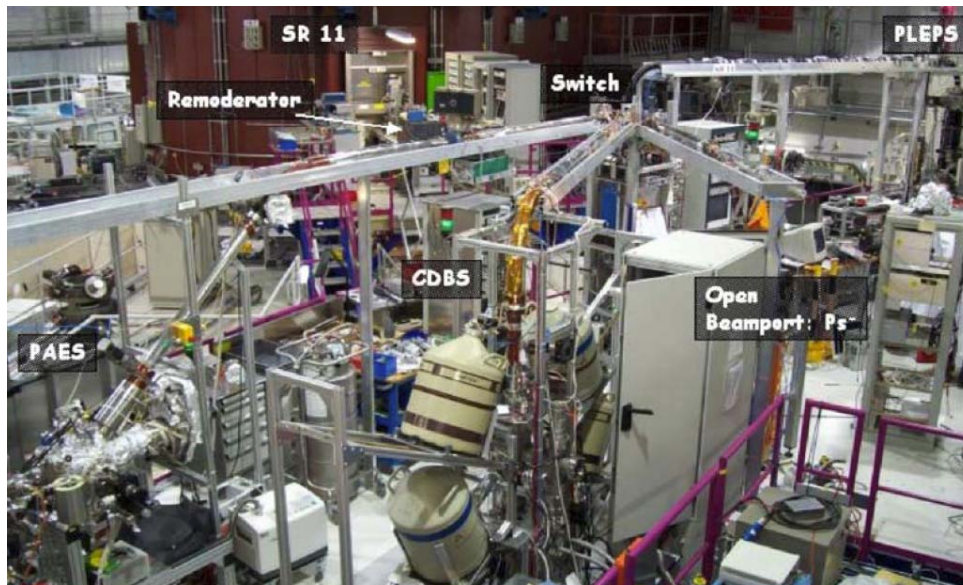


positron energy distribution⁴

1. Positron generation: pair production

For high-flux positron facilities: Positrons are obtained by pair production

- pair production using bremsstrahlung of a decelerated beam of MeV-electrons of a LINAC onto a target (EPOS in Rossendorf, Germany; KEK in Tsukuba, Japan; AIST in Tsukuba, Japan; ANL in Argonne, USA; ...)
- Gamma background from fission reactions in a reactor can be used: Reactor Centre at Delft University, The Netherlands
- Gamma generation from nuclear reaction: $^{113}\text{Cd}(n,\gamma)^{114}\text{Cd} \rightarrow$ three γ rays and pair production; continuous positron beam; $\approx 5 \times 10^8$ e⁺/s (Research Reactor in Garching, Germany)



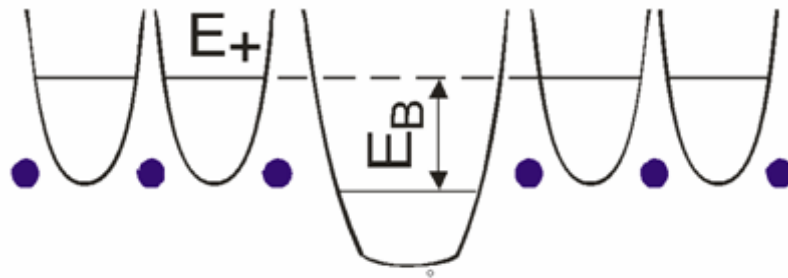
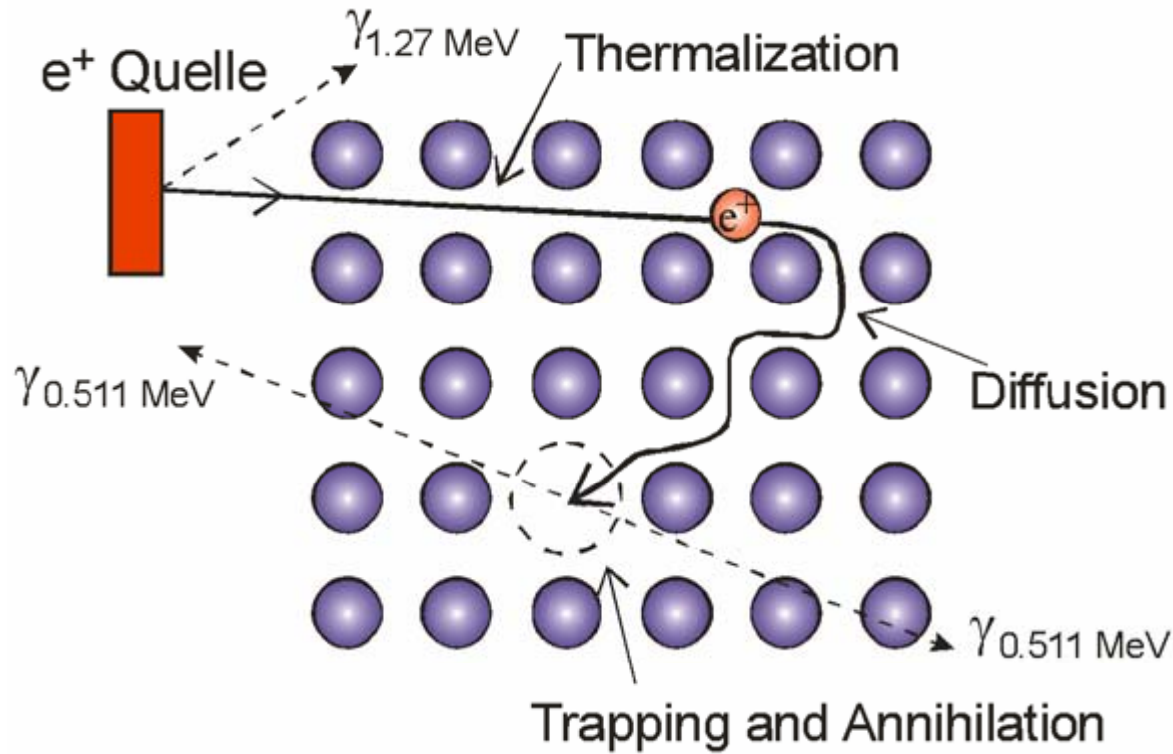
NEPOMUC Source in Garching



The electron to gamma to positron converter at EPOS (Rossendorf)

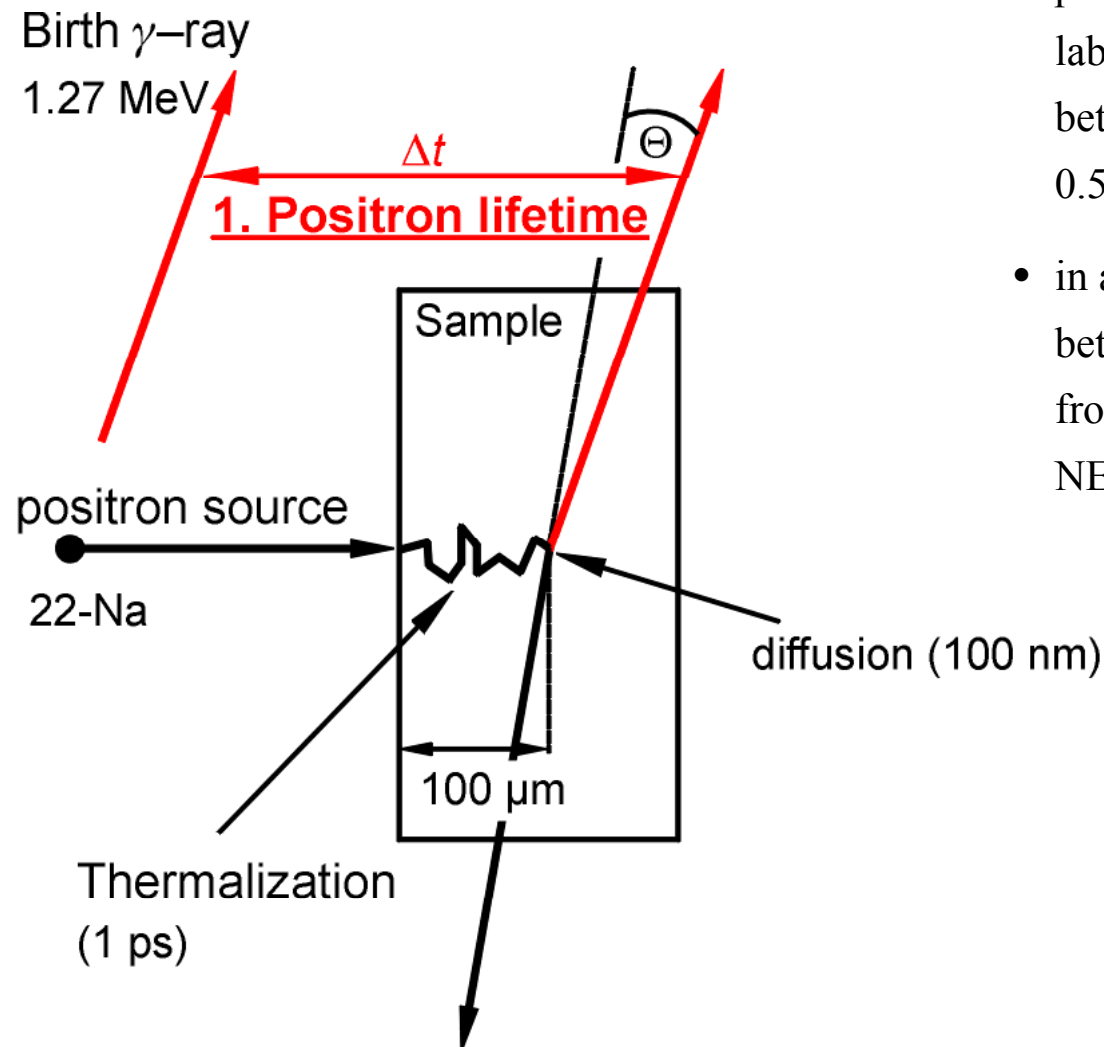
2. Methods of Positron Annihilation Spectroscopy

^{22}Na



- positron wave-function can be localized in the attractive potential of a defect
- annihilation parameters change in the localized state
- e.g. positron lifetime increases in a vacancy
- lifetime is measured as time difference between appearance of 1.27 (start) and 0.51 MeV (stop) quanta
- defect identification and quantification possible

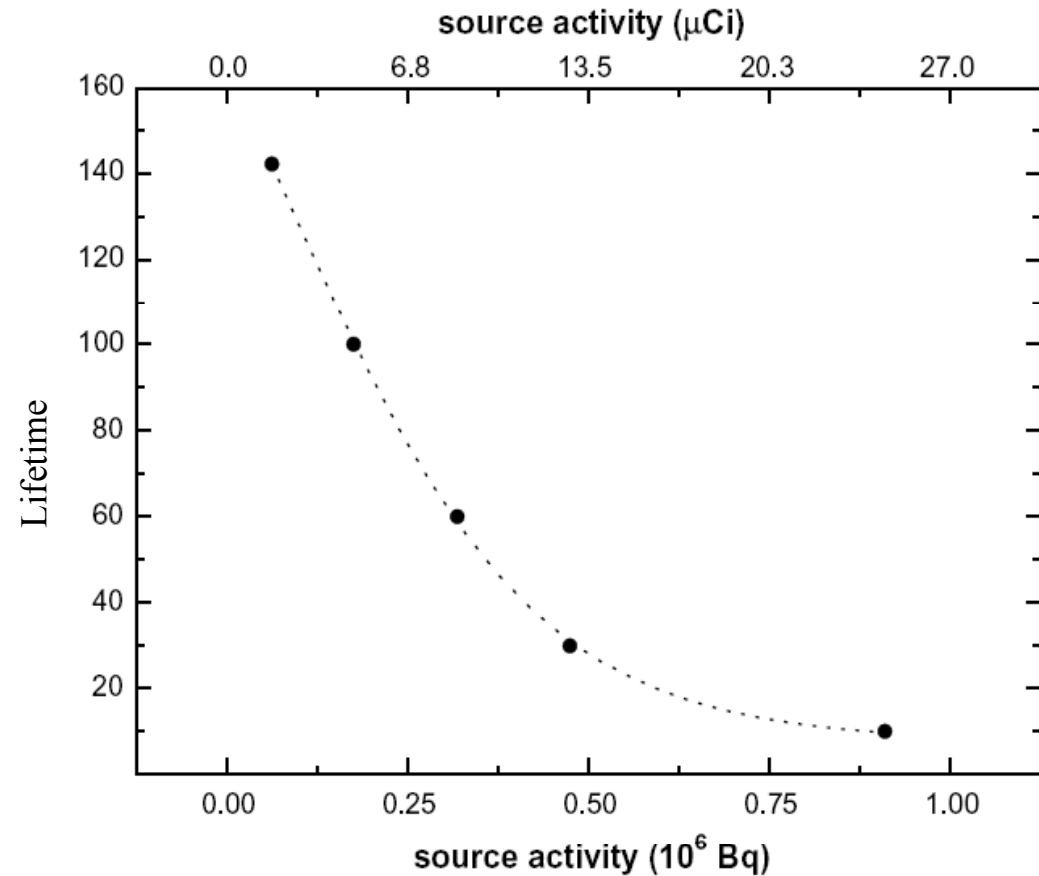
2. Methods of Positron Annihilation Spectroscopy: Positron Lifetime Spectroscopy - PALS



- positron lifetime is measured in a ^{22}Na laboratory setup as the time difference between the 1.27 MeV and the annihilation 0.511 MeV gamma quanta
- in a pulsed positron beam: time difference between 0.511 quantum and machine pulse from timing system (e.g. PLEPS system at NEPOMUC)

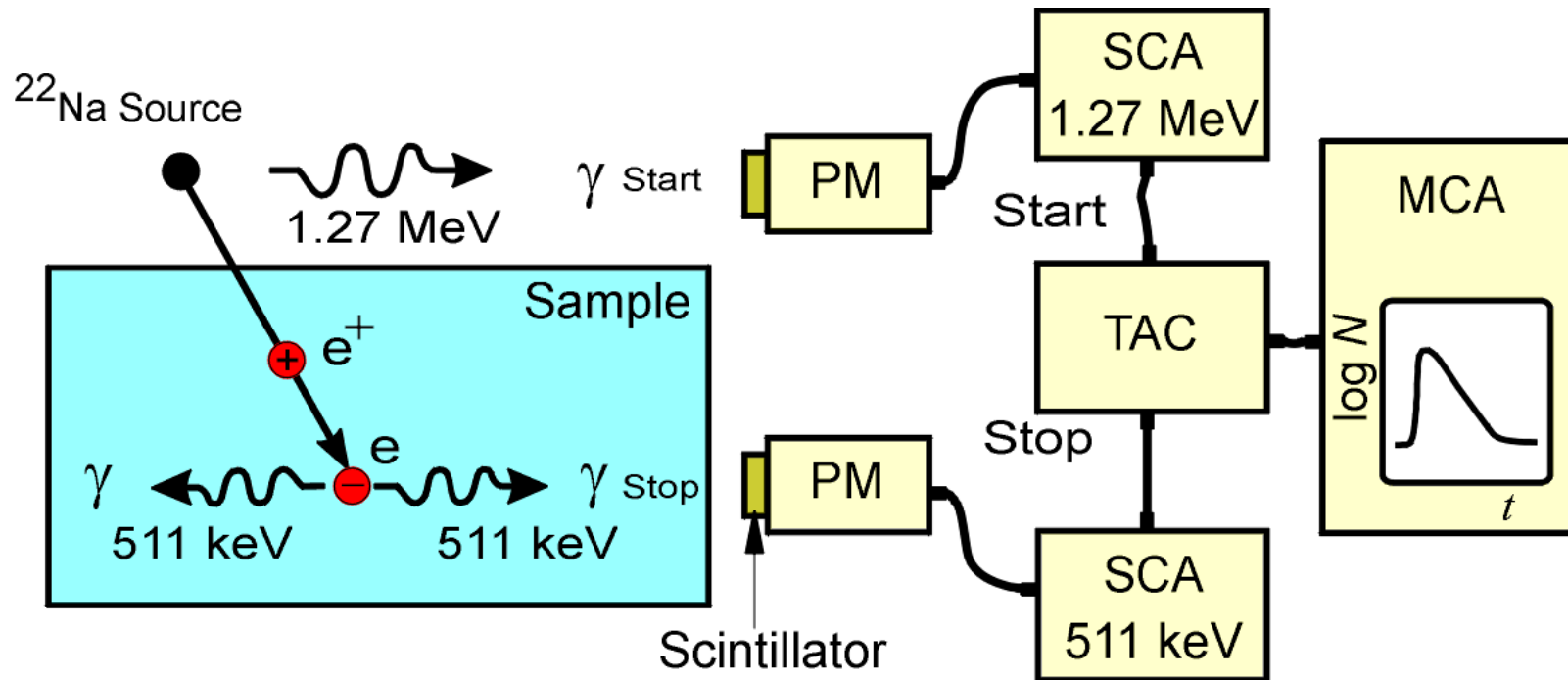
Isotope source: Maximum source strength

- in case of non-periodic sources (isotope sources):
- positron source activity must be adopted to maximum lifetime to be measured
- mean time between 2 positron must be much larger than positron lifetime
- we performed MC simulations to determine this correlation
- to have reasonable background in metals/semiconductors ($t < 0.5$ ns): source should be ≤ 25 μCi
- for porosimetry (e.g. pore diameter = 10 nm) source should have ≤ 5 μCi



S. Thraenert, E.M. Hassan, R. Krause-Rehberg, NIM B248 (2006) 336.

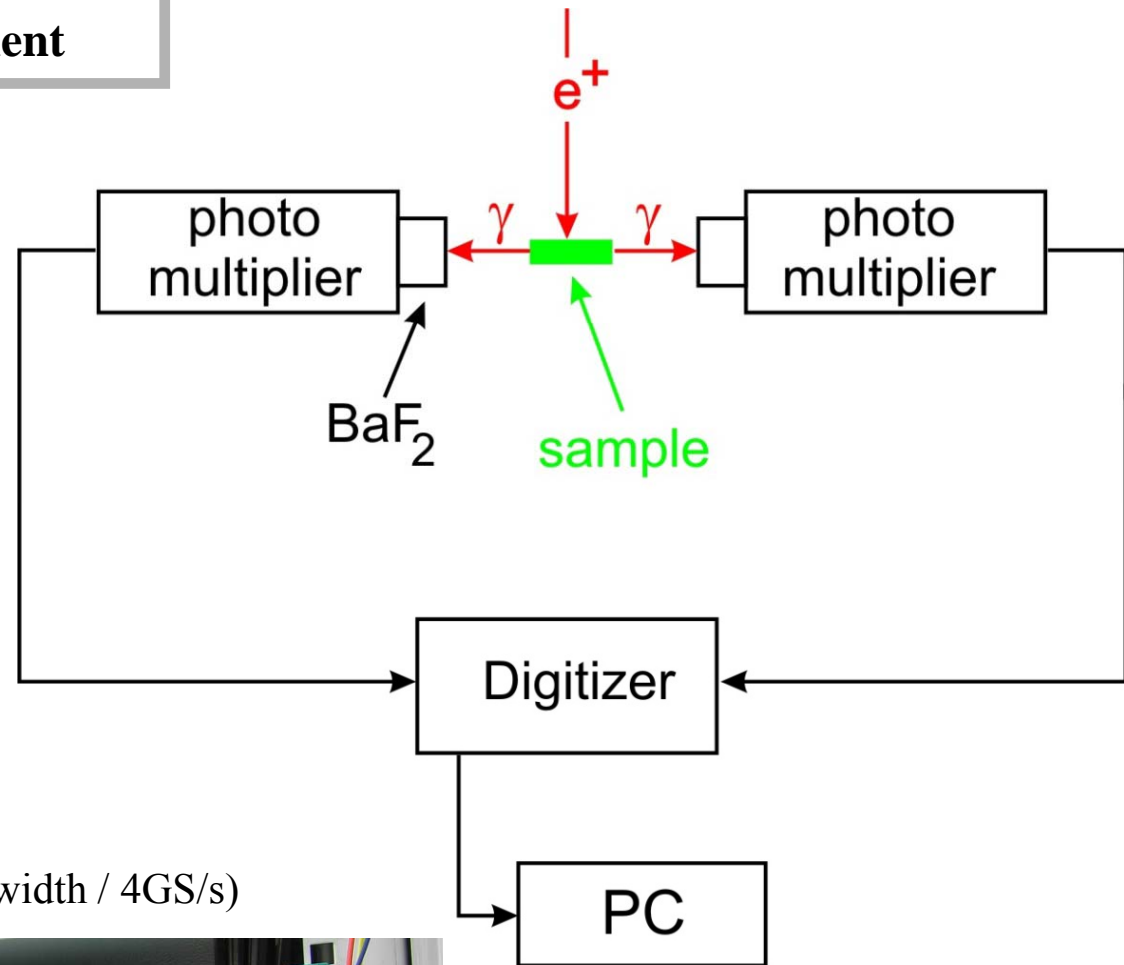
The conventional Positron Lifetime Measurement



- Positron lifetime is measured as time difference between 1.27 MeV quantum (β^+ decay) and 0.511 MeV quanta (annihilation process)
- PM...photomultiplier; SCA...single channel analyzer (constant-fraction type); TAC...time to amplitude converter; MCA... multi channel analyzer

Digital lifetime measurement

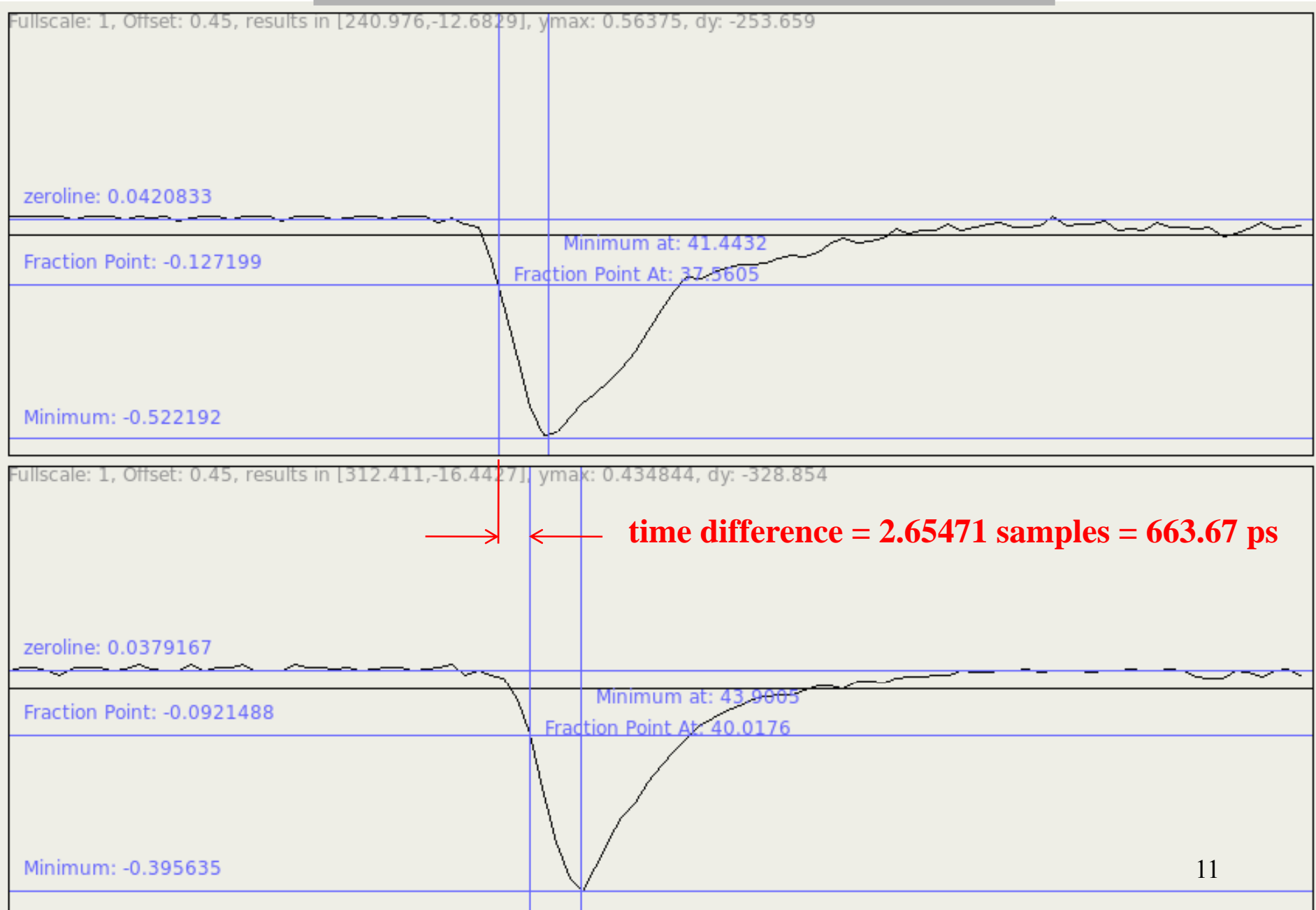
- much simpler setup
- like a dual-channel oscilloscope
- timing very accurate (10^{-6})
- pulse-shape discrimination (suppress “bad pulses”)
- each detector for start & stop (double statistics)



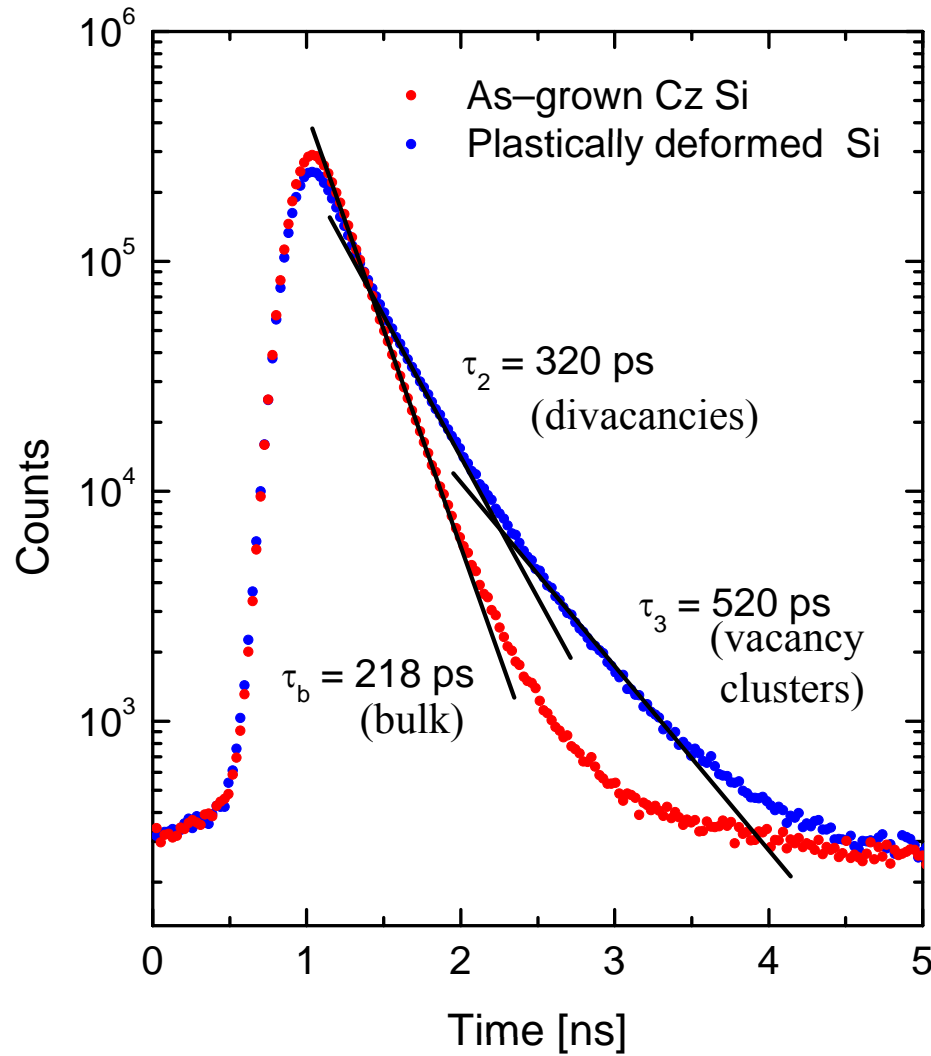
2 acqiris digitizer DP211 (1 GHz bandwidth / 4GS/s)



Screenshot of two digitized anode pulses



Positron lifetime spectroscopy



- positron lifetime spectra consist of exponential decay components
- positron trapping in open-volume defects leads to long-lived components
- longer lifetime due to lower electron density
- analysis by non-linear fitting: lifetimes t_i and intensities I_i

positron lifetime spectrum:

$$N(t) = \sum_{i=1}^{k+1} \frac{I_i}{\tau_i} \exp\left(-\frac{t}{\tau_i}\right)$$

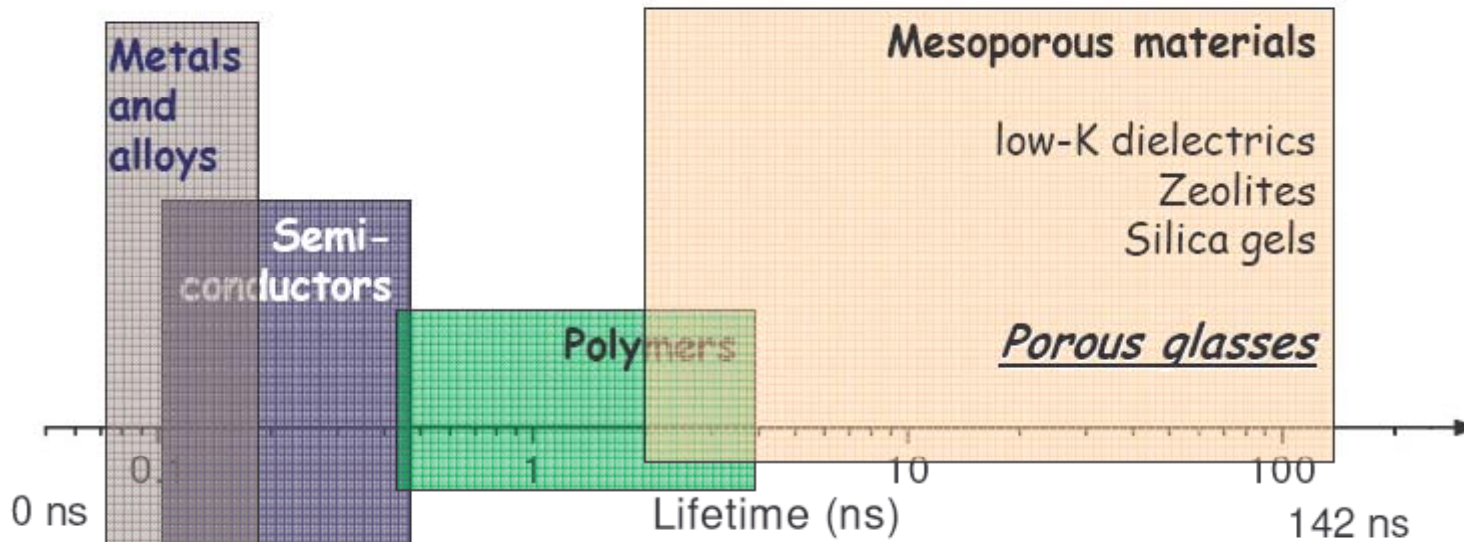
trapping coefficient

$$\kappa_d = \mu C_d = \frac{I_2}{I_1} \left(\frac{1}{\tau_b} - \frac{1}{\tau_d} \right)$$

trapping rate

defect concentration

Typical Lifetimes



V_1
 V_2, V_{etc}
 V_X

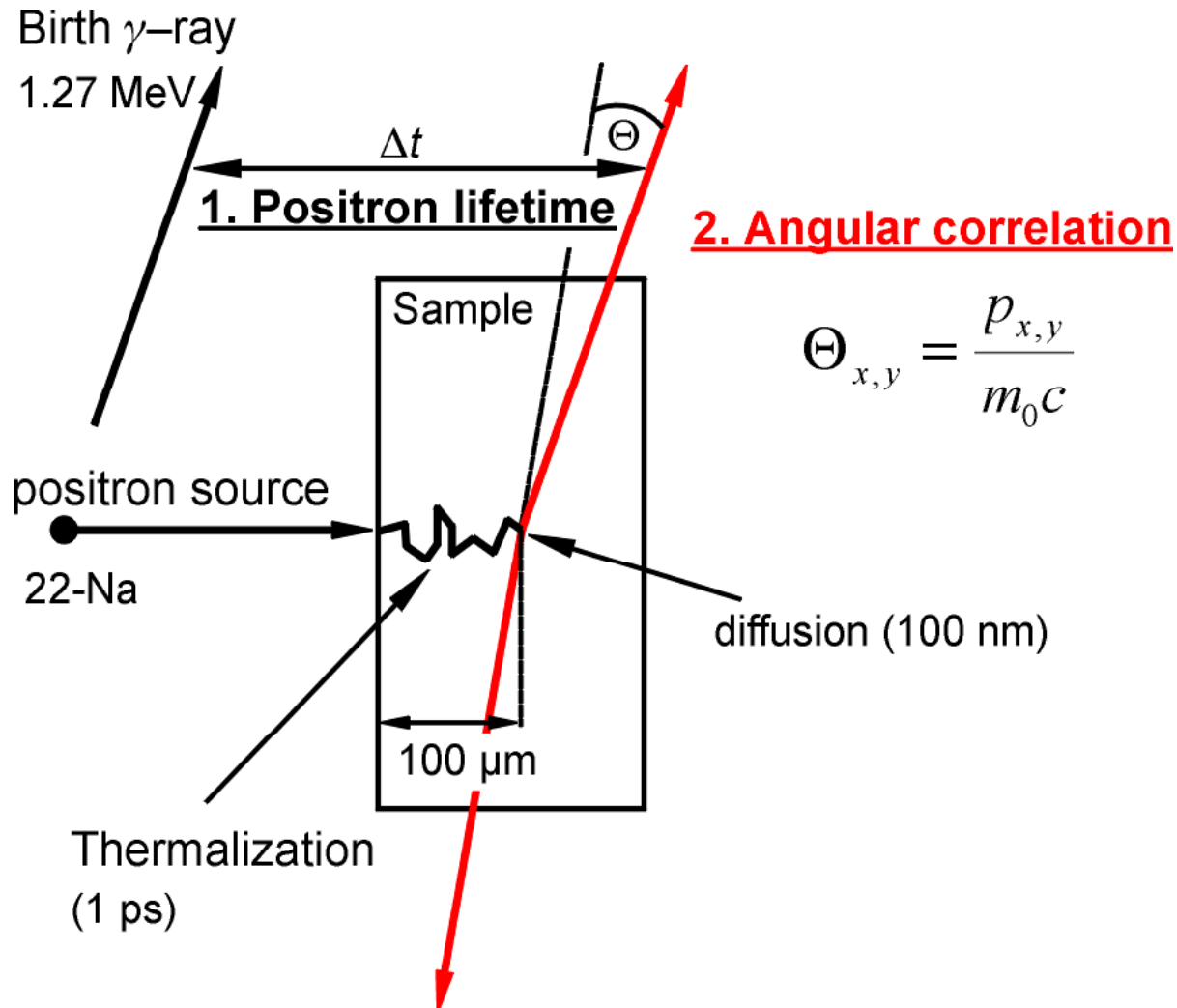


Positron

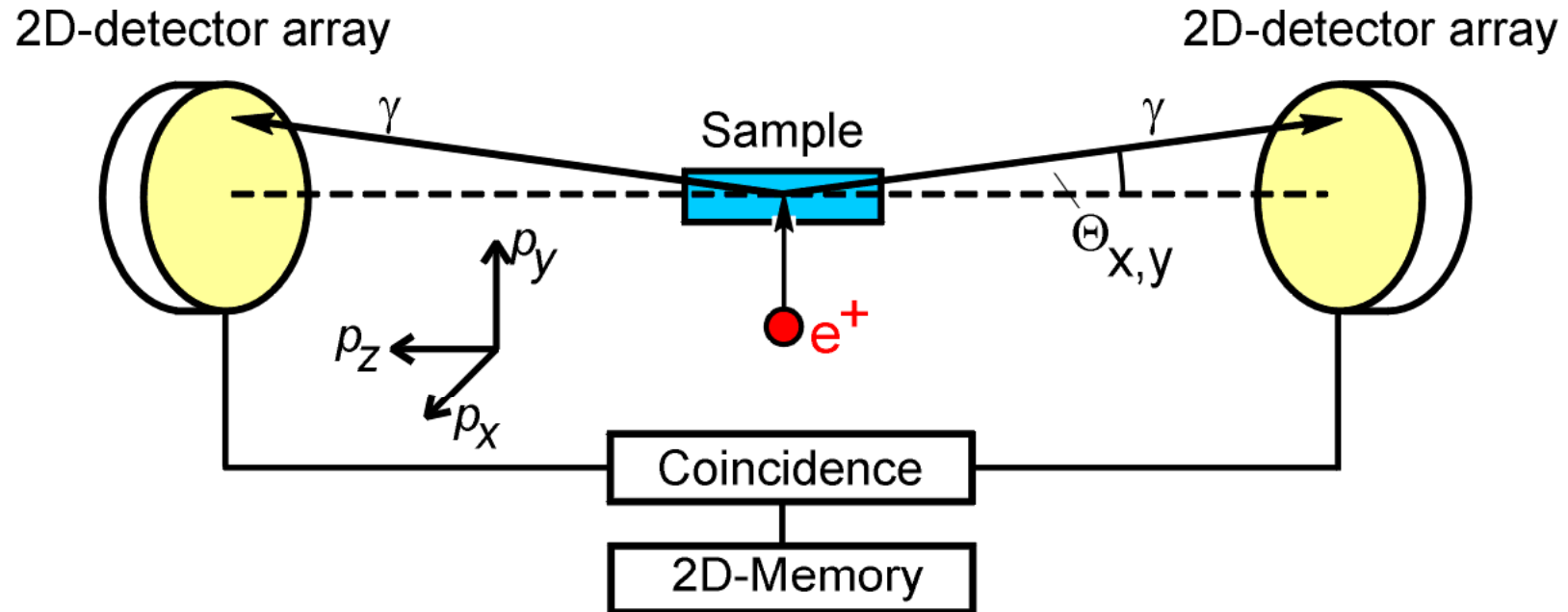


Positronium

2. Methods of Positron Annihilation Spectroscopy: Angular Correlation of Annihilation Radiation - ACAR



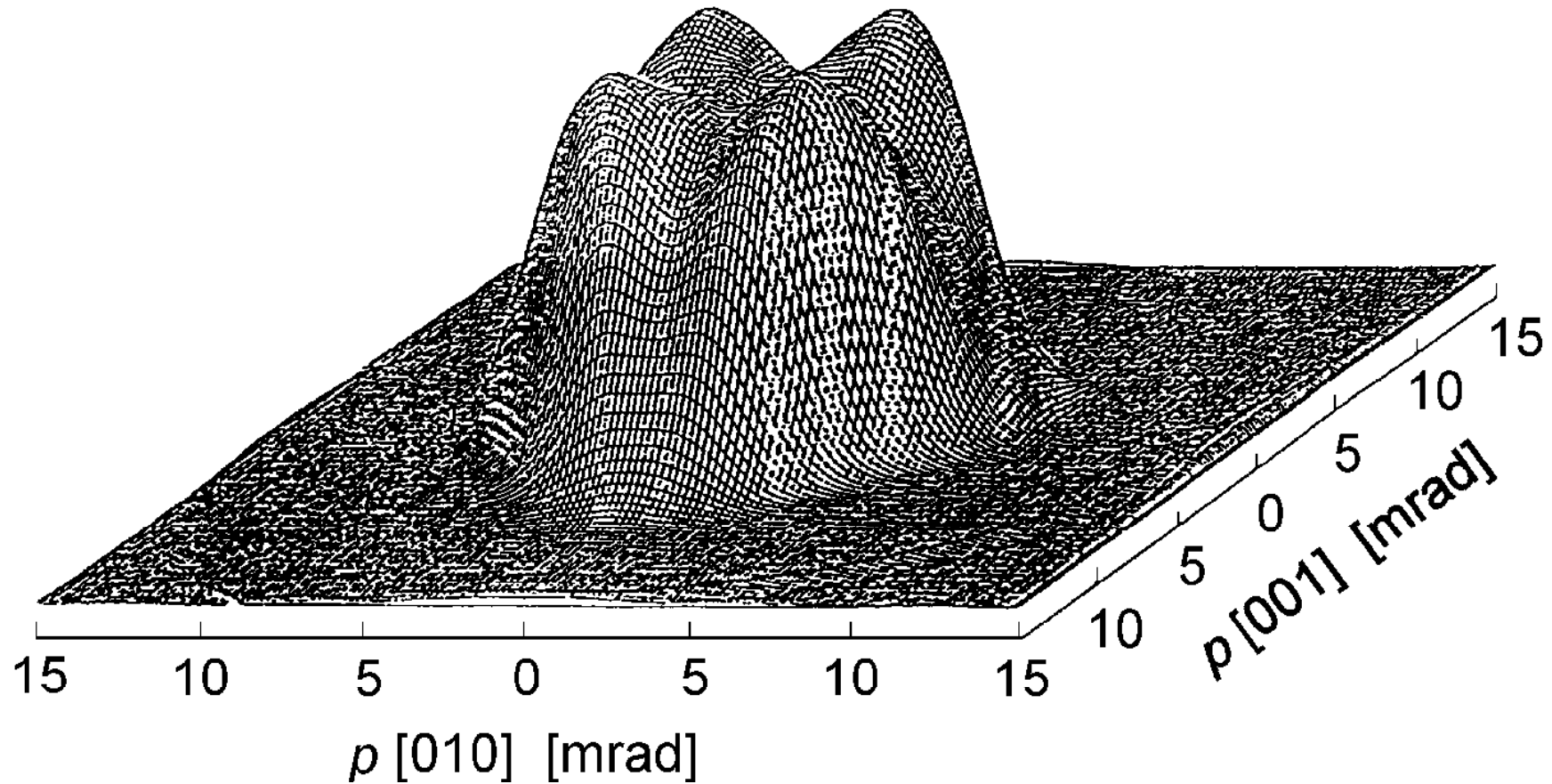
2-D Angular Correlation of Annihilation Radiation



Coincidence counting rate N_c :

$$N_c(\Theta_x, \Theta_y) = A_c \int_{-\infty}^{\infty} \sigma(\Theta_x m_0 c, \Theta_y m_0 c, p_z) dp_z$$

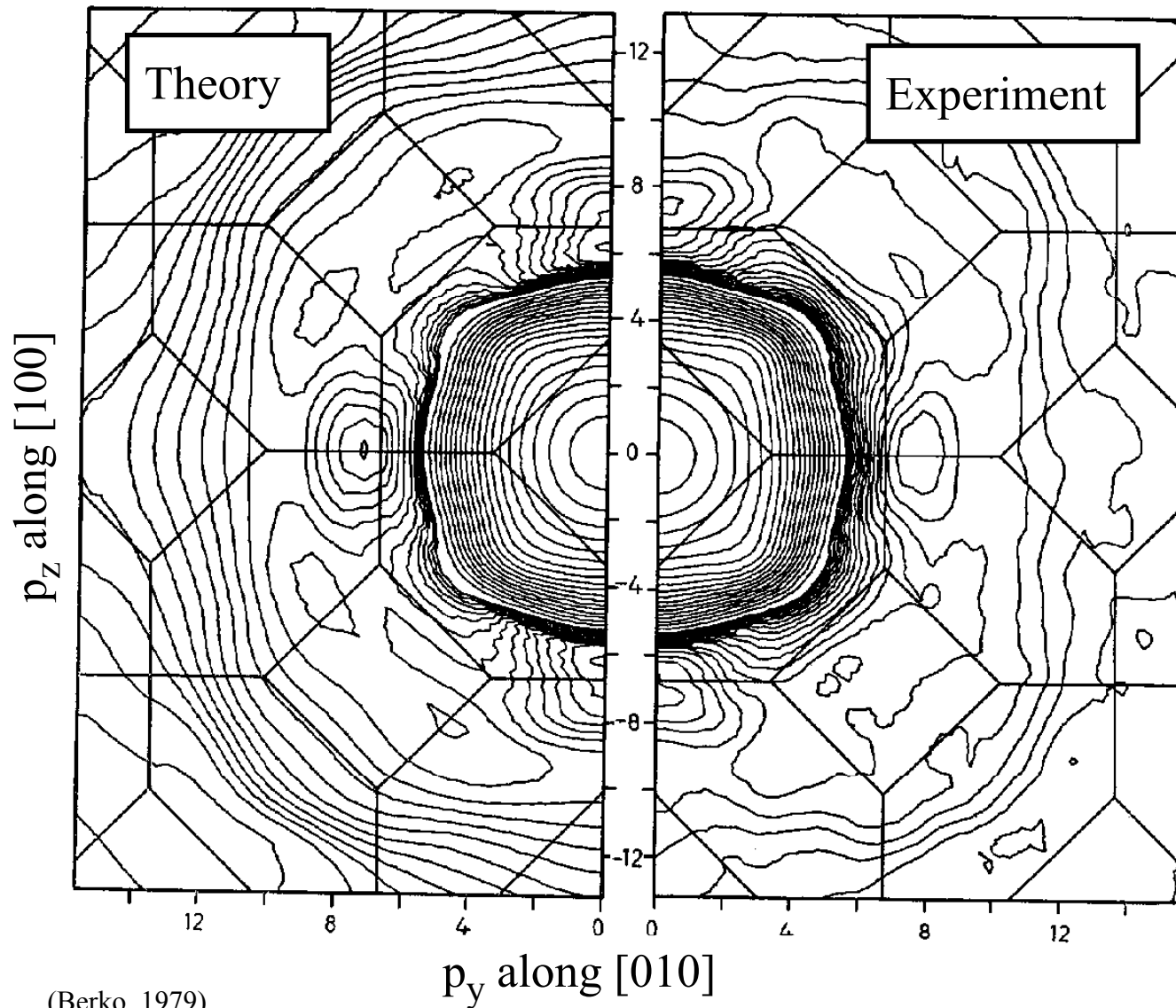
2D-ACAR of defect-free GaAs



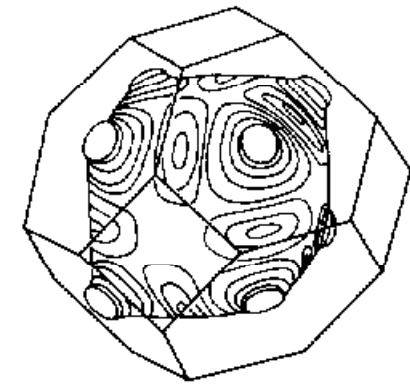
(Tanigawa et al., 1995)

3D-Fermi surface can be reconstructed from measurements in several directions of a single crystal

2D-ACAR of Copper

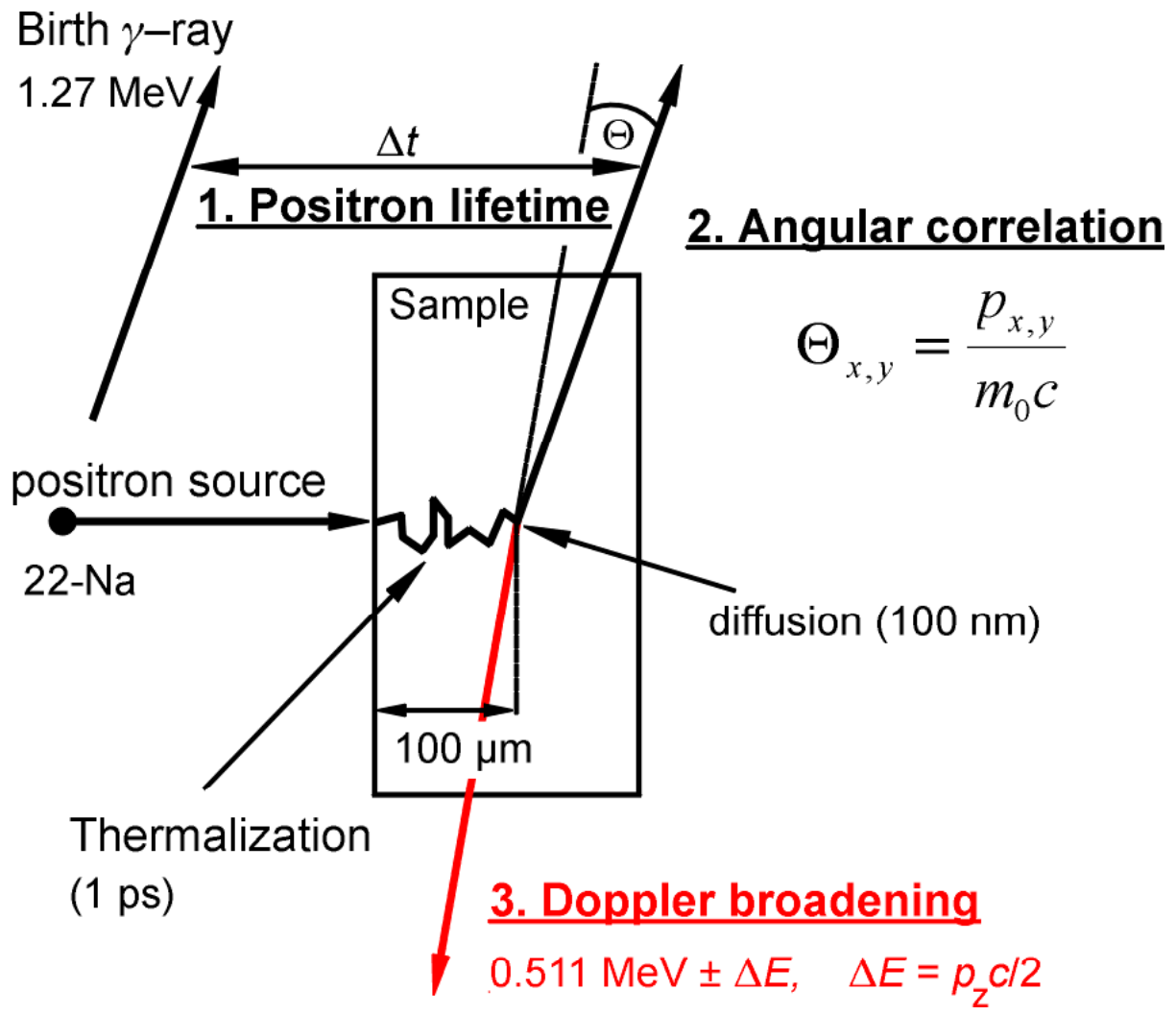


(Berko, 1979)

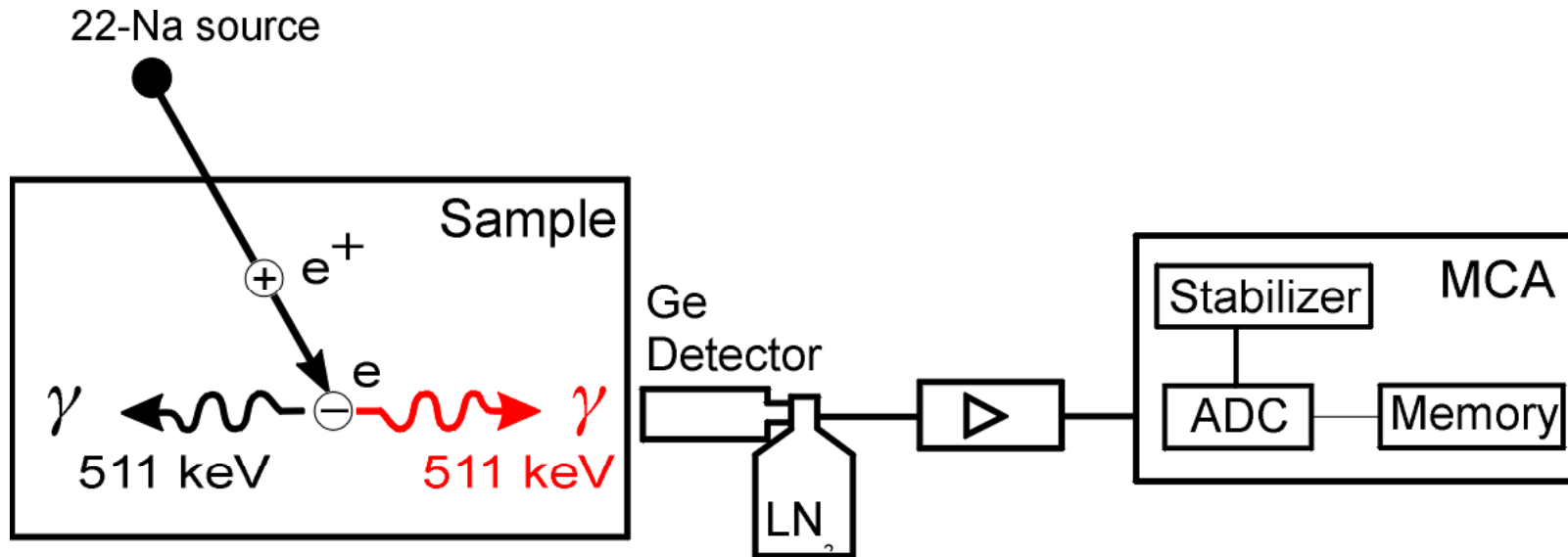


Fermi surface
of copper

2. Methods of Positron Annihilation Spectroscopy: Doppler Broadening Spectroscopy - DBS

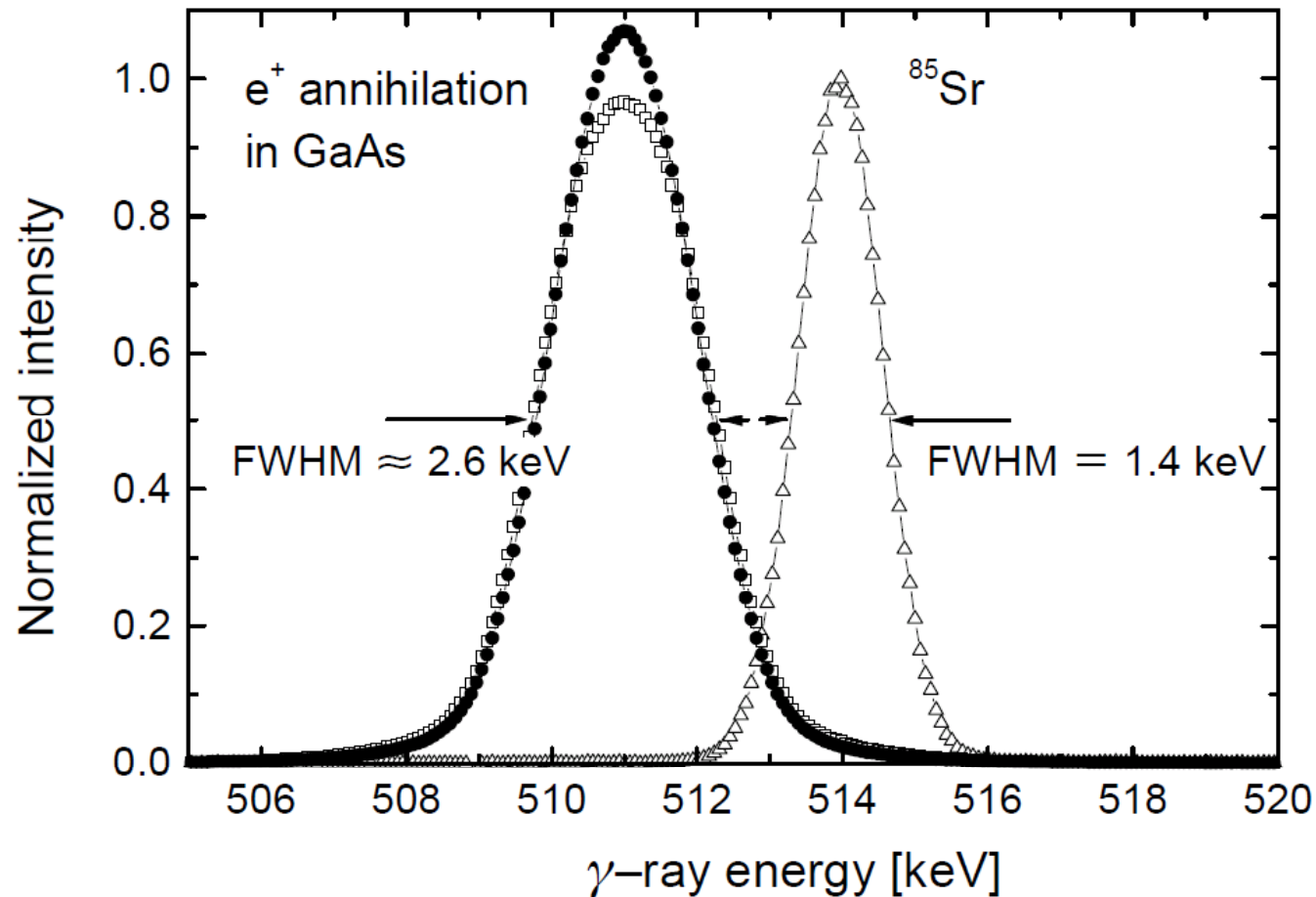


Measurement of Doppler Broadening



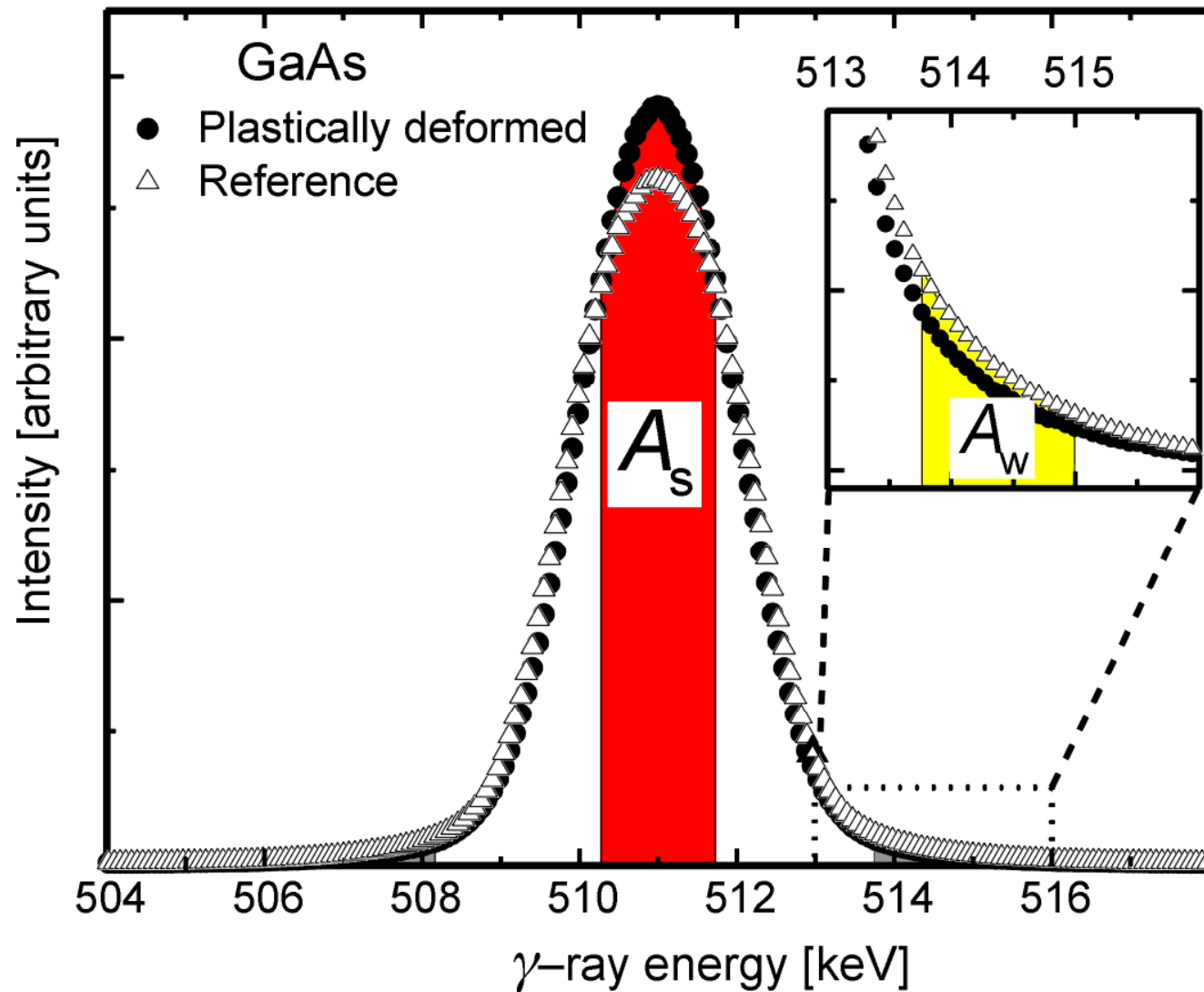
- electron momentum in propagation direction of 511 keV γ -ray leads to Doppler broadening of annihilation line
- can be detected by conventional energy-dispersive Ge detectors and standard electronics

Effect of Doppler Broadening



- width of ⁸⁵Sr line corresponds to the energy resolution of Ge detector
- 511 keV annihilation line distinctly broader due to momentum of annihilating electrons
- defect-rich sample show more narrow curves
- Effect due to enhanced annihilation with valence electrons in open-volume defects (e.g. in vacancies)
- they have smaller momenta: smaller Doppler shift

Line Shape Parameters



S parameter (shape):

$$S = A_S/A_0$$

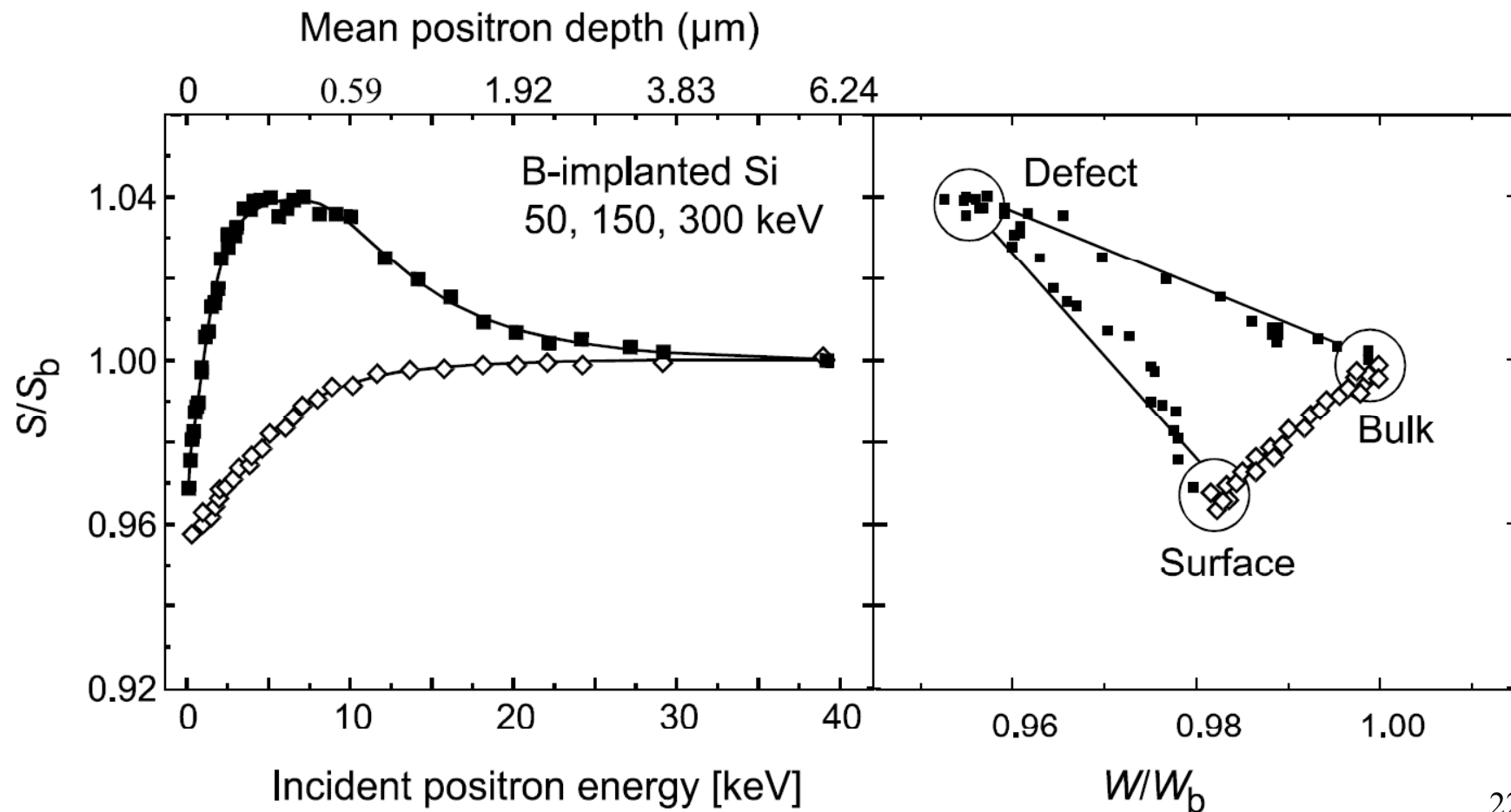
W parameter (wing):

$$W = A_W/A_0$$

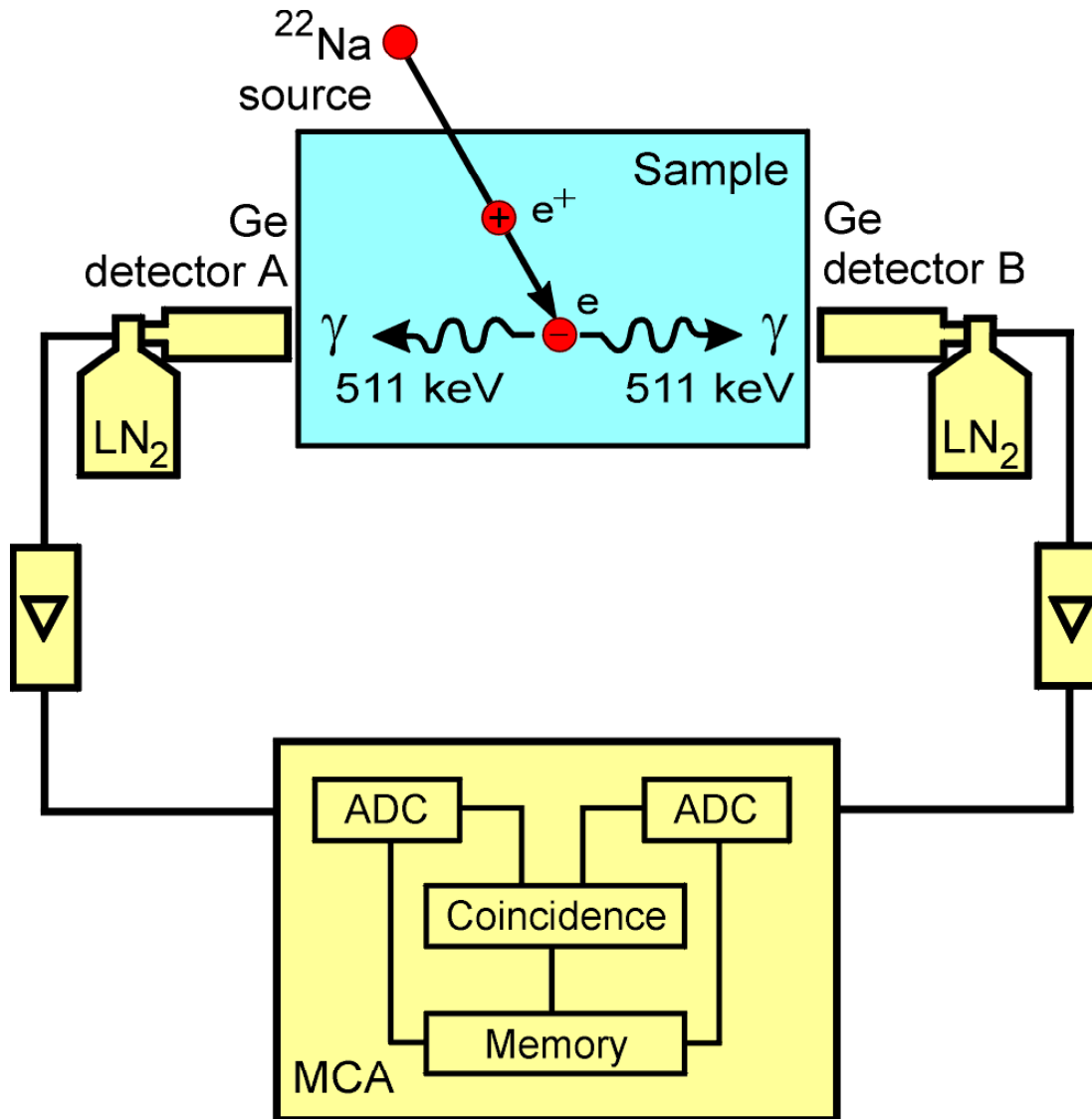
- W parameter mainly determined by annihilations of core electrons (chemical information)
- however: almost in background
- very useful S-versus-W plot

S versus W plot

- Doppler results after ion implantation in Si obtained by a slow-positron beam
- S and W values were normalized to the respective bulk values
- the S-W-plot allows to identify the annihilation site

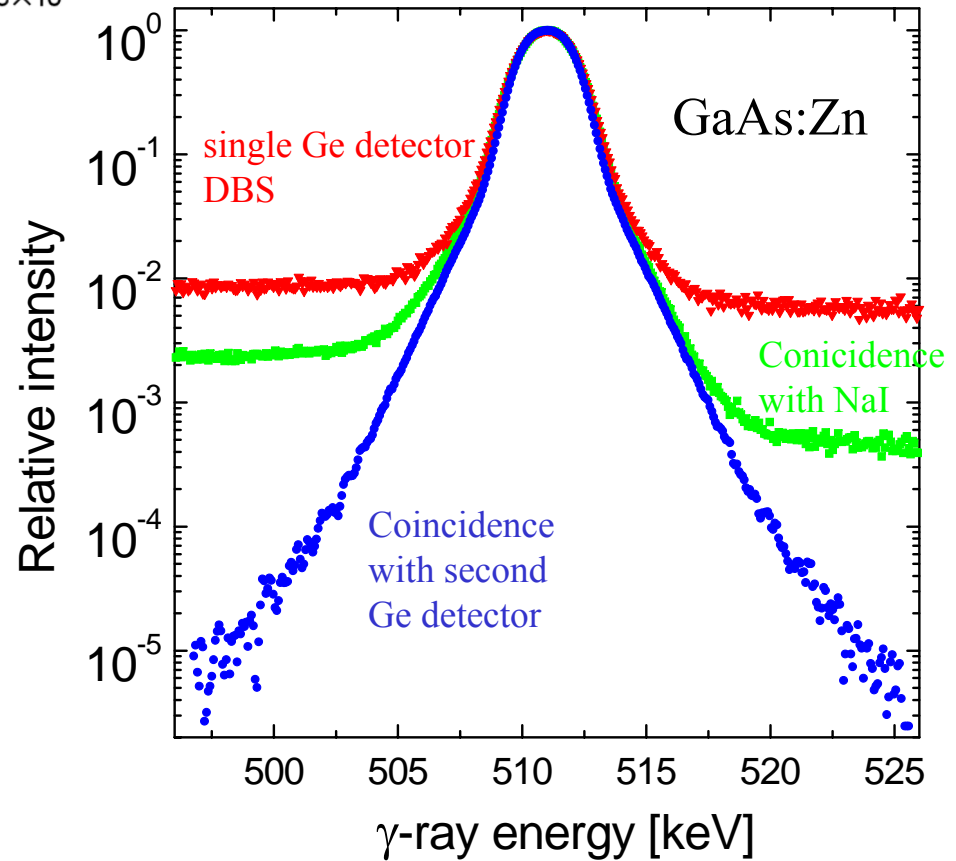
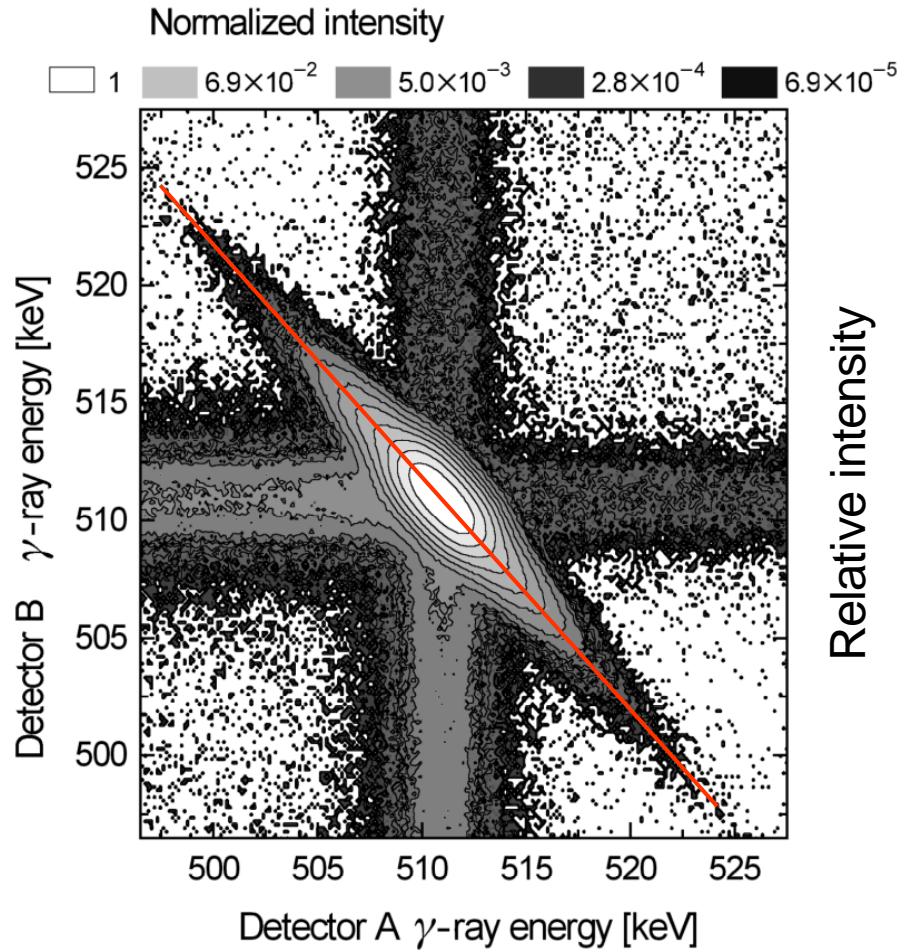


Coincidence Doppler Broadening Spectroscopy - CDBS



- coincident detection of second annihilation γ reduces background by 3...4 orders of magnitude
- sum of both energies is 1022 keV
- when 515 keV is detected in detector A: detector B shows 507 keV
- thus, electron energy is detected twice
- energy resolution of system is improved by a factor of 0.707

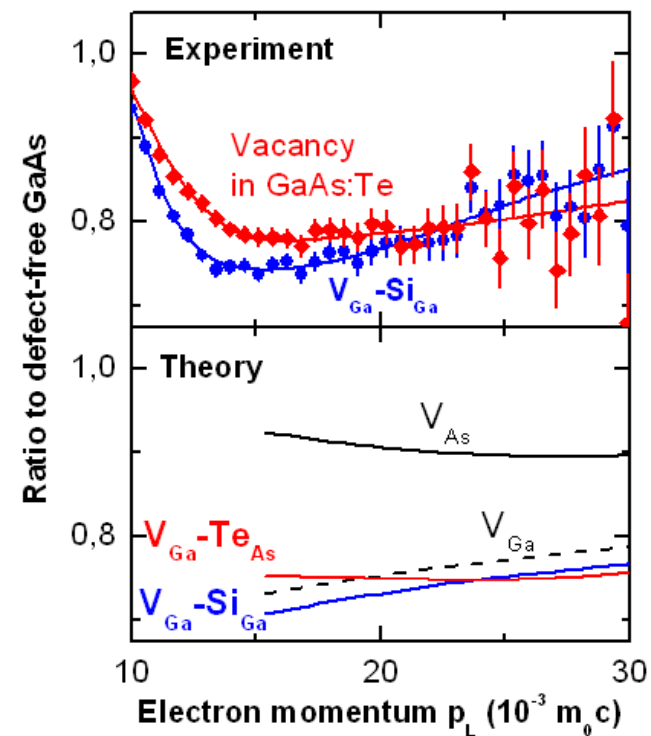
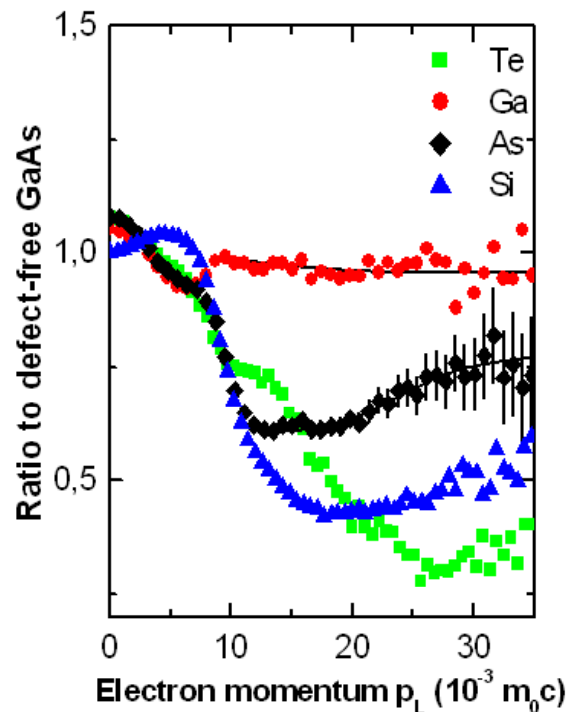
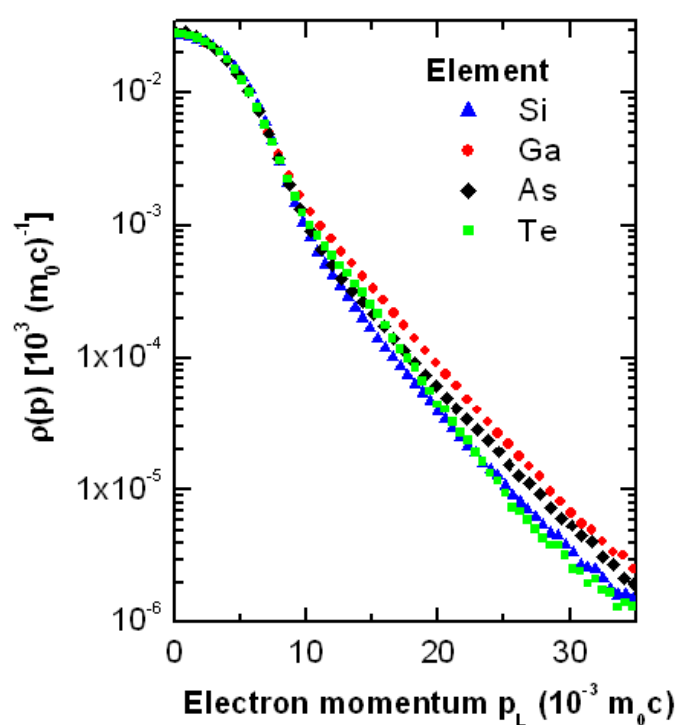
CBDS Spectra: the effect of coincident detection



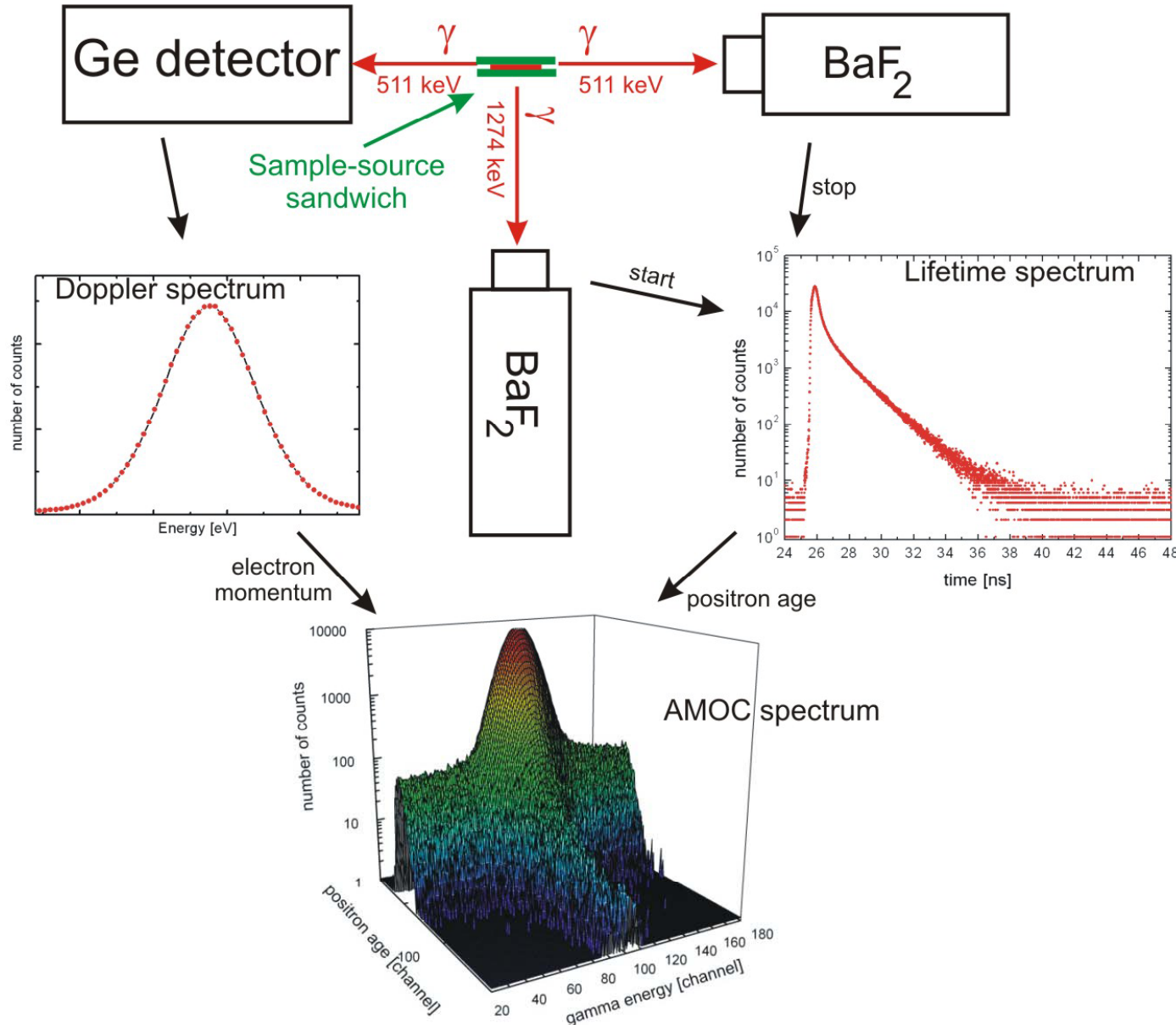
$$E_{\gamma_1} + E_{\gamma_2} = 2 m_0 c^2 = 1022 \text{ keV}$$

CDBS spectra in GaAs

- Chemical sensitivity due to electrons at high momentum (core electrons)
- a single impurity atom aside a vacancy is detectable
- examples: $V_{\text{Ga}}\text{-Te}_{\text{As}}$ in GaAs:Te

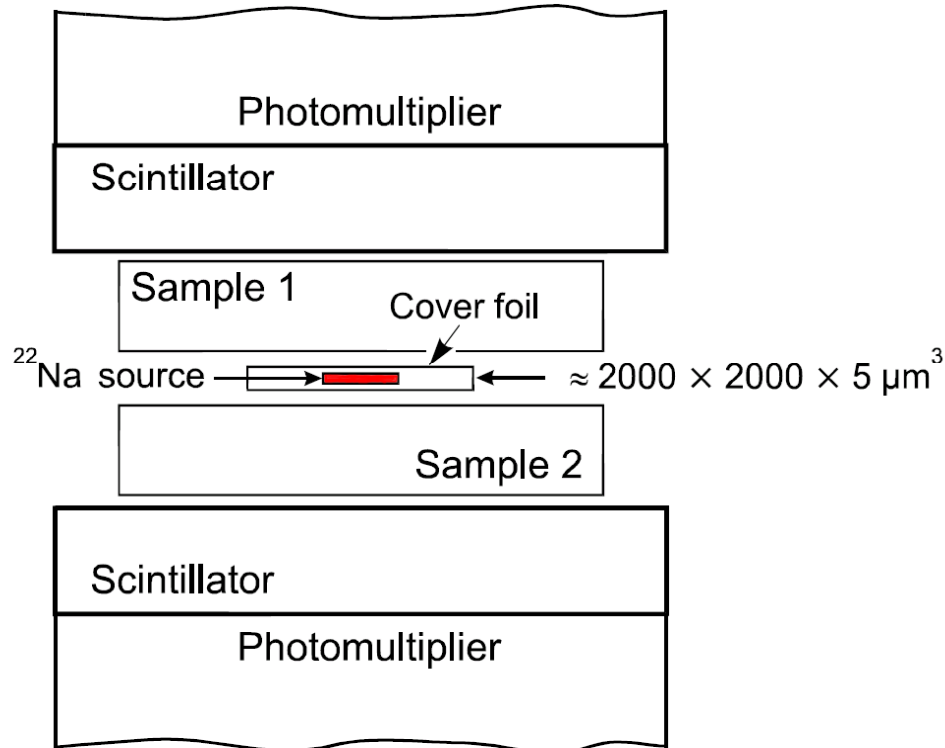


2. Methods of Positron Annihilation Spectroscopy: Age-Momentum Correlation - AMOC



- lifetime and Doppler shift are measured for the **same** positron in triple coincidence
- electron momentum is plotted as function of positron age
- interesting application for soft matter research
- count rate extremely low ($< 10 \text{ s}^{-1}$)
- better to be performed at bunched intense lifetime beams
- example was measured in Dec08 in Rossendorf

3. Possible experimental Setups: The Sandwich Geometry



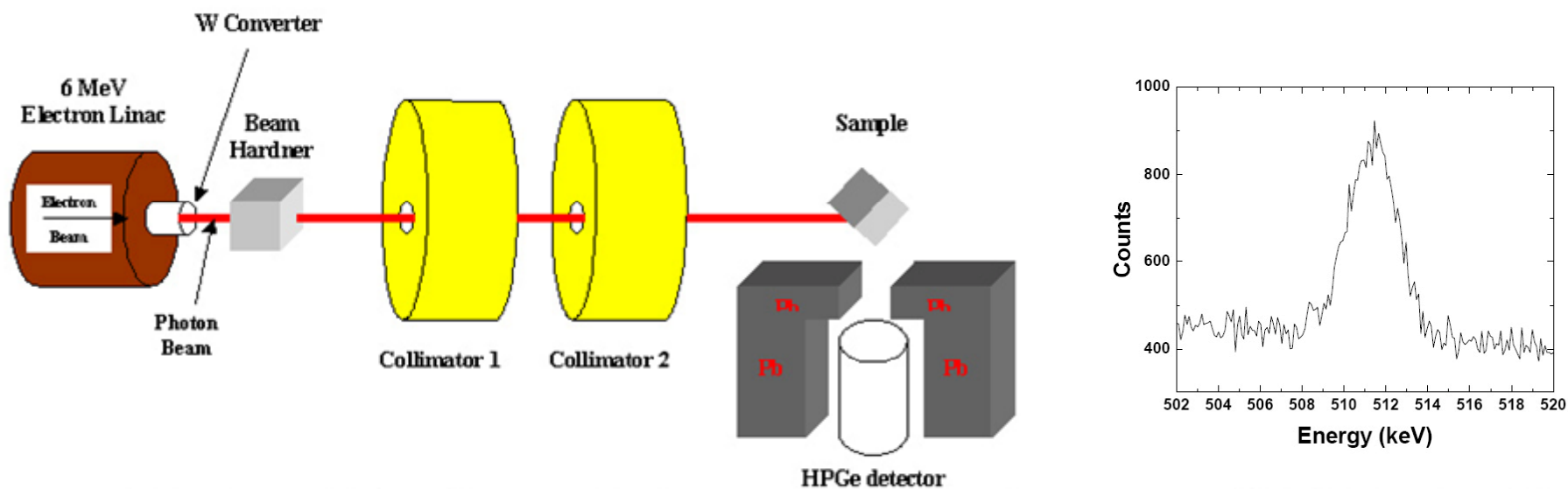
- small isotope sources (mostly ^{22}Na) are used for lifetime and Doppler spectroscopy
- covered by thin foils (Al, Ni, Kapton, ...)
- foil thickness: 1...5 μm
- two identical samples are needed on both sides of the source
- sample thickness 0.3 ... 1 mm to stop > 99% of positrons in sample (depends on density)
- positrons exhibit exponential stopping profile
- main information depth 10...50 μm
- positrons annihilating in the source can be subtracted from lifetime spectra as so-called source correction
- can be determined by measuring known (one-component) spectra (pure annealed metals; as-grown Si) – depend on z

$$S_p(z) = 1 - \bar{P}(z) = 1 - \exp(-\alpha z) \quad \text{with} \quad \alpha[\text{cm}^{-1}] = 17 \frac{\rho[\text{g cm}^{-3}]}{E_{\text{max}}^{1.43}[\text{MeV}]}$$

$S_p(z)$... number of positrons stopped in surface-near layer of thickness z; E_{max} is the maximum positron energy (540 keV for ^{22}Na); ρ is the mass density

3. Possible Experimental Setups: Gamma-induced Positron Spectroscopy - GiPS

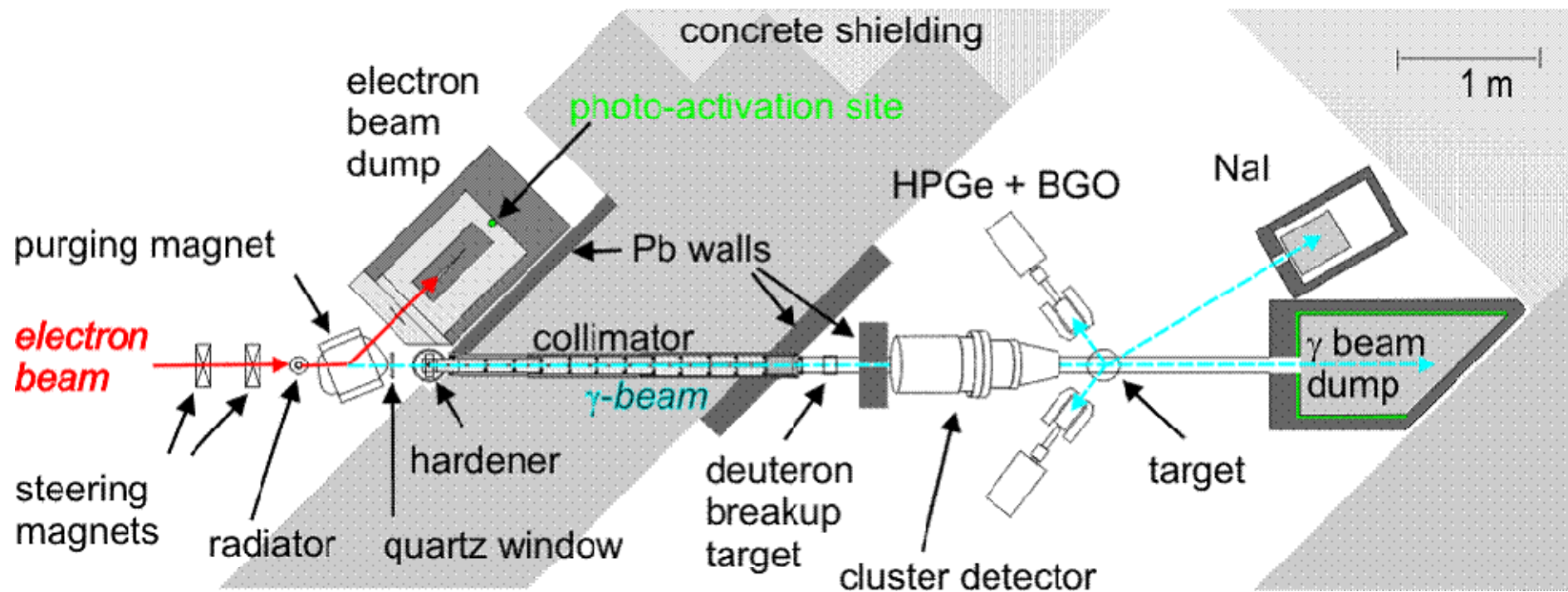
- positrons are generated inside the whole volume of sample by bremsstrahlung of MeV electron beam
- information from the whole sample (several cm thickness)
- ideal for non-destructive testing of large components or e.g. liquids; biological samples
- with usual Linacs ($< 1\text{kHz}$): many gammas in a few bunches; not suitable for lifetime spectroscopy
- very low statistics and poor Peak/Background ratio of about 1:1
- improvement: superconducting Linac with high repetition rate (26 MHz at ELBE)



The experimental set-up of Doppler broadening spectroscopy using 6 MeV electron Linac

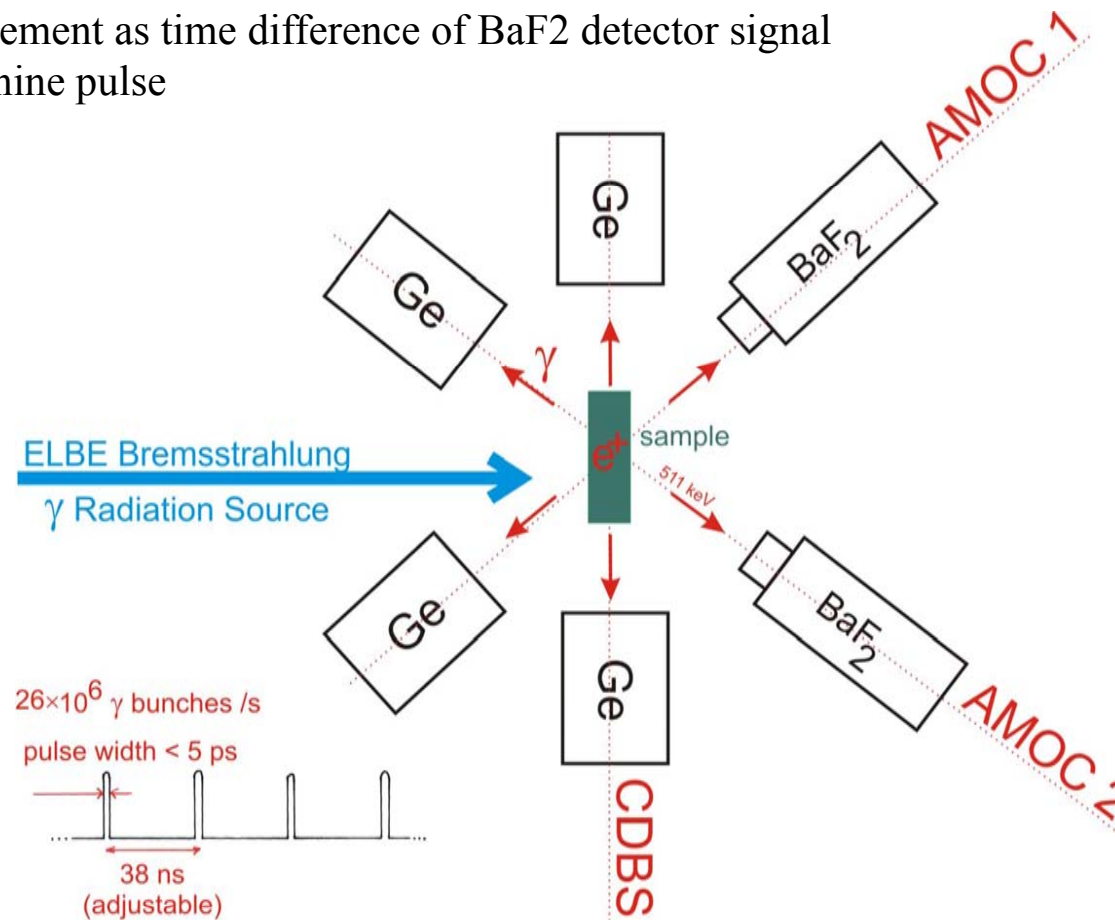
Gamma-induced Positron Spectroscopy (GiPS) at ELBE (in Rossendorf)

- ELBE provides a pulsed electron beam with extremely sharp bunches (5 ps bunch length; up to 40 MeV; 1 mA average current)
- among 5 experiments at ELBE: a bremsstrahlung gamma source exists
- provides a collimated und pulsed gamma beam with high intensity
- time structure suitable for lifetime spectroscopy



Coincident Detector System of GiPS at ELBE

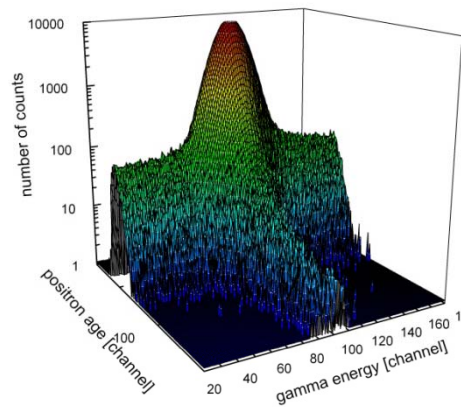
- detector system was modified to have 2 AMOC and 1 CDBS spectrometer at the same time
- count rate can be adapted by electron current of primary ELBE beam
- lifetime measurement as time difference of BaF₂ detector signal and ELBE machine pulse



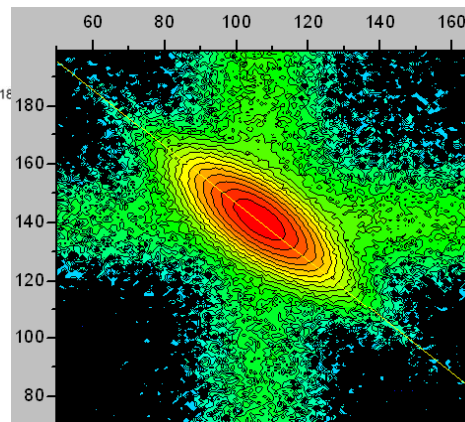
AMOC: Age-Momentum Correlation
 CDBS : Concidence Doppler-Broadening Spectroscopy

First GiPS spectra at ELBE

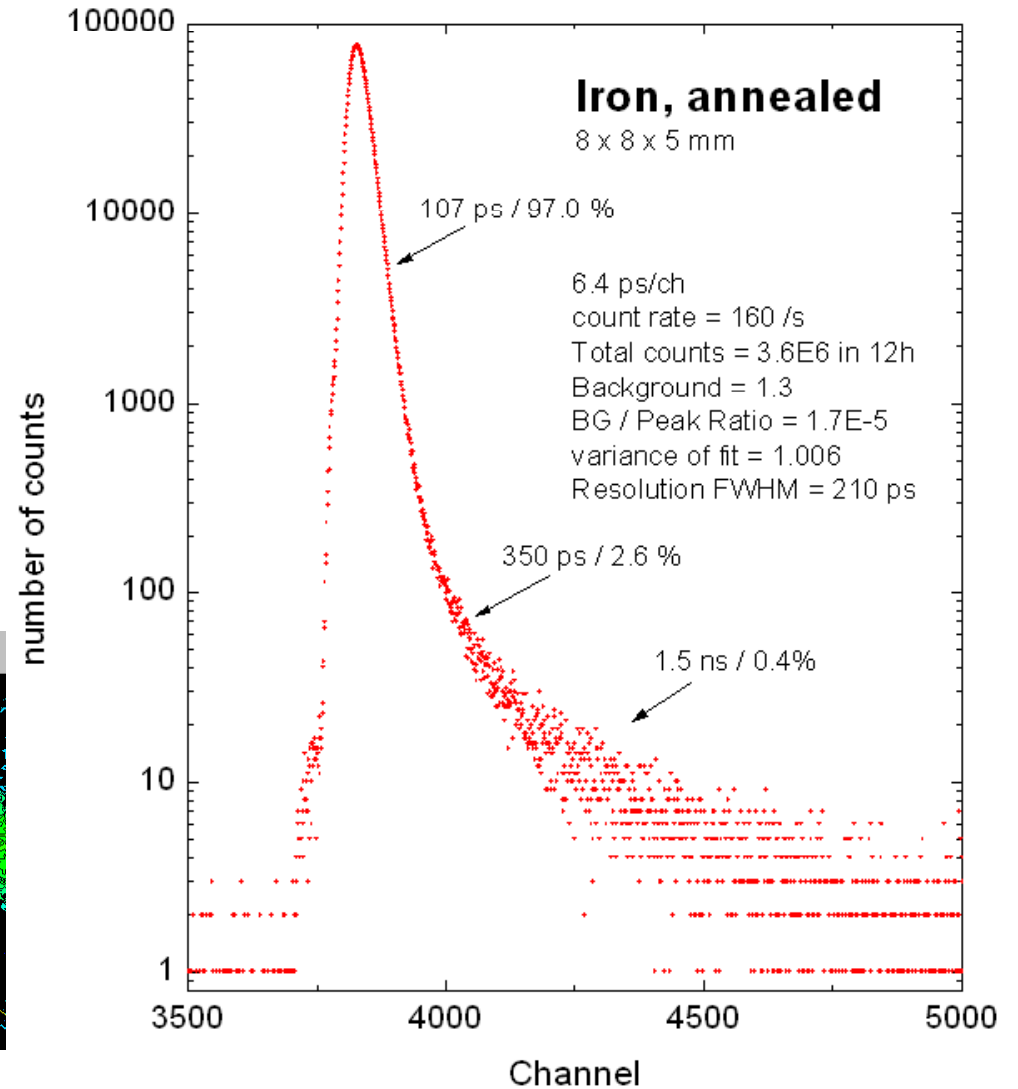
- lifetime spectrum is obtained in coincidence with Ge detector to reduce background
- good spectra quality obtained:
- Count rate for one AMOC spectrum = 160 /s
- Time resolution = 210 ps
- $BG / Peak = 1.7 \times 10^{-5}$
- AMOC and CDBS is measured at the same time:



AMOC spectrum of Fe

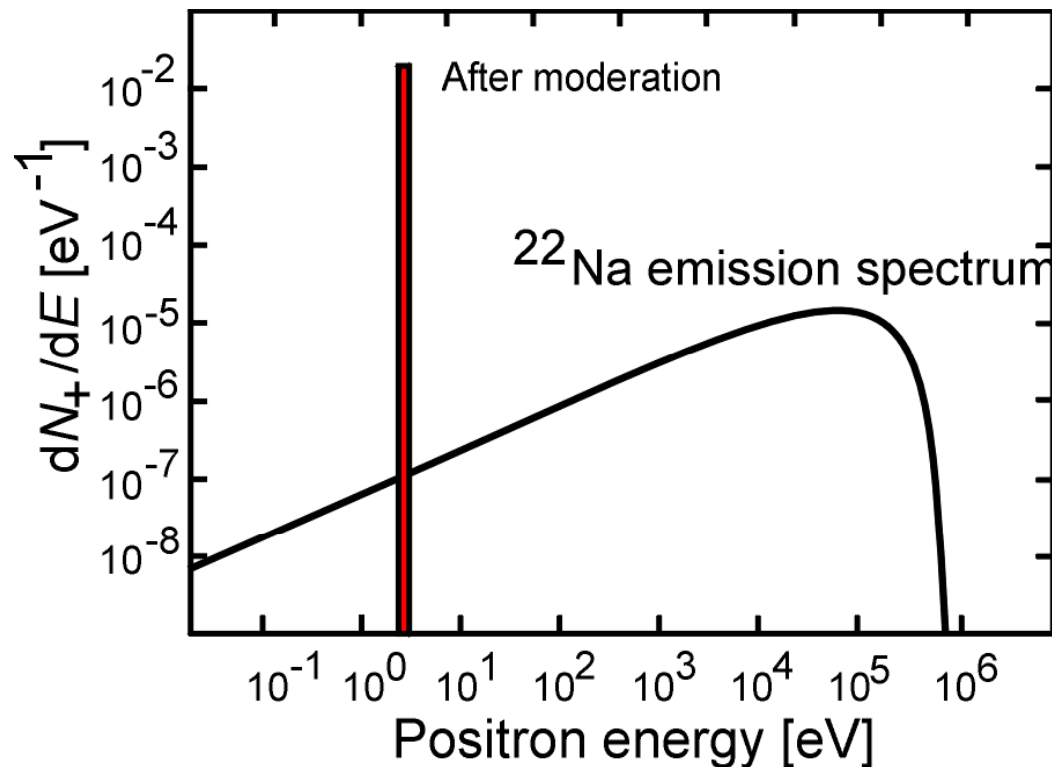


CDBS spectrum of Fe



3. Possible Experimental Setups: Positron beams Variable Energy Positron Annihilation Spectroscopy (VEPAS)

- often: only thin near-surface layers are of interest (surface modification; ion-implantation; epitaxy ...)



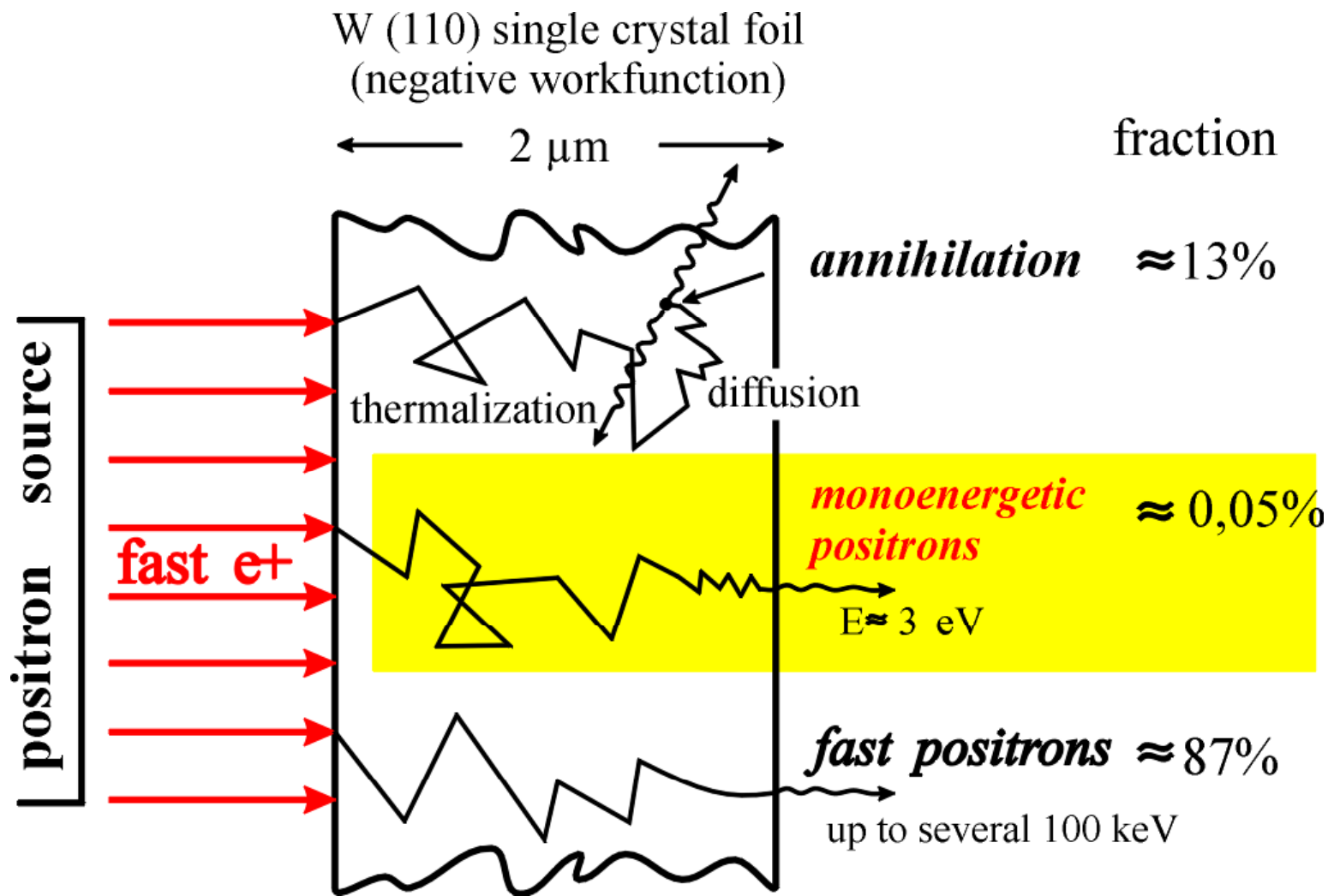
- isotope β sources: broad positron emission spectrum up to 540 keV (^{22}Na)
- deep implantation into solids

Mean (maximum) depth in:

- Si: 50 μm (770 μm)
- GaAs: 22 μm (330 μm)
- PbS: 15 μm (220 μm)

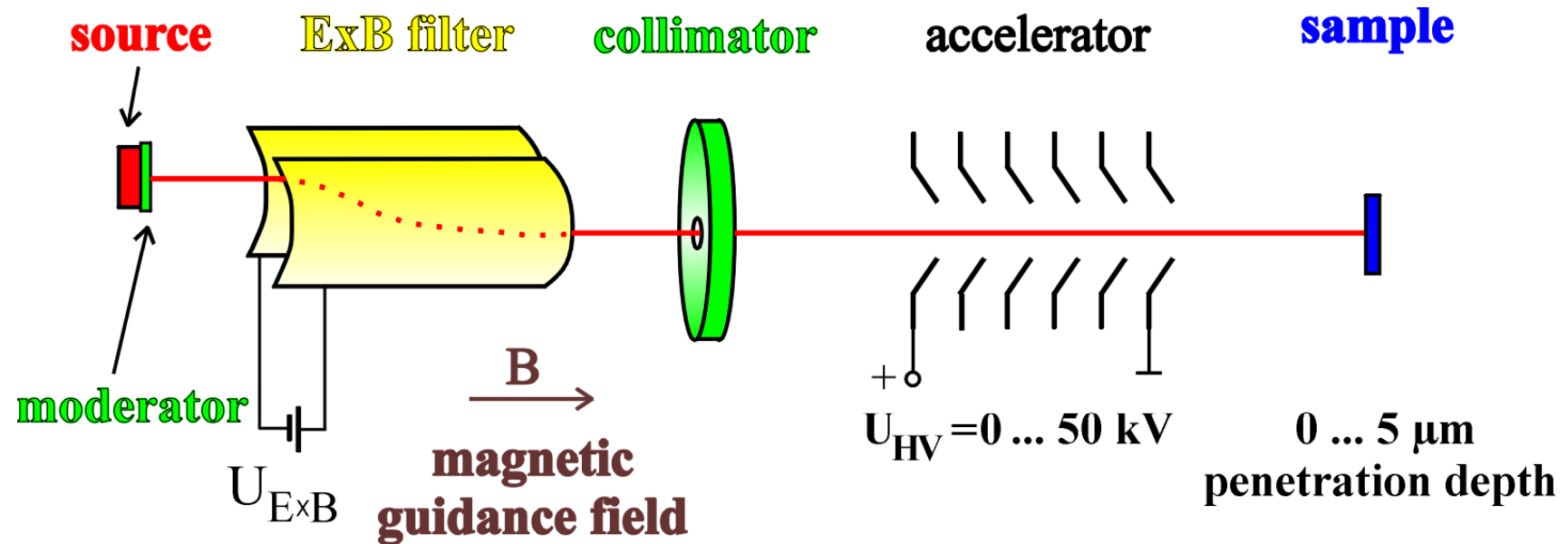
- “moderation” necessary
- provides monoenergetic positrons
- can be guided as slow-positron beam to the sample

Moderation of Positrons



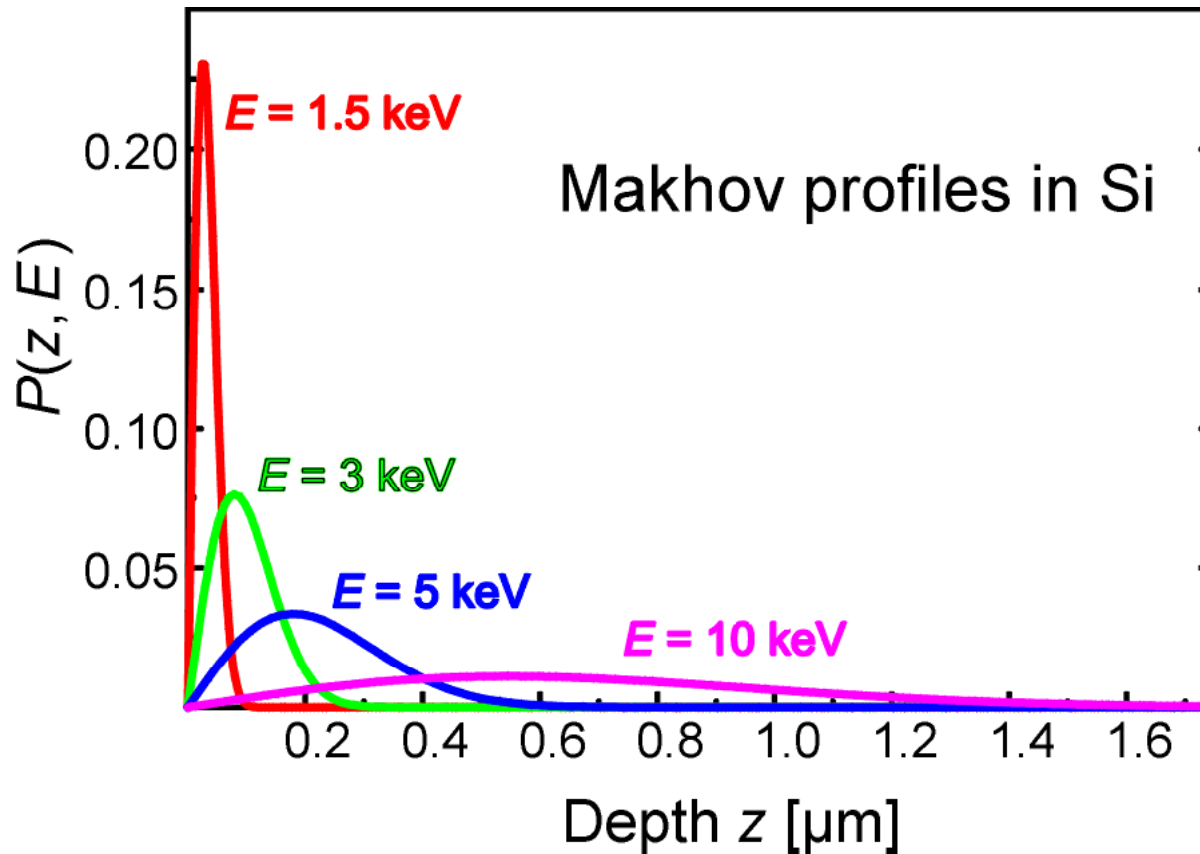
moderation efficiency: $\approx 10^{-4}$

The Positron Beam System at Halle University



- typical continuous laboratory positron beam
- defect-depth profiles can be measured by variation of acceleration voltage
- ExB filter can be replaced by a bended tube for simplicity
- no lifetime spectroscopy possible

Implantation Profiles of monoenergetic Positrons



- depth resolution is function of implantation depth
- exact implantation profiles are obtained by Monte-Carlo simulations

$$P(z, E) = \frac{mz^{m-1}}{z_0^m} \exp\left[-\left(\frac{z}{z_0}\right)^m\right] \quad \text{with} \quad z_0 = \frac{AE^r}{\rho\Gamma\left(1 + \frac{1}{m}\right)} \quad z = f(E, \rho) \quad z_0 = \text{const.} \quad m = 2$$

(Makhov, 1961)

The Positron Beam System in Halle

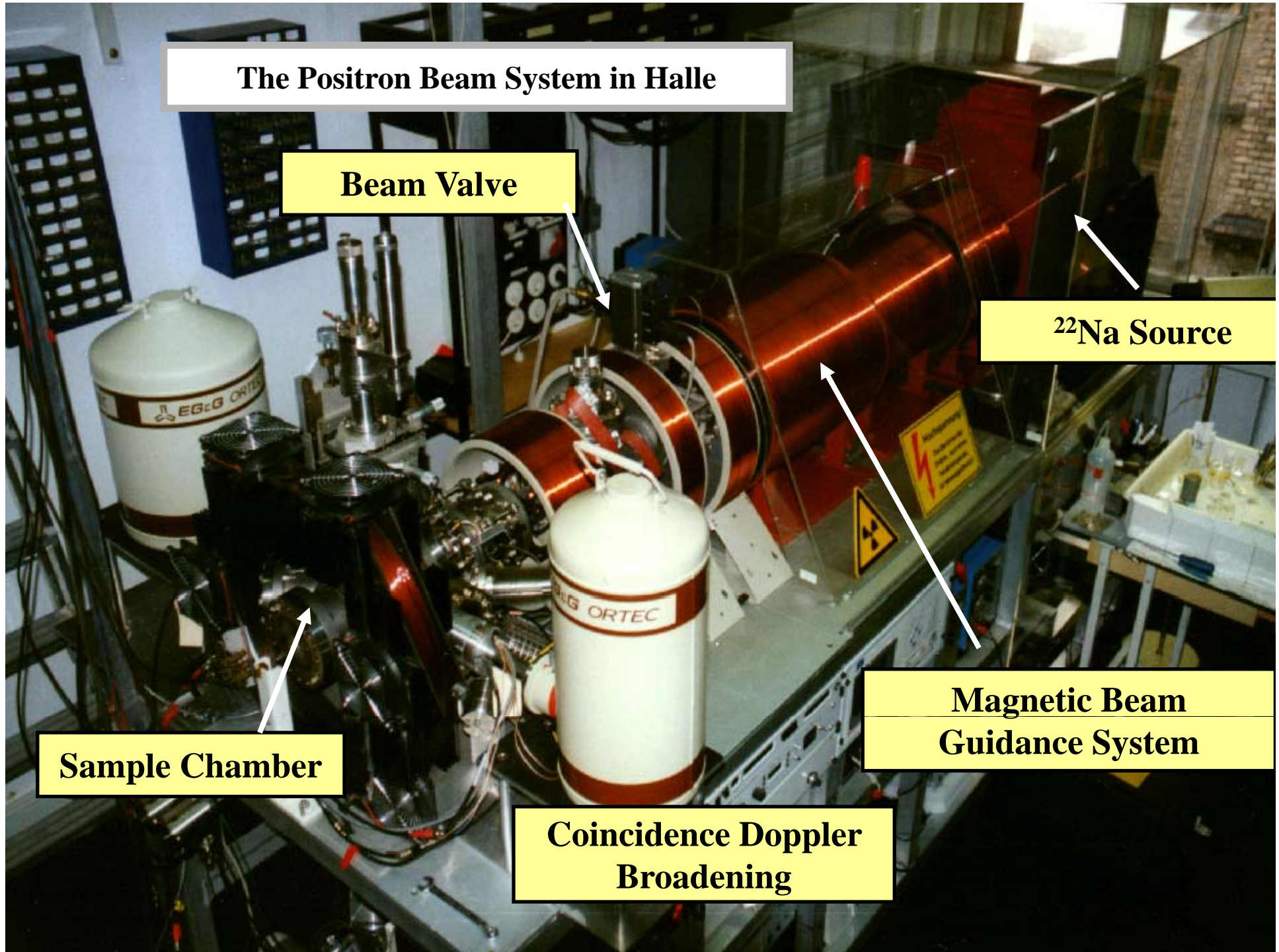
Beam Valve

^{22}Na Source

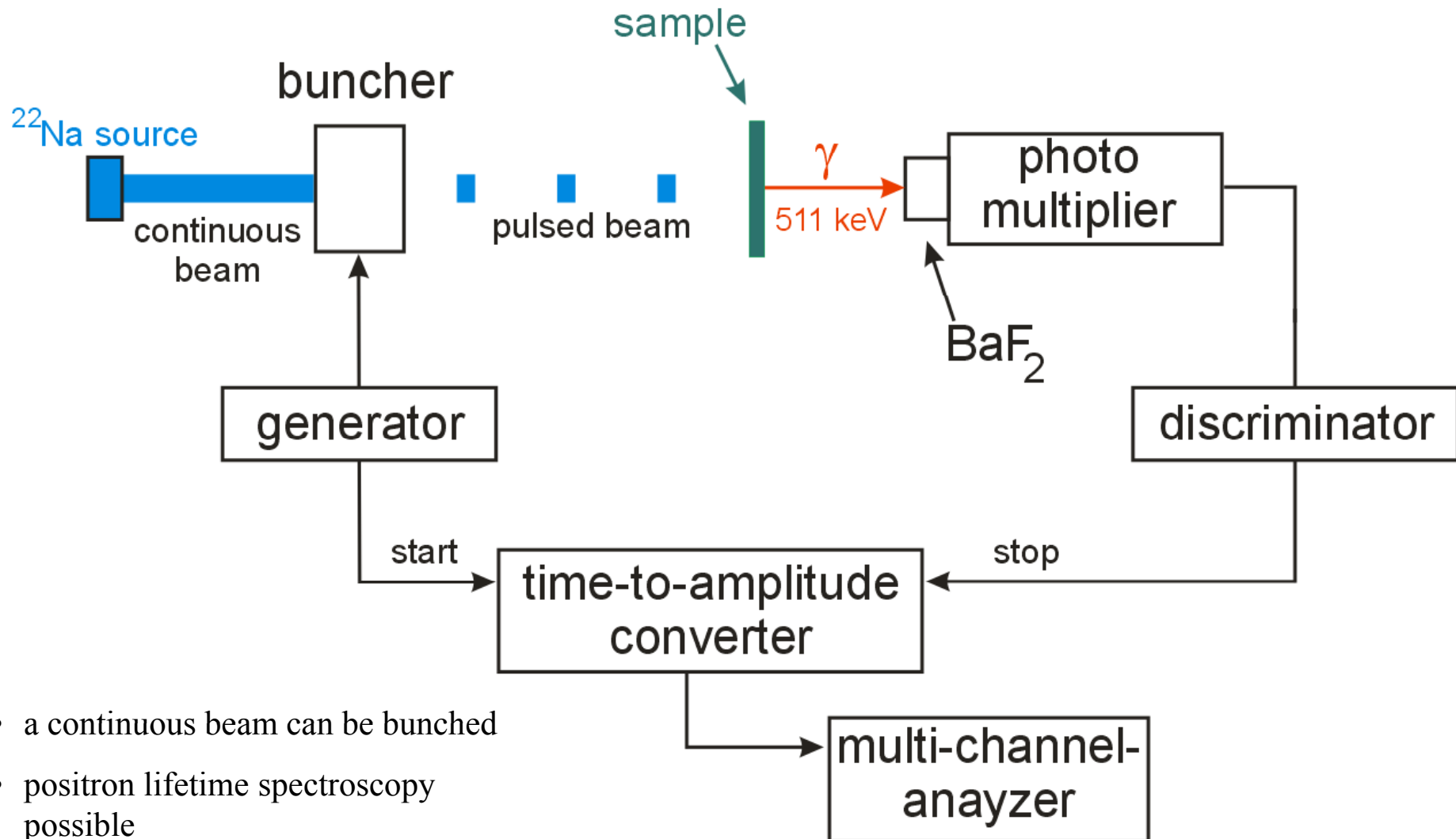
Magnetic Beam
Guidance System

Sample Chamber

Coincidence Doppler
Broadening



Positron Lifetime at a Beam System using Isotope Sources



- a continuous beam can be bunched
- positron lifetime spectroscopy possible
- e.g. PLEPS system at Garching

4. Large-scale user-dedicated Positron Facilities

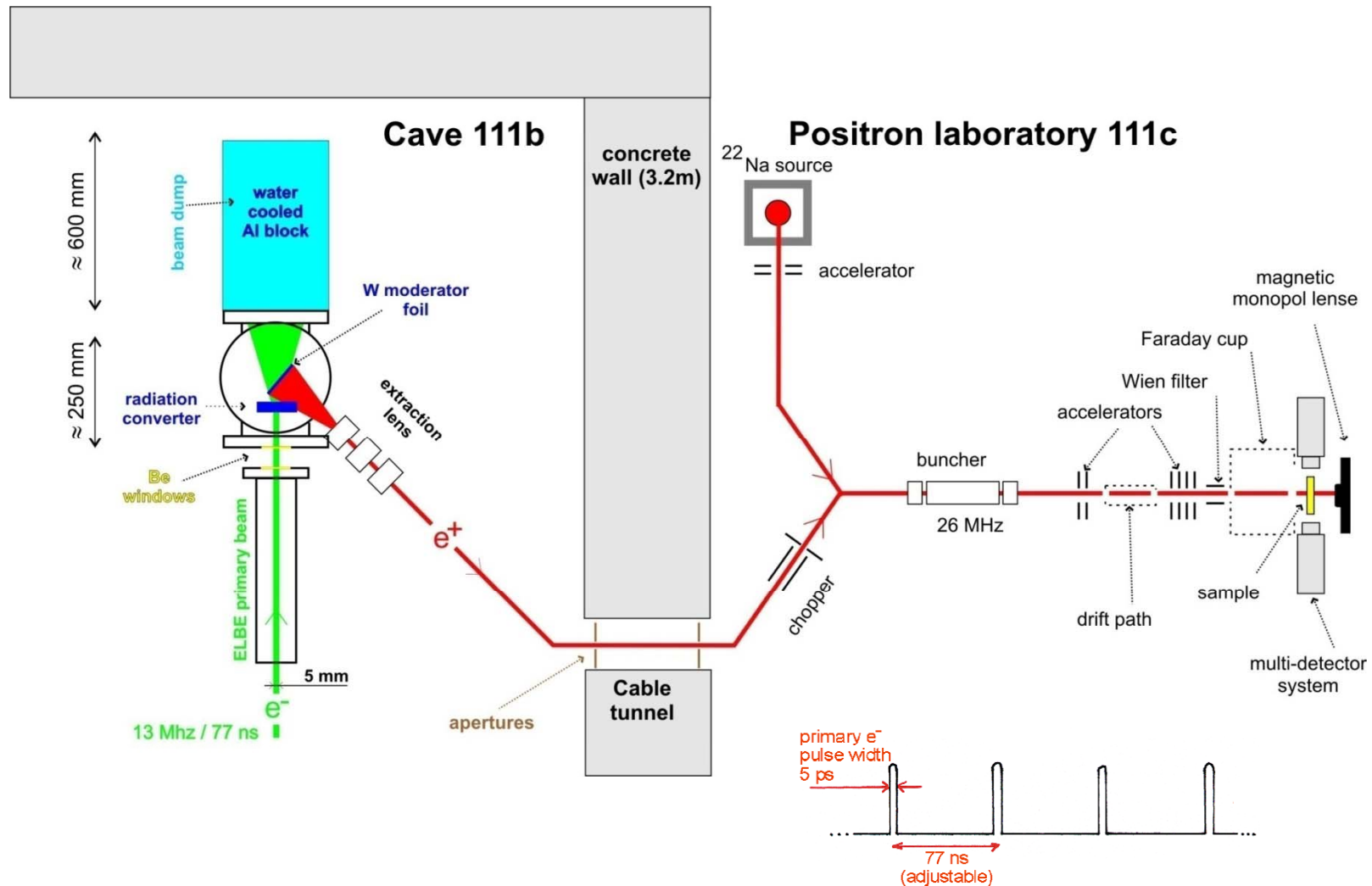
List not complete:

- **NEPOMUC at FRM-II in Garching (Munich) / Germany**
 - reactor-based; 5 beamlines: Lifetime; CDBS; PAES; Microscope (planned – see below); 1 free port for user experiments
 - 5×10^8 e⁺/s – highest slow-positron flux so far
- **Argonne Project APosS / USA**
 - Linac, 15.5 MeV, 0.1 mA, 60 Hz
 - First positrons detected – up to 3×10^9 e⁺/s expected
- **Helsinki Pulsed Positron Beam at HUT / Finland**
 - Slow-positron lifetime beam based on isotope source
- **SOPHI Project in Saclay / France – Mini LINAC for Gravity Experiment with Anti-H**
 - Tabletop commercial accelerator: 6 MeV, 300 Hz, 0.2 mA; 10 kW
 - Under construction (solid Ne moderator possible)
 - Aim 10^8 e⁺/s

- **Positron Microbeam for Transmission Positron Microscope at KEK (Japanese Collaboration)**
 - 60 μm diameter after remoderation
 - Amazing results for Ni transmission moderator (up to 20% efficiency)
- **Positron Beam at IHEP Beijing / China**
 - Many promising activities: lifetime, AMOC, CDBS
 - Isotope and LINAC-based bunched slow positron beams
- **Positron Probe Micro Analyzer (PPMA) at AIST (Tsukuba) /Japan**
 - 100 μm beam (10 μm expected); lifetime; 200...300 s/ pixel; 200ps FMHM expected
- **Australian Positron beam Facility**
 - 2 beam lines: materials science & atomic/bio/molecular
 - AMO beam line: Pulsed; rare gas moderator; 25 meV energy resolution expected
 - Materials beam line under construction; aim: bunched 200ps FWHM; 10^7 e⁺/s

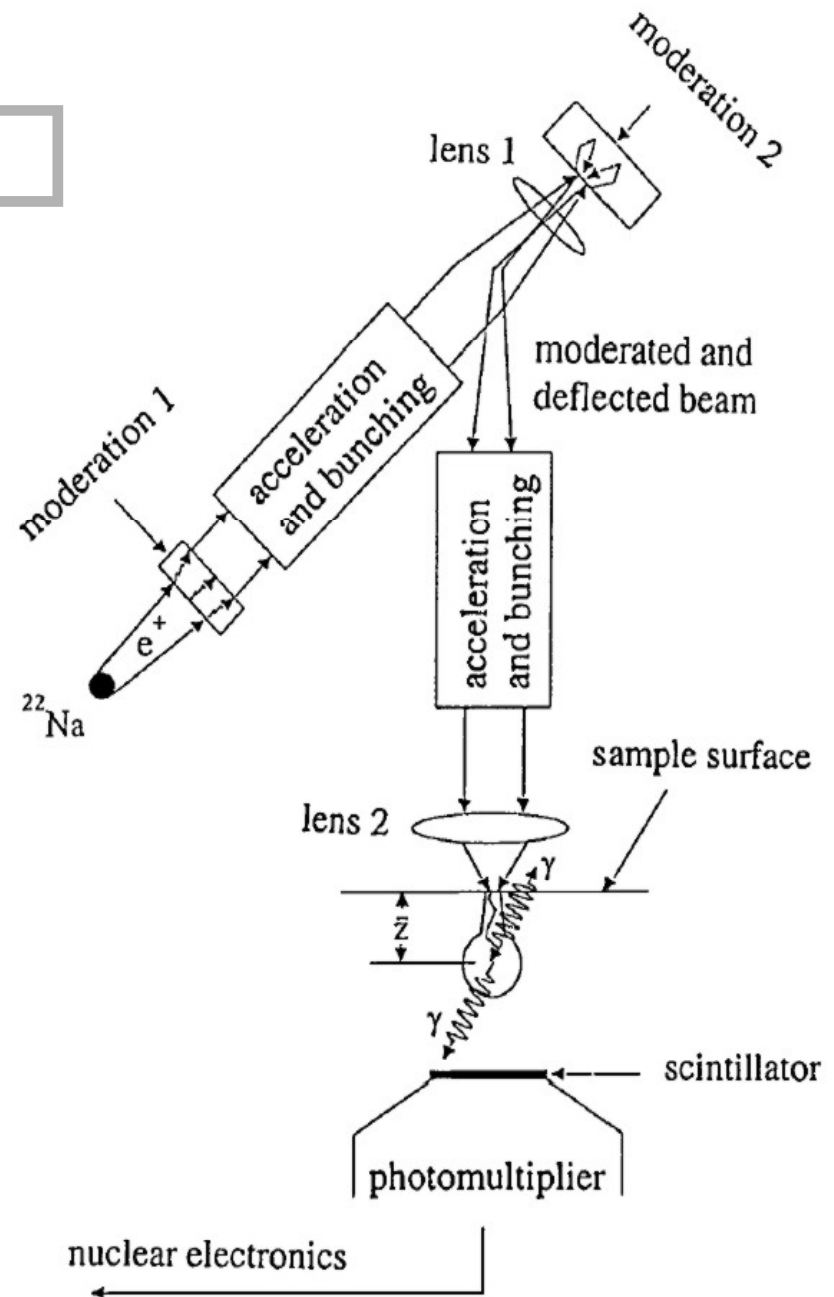
- **EPOS: ELBE Positron Source @ Research Centre Dresden Rossendorf / Germany**

- 40 MeV, 1 mA, 26 MHz repetition time in cw mode; lifetime, CDBS and AMOC with slow e^+
- Retain original time structure for simplicity and best time resolution
- Gamma-induced Positron Spectroscopy for bulky samples

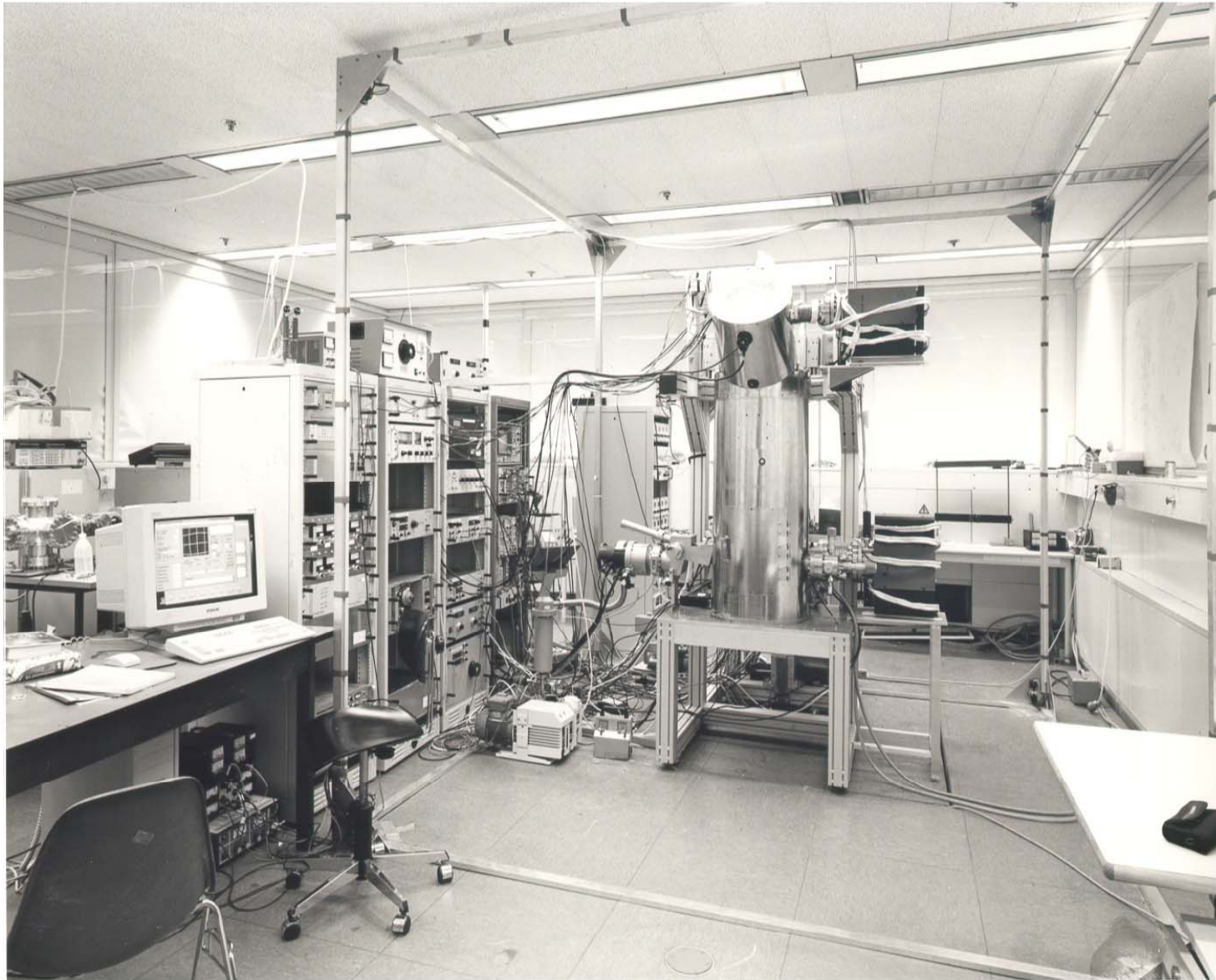


Scheme of the Munich Microscope

- moderated positrons are electrostatically focused, chopped and bunched
- second moderator stage allows focus down to about $2\ \mu\text{m}$
- positron penetration energy adjustable for depth information
- operated by ^{22}Na source
- instrument shall be adopted to the NEPOMUC source at FRM-II in the near future



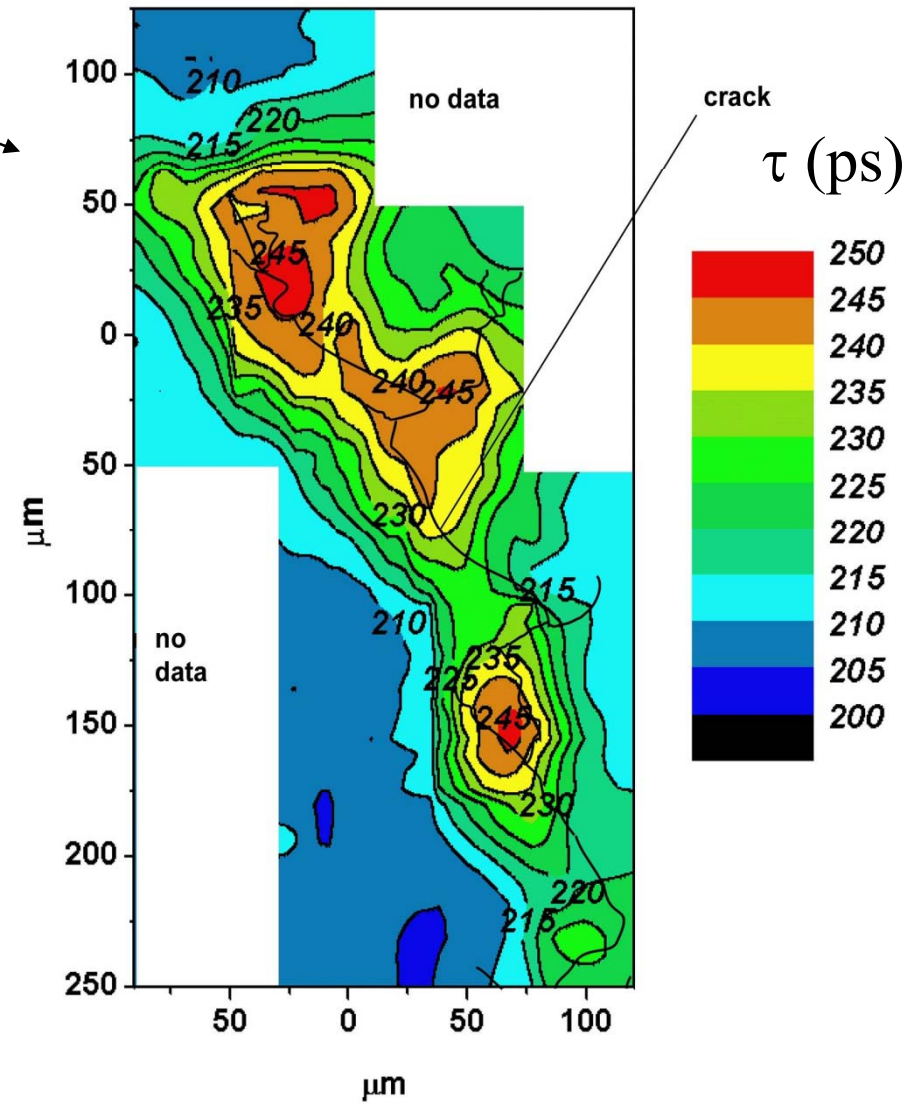
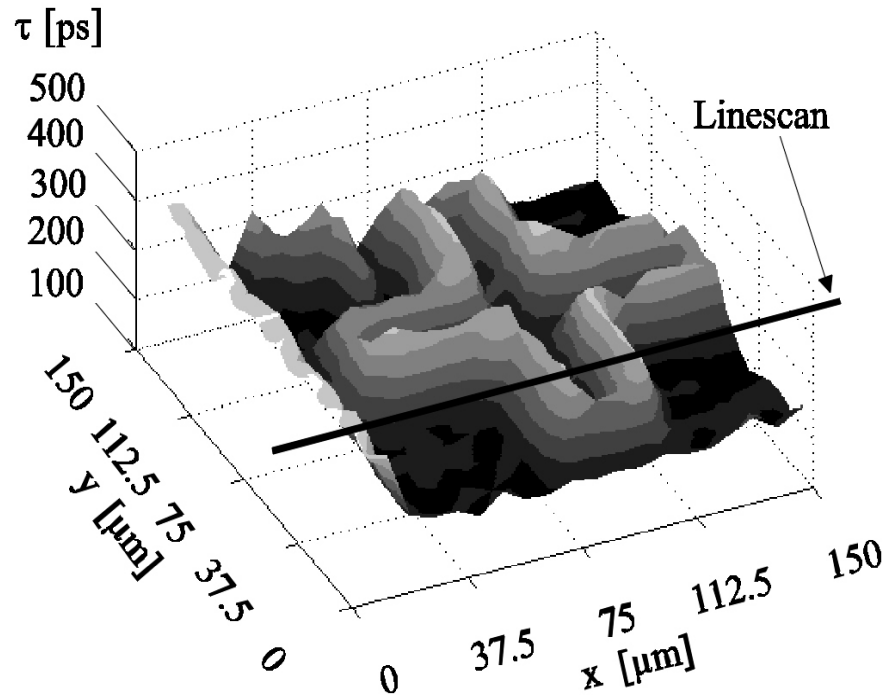
Scanning Positron Microscope in Munich



Scanning Positron Microscope in Munich

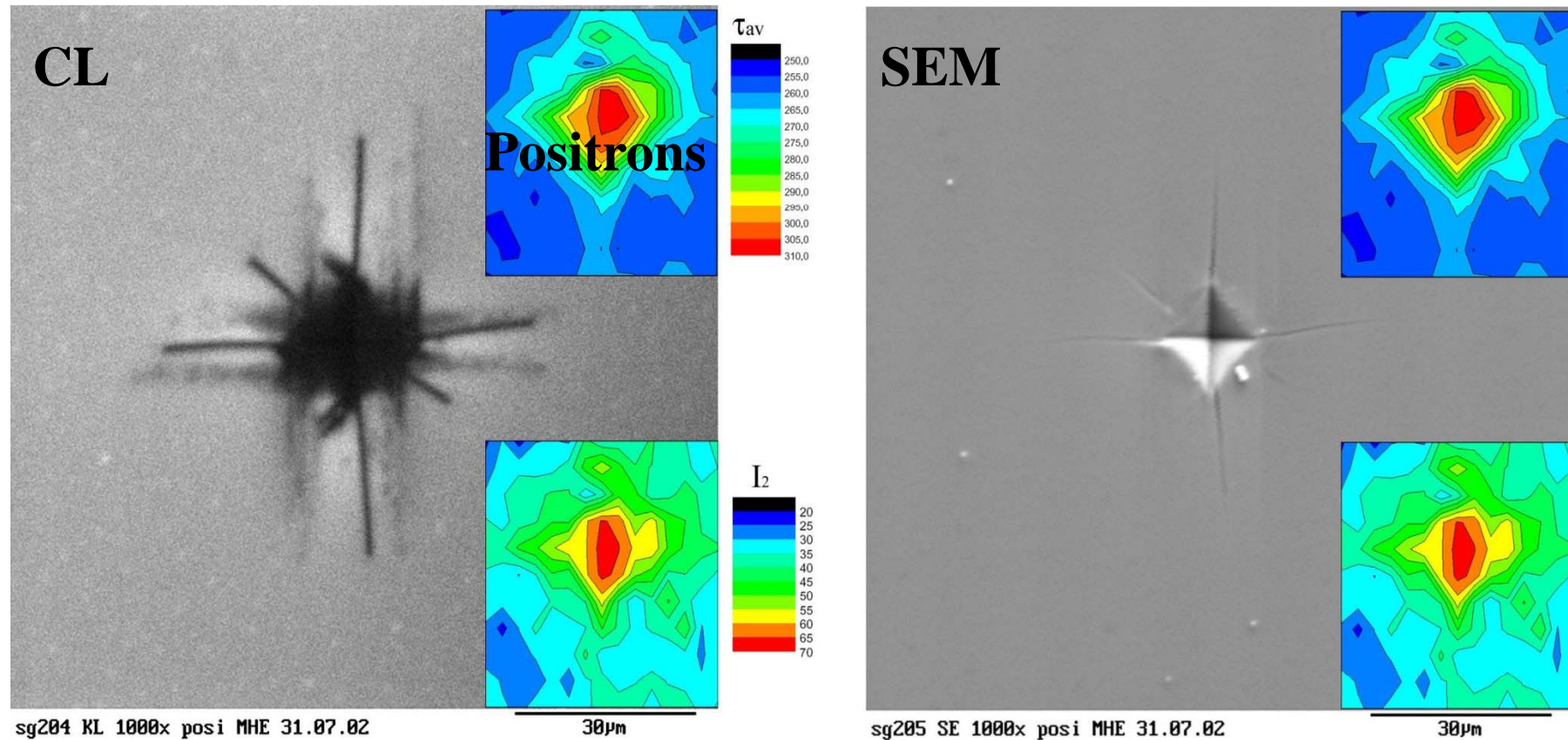
defects near a crack in fatigued Cu

Semiconductor test structure



Micro-hardness indentation in GaAs

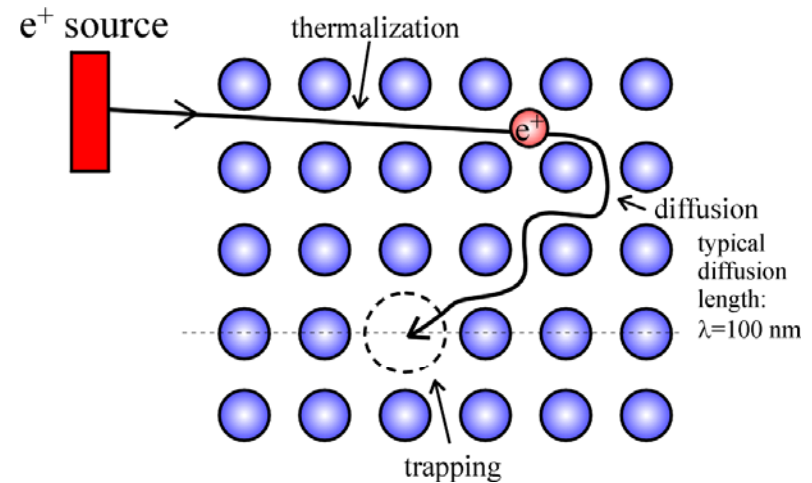
- Comparison of scanning electron microscopy (SEM), cathodoluminescence (CL) and Munich Positron Scanning Microscope
- problem here at the moment: intensity
- microscope will be transferred to NEPOMUC source at Garching Research Reactor



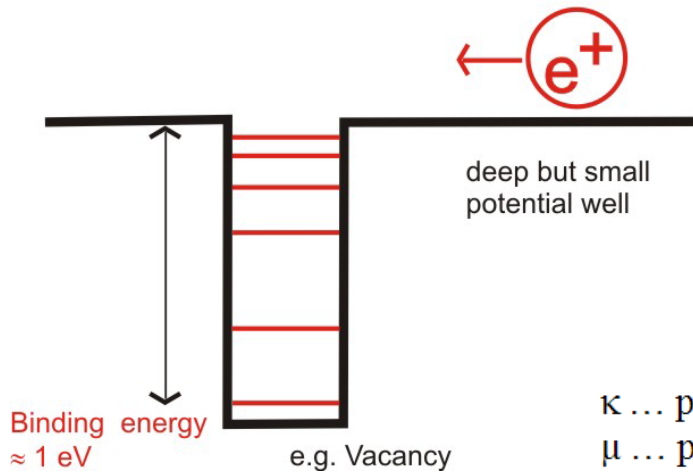
(Krause-Rehberg et al., 2002)

5. Defect Spectroscopy using Positrons

- Positrons are trapped by lattice defects
- trapping can be limited by
 - the diffusion to the defect
 - or by the trapping process itself, i.e. by the energy release during transition into bound state
- trapping rate κ is proportional to defect density C

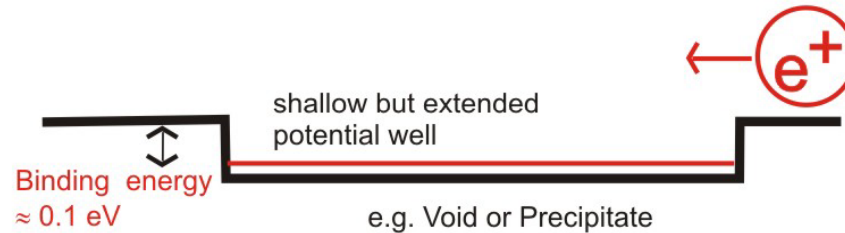


Transition-limited Trapping



$$\kappa = \mu \cdot C$$

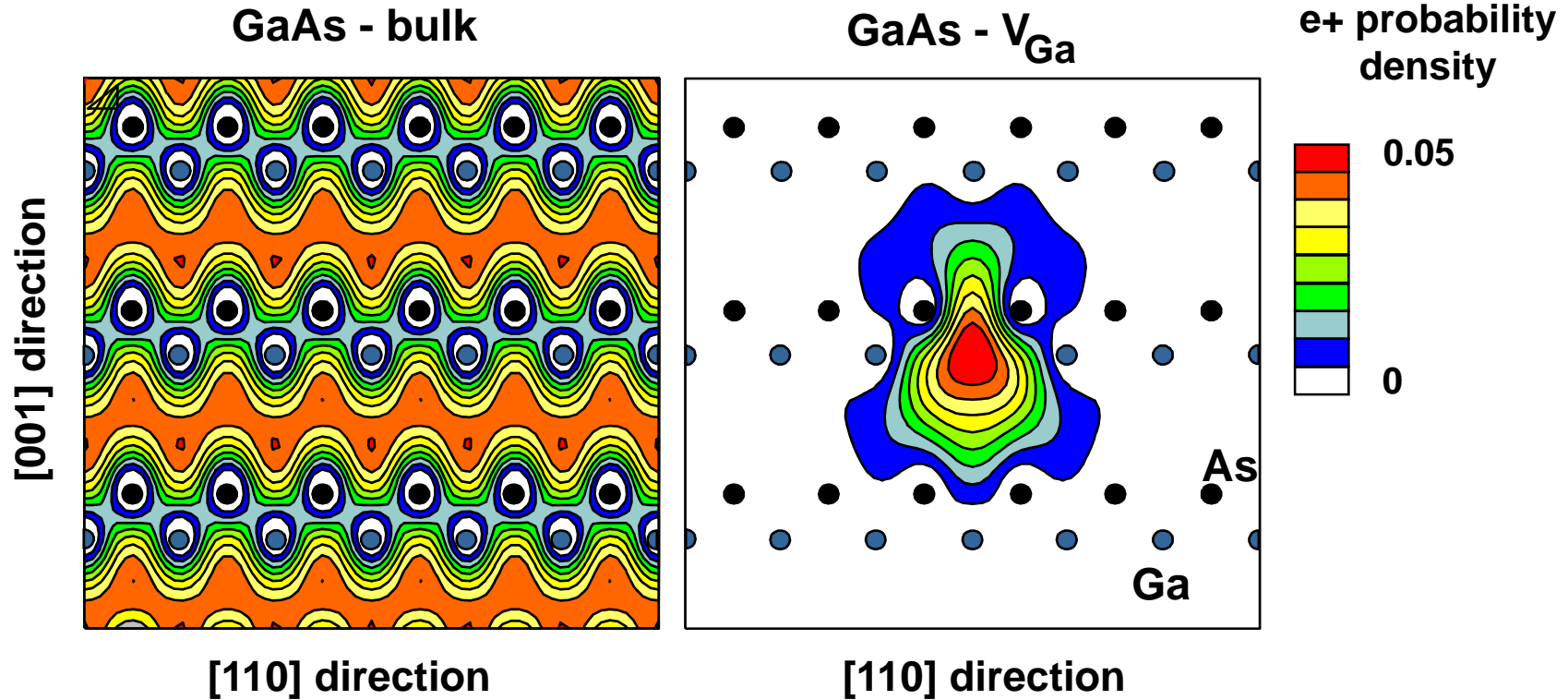
Diffusion-limited Trapping



$$\kappa = 4\pi r_d D_+ C$$

- κ ... positron trapping rate
- μ ... positron trapping coefficient
- C ... defect density
- r_d ... radius of defect
- D_+ ... positron diffusion coefficient

Localization of the positron wave-function: GaAs bulk vs. V_{Ga}



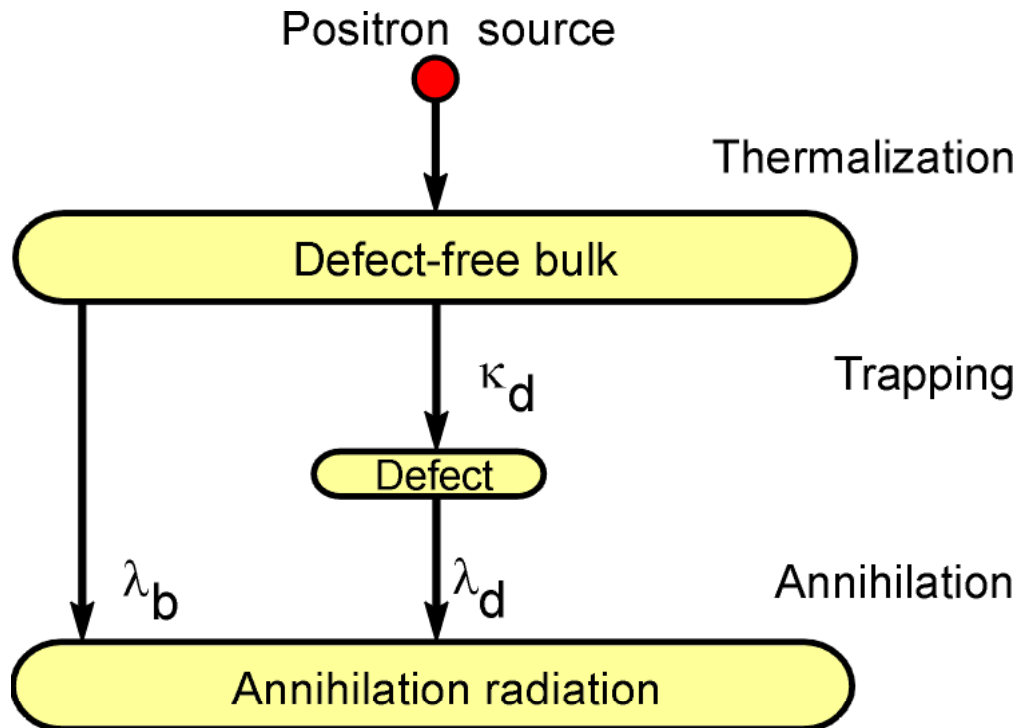
$$\tau_{\text{bulk}} = 230 \text{ ps}$$

$$\tau_{\text{vacancy}} = 260 \text{ ps}$$

$$1/\tau = \lambda \sim \int dr n_{\text{electron}} n_{\text{positron}} \gamma(n(r))$$

τ ...lifetime
 λ ...annihilation rate

Trapping Model: Positron Trapping in a Single Defect Type



$$\frac{dn_b(t)}{dt} = -(\lambda_b + \kappa_d)n_b(t)$$

$$\frac{dn_d(t)}{dt} = -\lambda_d n_d(t) + \kappa_d n_b(t)$$

solution: decay spectrum

$$D(t) = I_1 \exp\left(-\frac{t}{\tau_1}\right) + I_2 \exp\left(-\frac{t}{\tau_2}\right)$$

abbreviations:

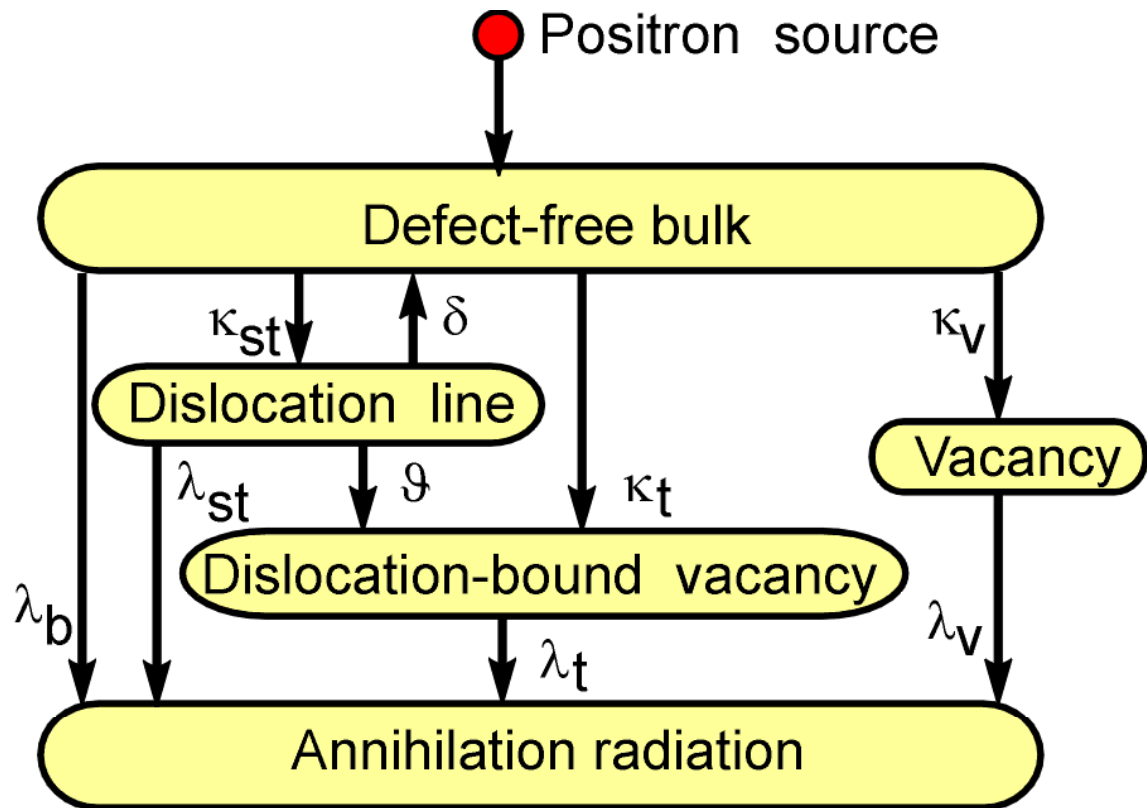
$$\tau_1 = \frac{1}{\lambda_b + \kappa_d}, \quad \tau_2 = \frac{1}{\lambda_d}$$

$$I_1 = 1 - I_2, \quad I_2 = \frac{\kappa_d}{\lambda_b - \lambda_d + \kappa_d}$$

The t_i and I_i are measured \Rightarrow κ is obtained:

$$\boxed{\kappa_d = \mu C_d} = \frac{I_2}{I_1} \left(\frac{1}{\tau_b} - \frac{1}{\tau_d} \right)$$

Complex Example: Positron Trapping in a Dislocation



the dislocation line (shallow trap) acts as a “funnel” for the trapping in deep traps

b ... bulk

v ... vacancy

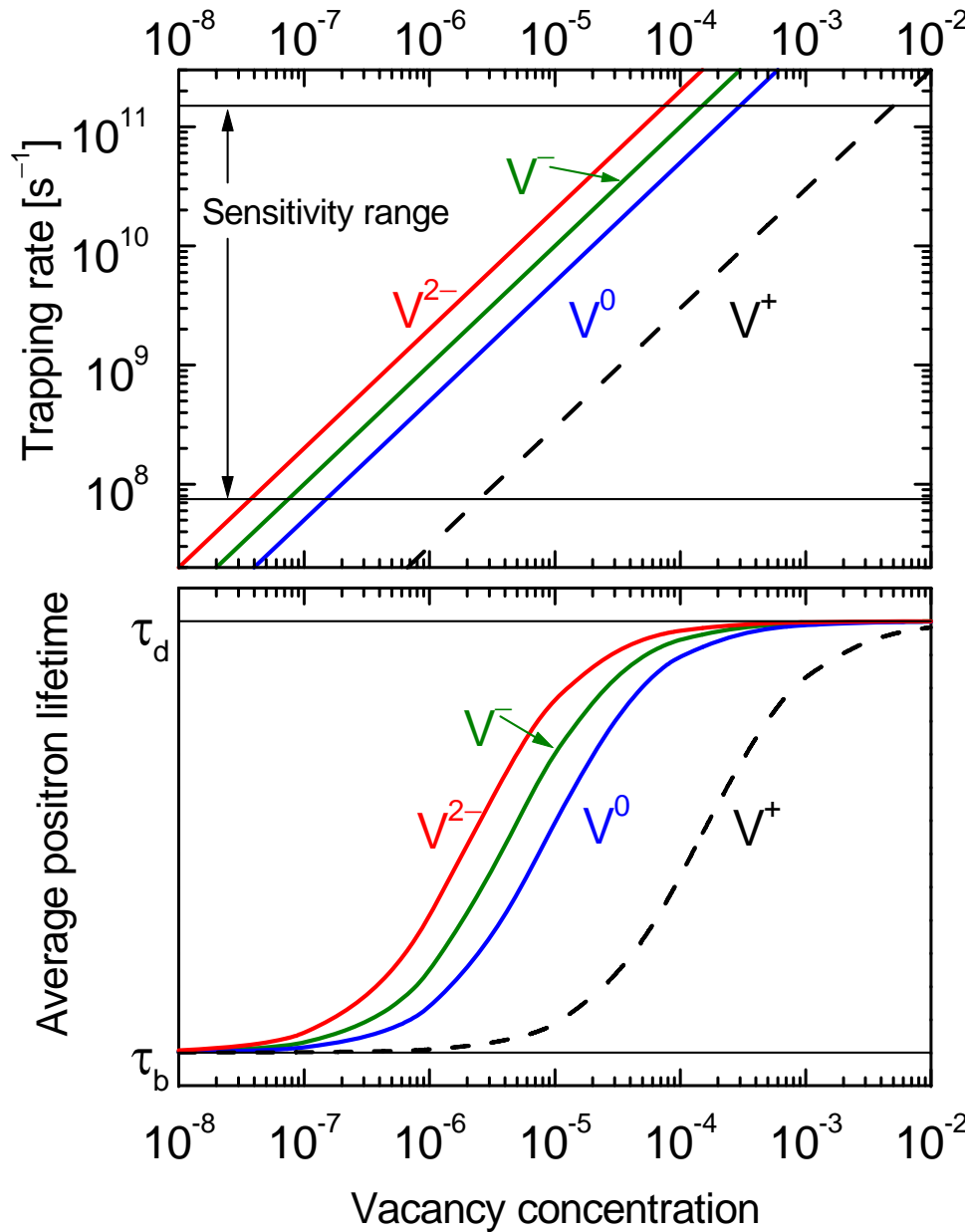
t ... deep trap

st ... shallow trap

λ_i ... annihilation rates κ_i, ϑ ... trapping rates

δ ... detrapping (escape) rate

Determination of absolute Defect Densities



- the trapping coefficient μ must be determined by an independent method

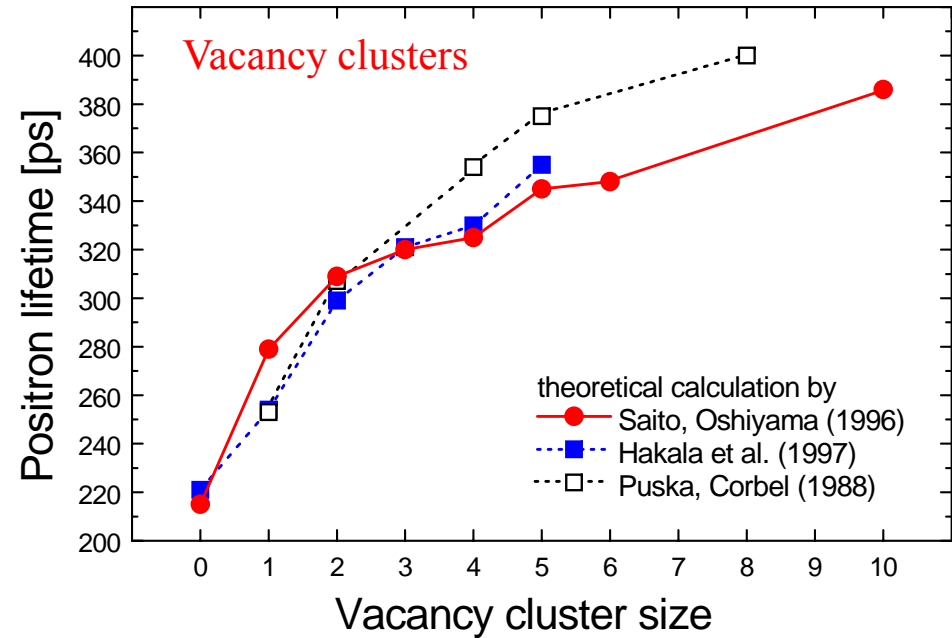
$$\kappa = \mu \cdot C$$

- positron trapping may be strongly temperature-dependent: $\mu = f(T)$

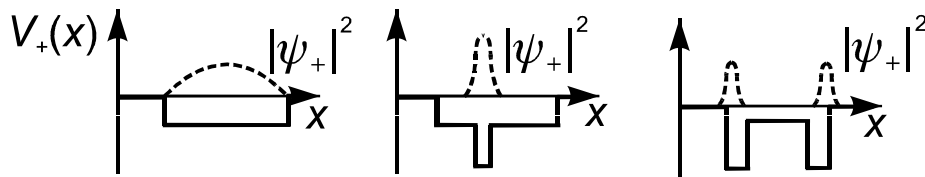
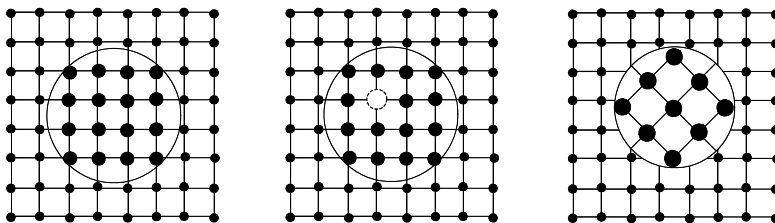
defect in Si_{300K}	μ ($10^{15} s^{-1}$)
V^-	1
V^{2-}	2
V^0	0.5
V^+	< 0.1
dislocation	$1 cm^2 s^{-1}$
vacancy cluster	$n \cdot \mu_{1V}$

What defects can be studied in crystalline solids?

- Defects with open-volume
 - vacancies
 - vacancy clusters / voids
 - dislocations
 - grain boundaries (for grains $< 1\mu\text{m}$)
 - surface (outer and inner)
- Defects without open-volume
 - Precipitates
 - negatively charged defects /shallow traps (e.g. ionized acceptors in semiconductors)

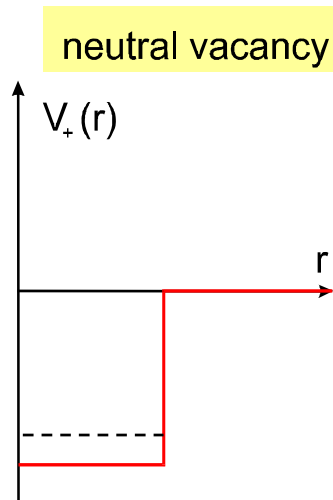


Positron trapping in / at Precipitates



6. Peculiarities of Positron Annihilation in Semiconductors

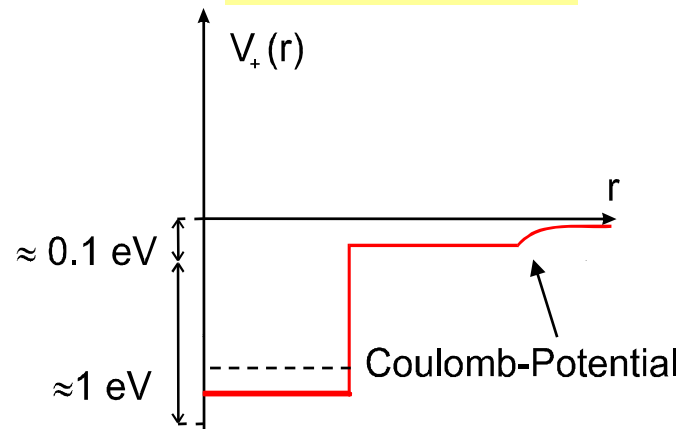
Positron trapping at vacancies



- deep, localized states due to missing ion core, no detrapping
- lifetime $> \tau_{\text{bulk}}$, Doppler broadening decreases

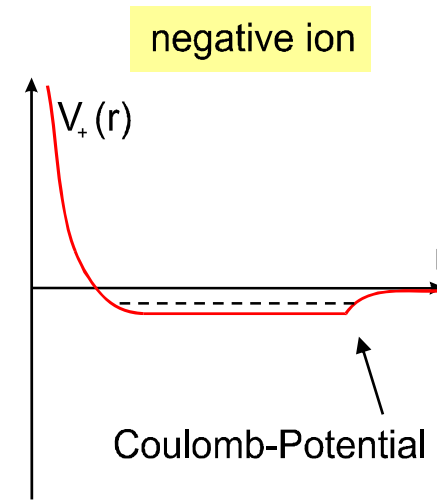
trapping independent
of temperature

negative vacancy



trapping increases with
decreasing temperature

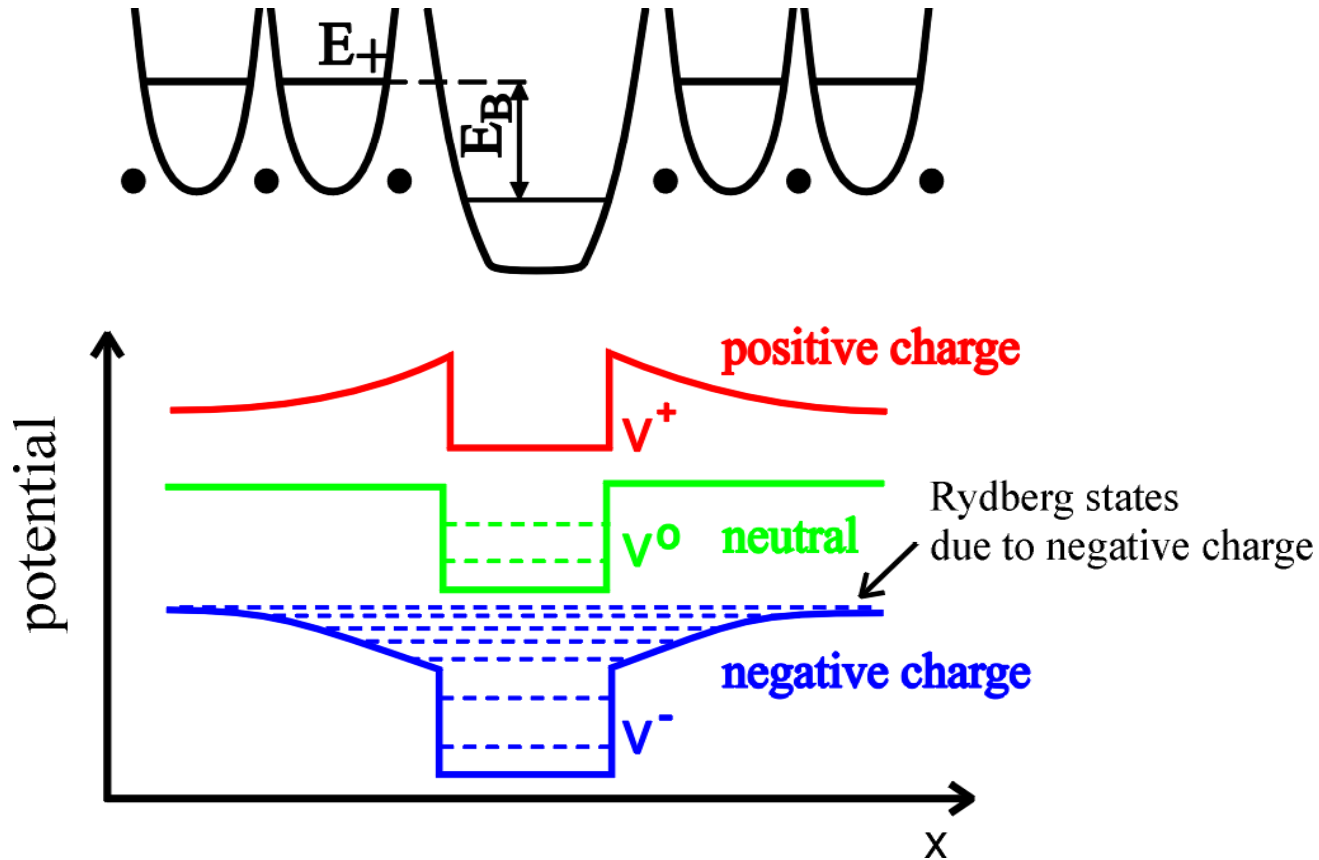
... at shallow traps



- shallow, delocalized state
- thermal detrapping at 300 K

lifetime = τ_{bulk}

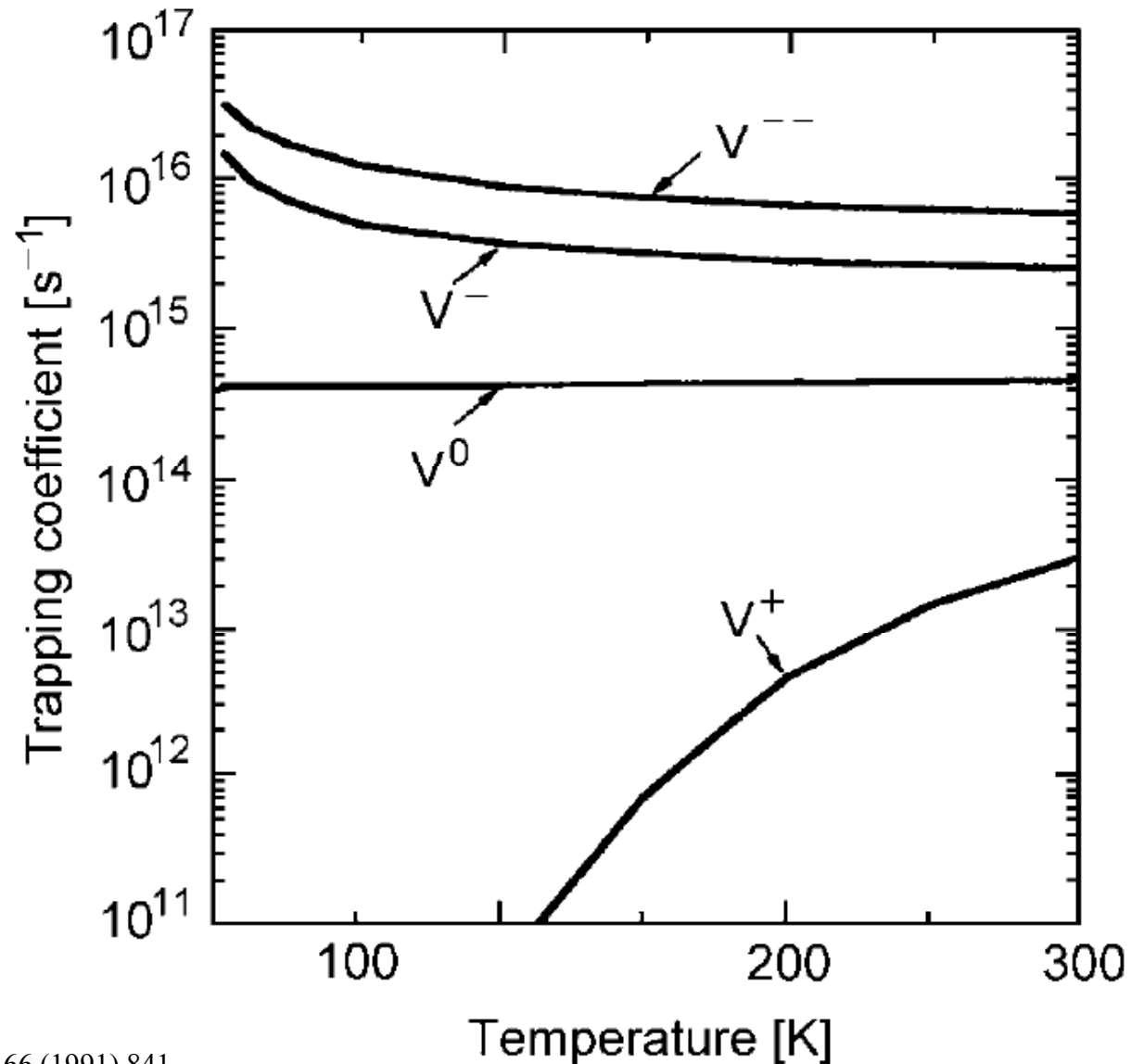
Positron Trapping Potential



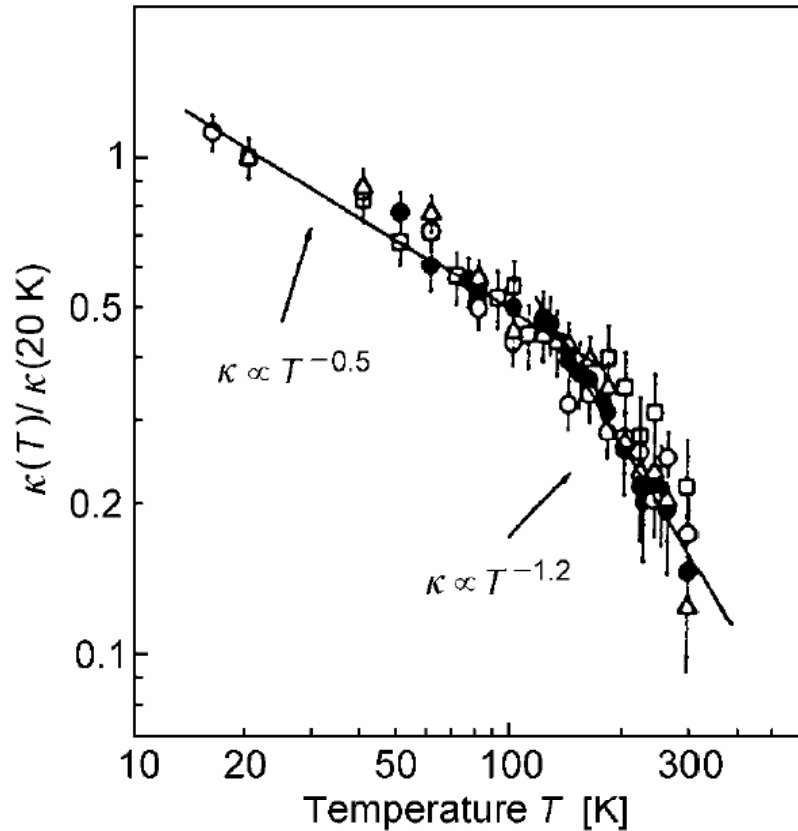
- Attractive potential mainly due to missing ion (repelling core is absent)
- in semiconductors: additional Coulomb tails (rather extended)
- no positron trapping by positive vacancies (positrons are repelled)
- temperature dependence expected

Different sensitivity for differently charged vacancies

- defects in semiconductors can be charged
- large influence on trapping behavior especially at low temperatures
- trapping coefficient is function of T
- positive vacancies repel positrons



Negative vacancies show temperature-dependent positron trapping



positron trapping in negatively charged Ga vacancies in SI-GaAs

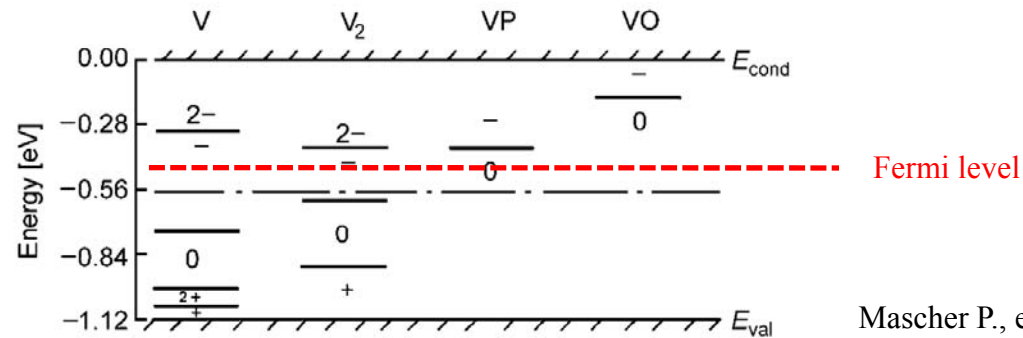
- temperature dependence of positron trapping is rather complex

$$\kappa = \frac{\vartheta_R \rho_v \kappa_{R0} T^{-1/2}}{\vartheta_R \rho_v + \kappa_{R0} \left(\frac{m^* k_B}{2\pi \hbar^2} \right)^{3/2} T \exp\left(-\frac{E_R}{k_B T} \right)}$$

- low temperature: $\kappa \sim T^{-0.5}$ due to diffusion limitation in Rydberg states
- higher T: stronger temperature dependence due to thermal detrapping from Rydberg state

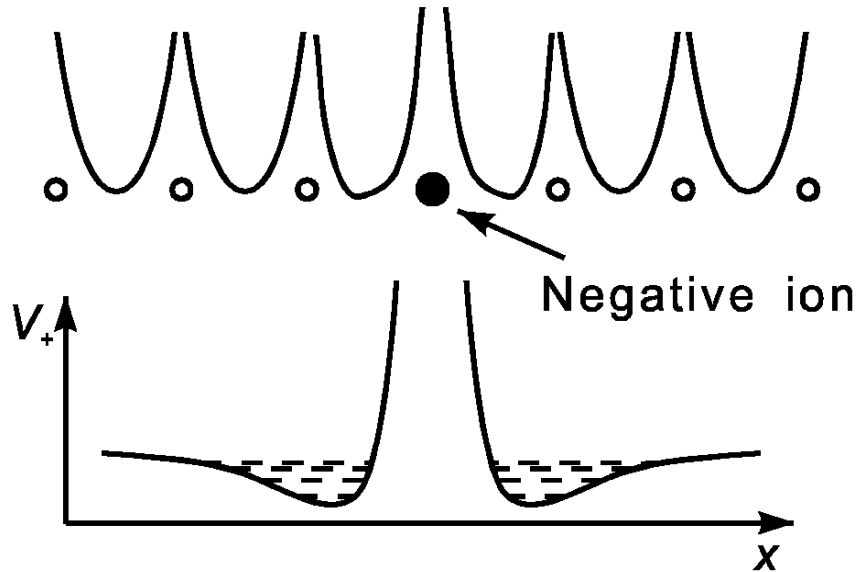
Fermi-level Dependence of Charge State

- charge state of defect depend on position of Fermi level



- in the above example: mono- and di-vacancies carry a single negative charge while the vacancy-phosphorus pair and the A center (vacancy-oxygen pair) remain neutral
- Fermi level can be shifted by
 - temperature change
 - doping (impurity in-diffusion)
 - defect generation (e.g. by irradiation)
 - light illumination (wavelength dependence)

Negative ions act as shallow positron traps



- at low T: negatively charged defects without open volume may trap positrons
- “shallow” due to small positron binding energy
- annihilation parameters close to bulk parameters
- thermally stimulated detrapping δ can be described by:

$$\delta = \frac{\kappa}{\rho_{\text{st}}} \left(\frac{m^* k_B T}{2\pi \hbar^2} \right)^{3/2} \exp\left(-\frac{E_{\text{st}}}{k_B T}\right)$$

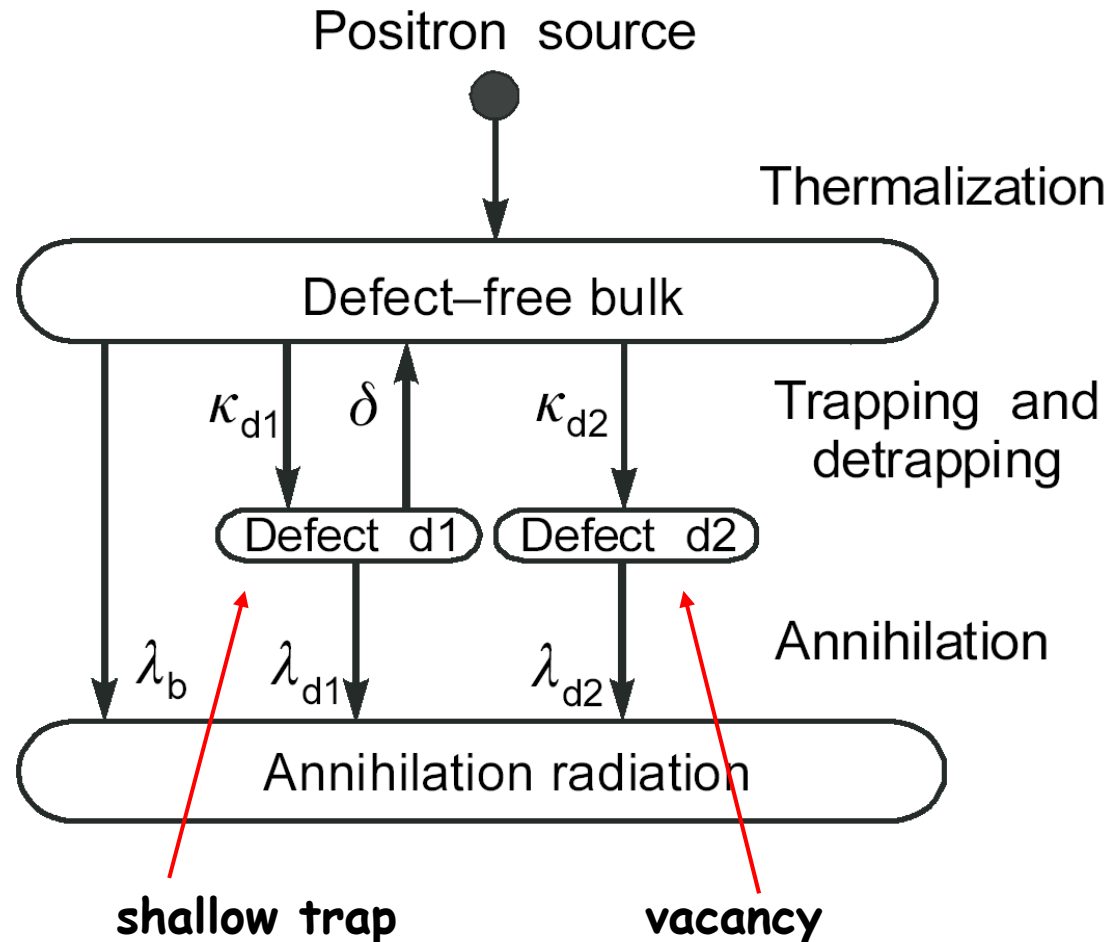
Examples:

- negatively charged point defects without open volume
- ionized acceptors
- negatively charged antisite defects
- vacancy defects with very small open volume: the A center in Si (Vac-O-complex)

κ ... trapping rate of shallow traps
 ρ_{st} ... density of shallow traps
 E_{st} ... positron binding energy to shallow traps

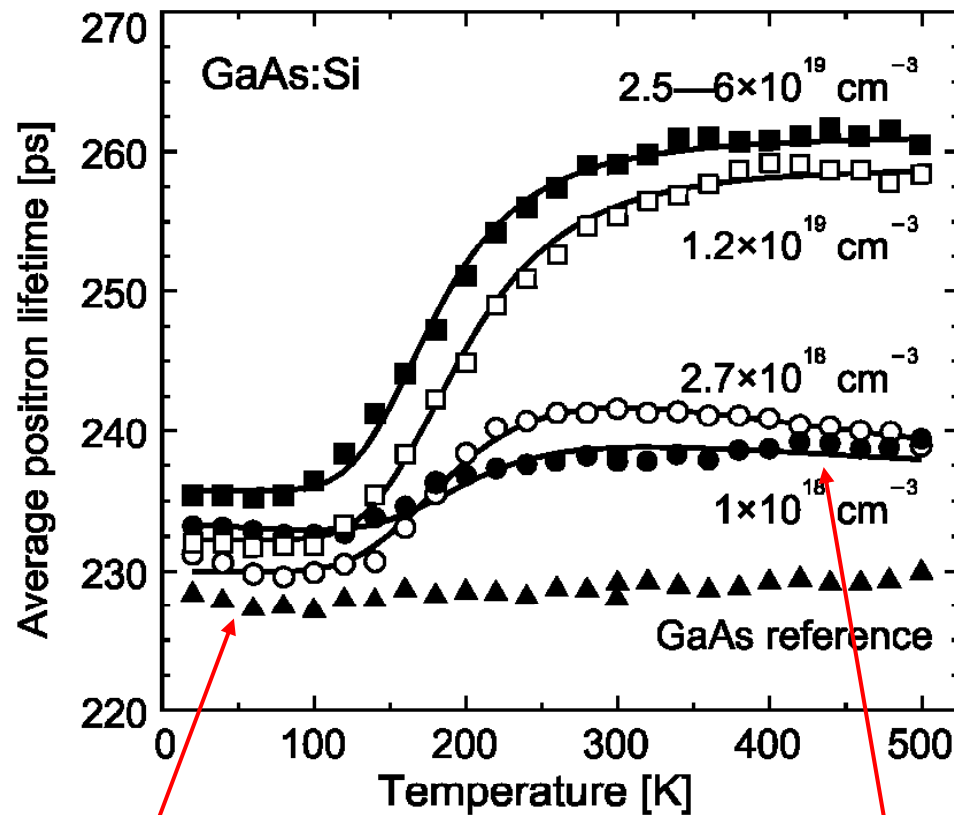
M. Manninen, R.M. Nieminen:
 Appl. Phys. A 26 (1981) 93

Trapping model of shallow Positron Traps



- positron trapping model gets more complex
- however: trapping at shallow traps can usually be avoided at high temperatures due to small positron binding energy
- shallow traps can only be seen in lifetime spectra when open-volume defects are present (e.g. vacancies)
- this is because positron defect lifetime is almost equal to bulk value

Effect of shallow positron traps in lifetime spectra



- temperature dependence is characterized by **competing trapping** by vacancies and shallow traps
- in GaAs:Si we observe $V_{\text{Ga}}\text{-Si}_{\text{Ga}}$ complexes at high temperatures
- and Si_{Ga}^- donors at low T in addition (shallow traps) at low temperatures
- when vacancies and shallow traps appear at the same time, lifetime spectra decomposition becomes very difficult or rather impossible

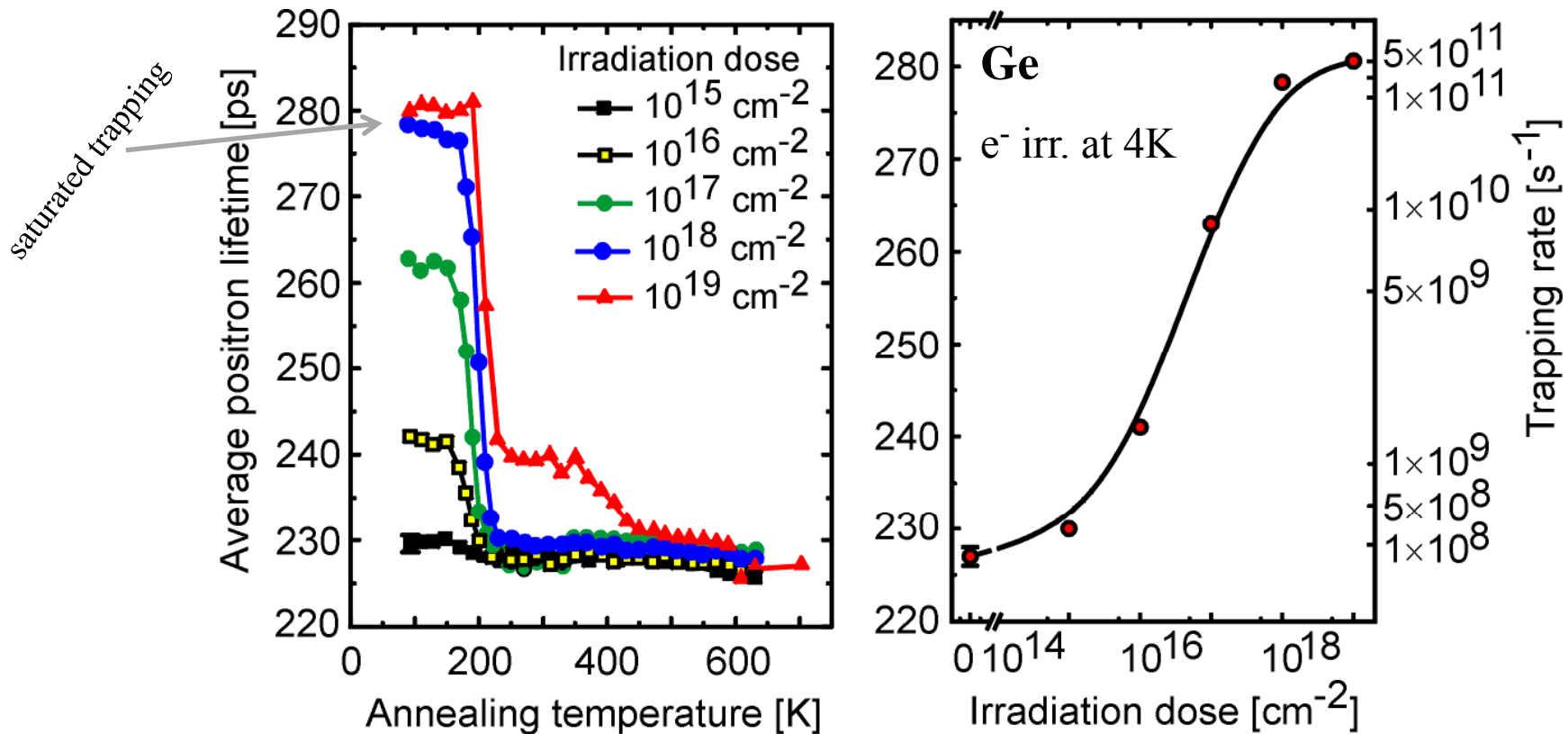
competing trapping centres at low T
shallow positron traps (Si_{Ga}^-)

trapping by vacancies
at elevated temperatures ($V_{\text{Ga}}\text{-Si}_{\text{Ga}}$)

7. Defect Studies in Semiconductors:

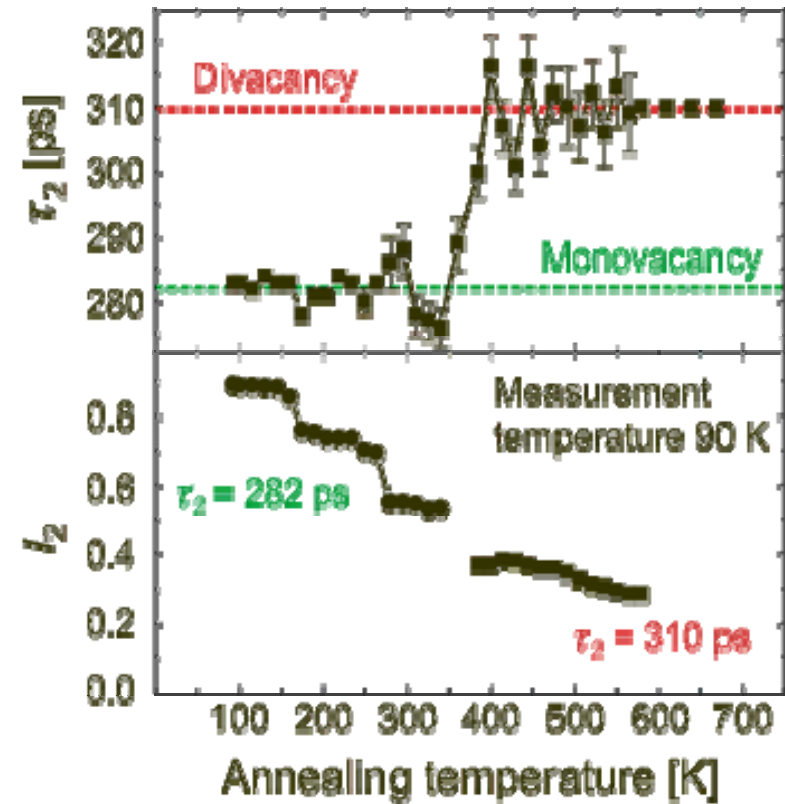
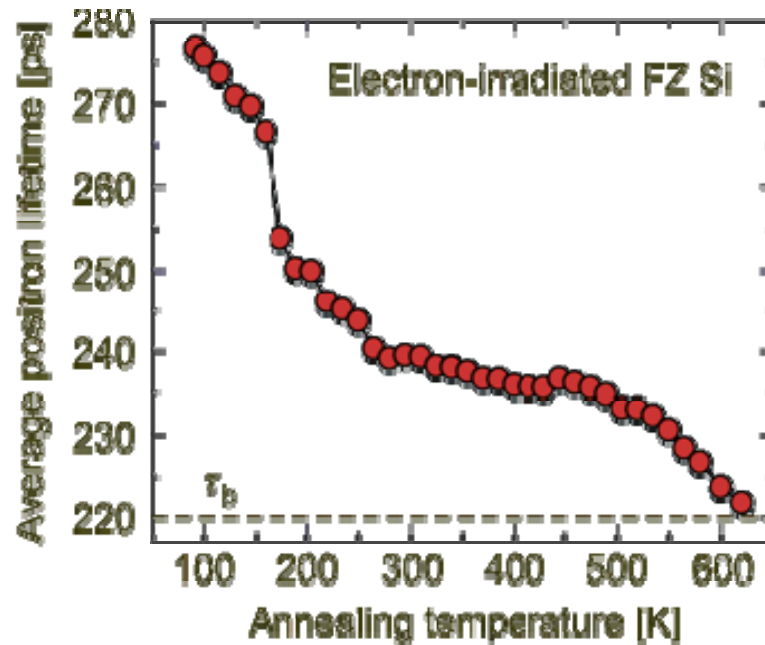
7.1. Example: Electron Irradiation of elemental semiconductors

- electron irradiation generates Frenkel pairs (vacancy-interstitial pairs)
- vacancy annealing and defect reactions may be studied easily by positrons
- **Example:** electron irradiation at 4K by 2 MeV electrons of different doses
- annealing experiment started at 90 K: clear annealing stage at 200K
- very high dose: formation of divacancies



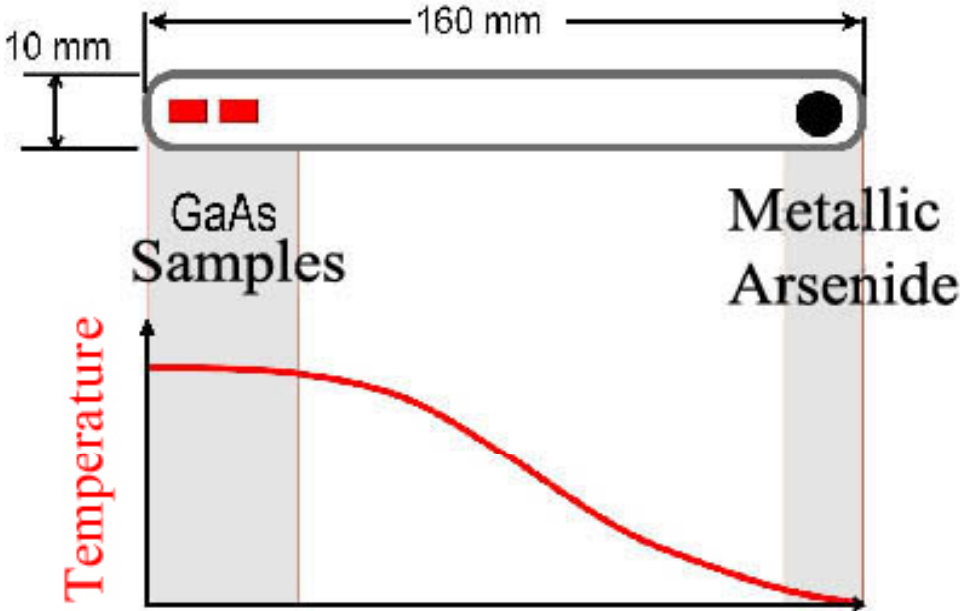
Electron irradiation of Si

- low-temperature electron irradiation was performed at 4K ($E_{e^-} = 2$ MeV)
- annealing stage of monovacancies at about 170 K
- moving V_{Si} partly form divacancies
- divacancies anneal at about 550...650 K



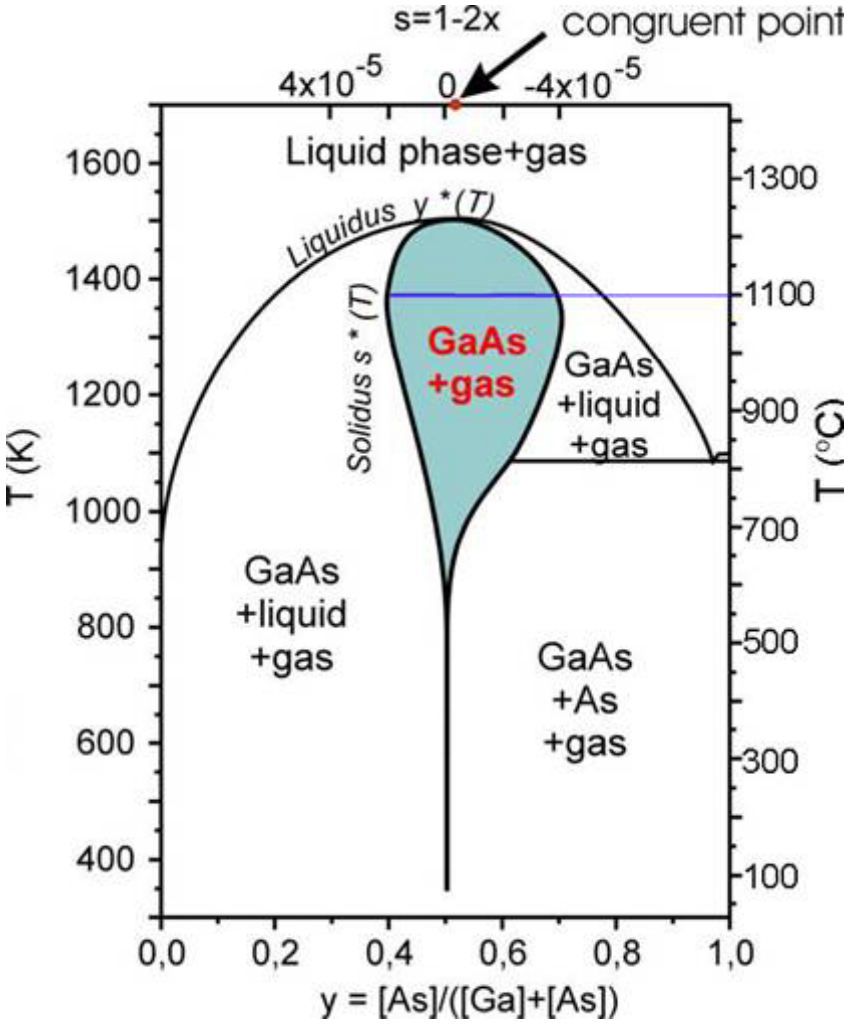
7.2. GaAs: annealing under defined As-partial pressure

- two-zone-furnace: Control of sample temperature and As partial pressure allows to navigate freely in phase diagram (existence area of compound)



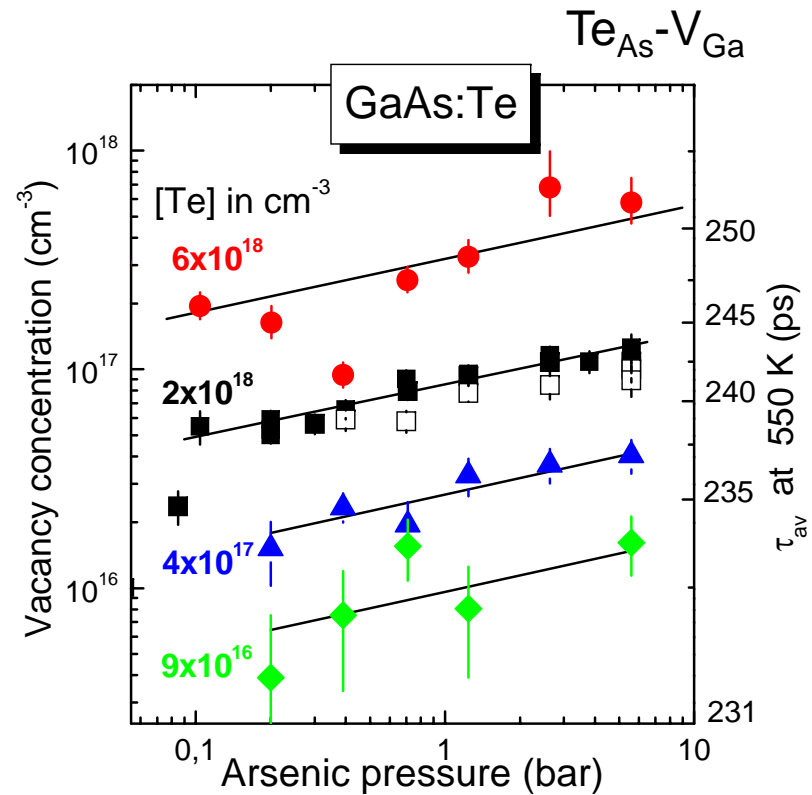
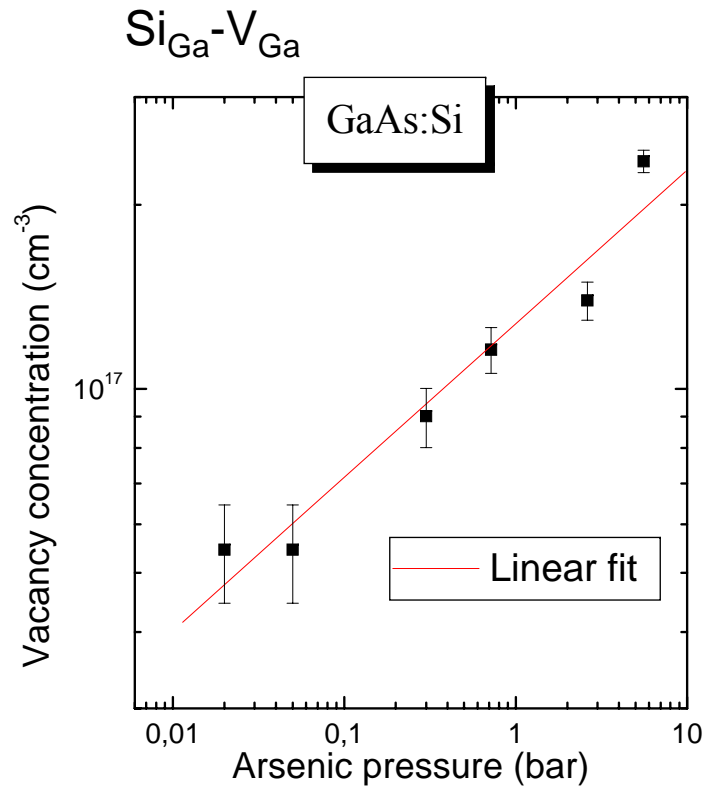
$T_{\text{sample}}: 1100^{\circ}\text{C}$

T_{As} : determines As-partial pressure

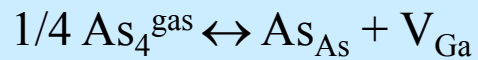


H. Wenzl et al., J. Cryst. Growth 109, 191 (1991).

GaAs: Annealing under defined As pressure



Thermodynamic reaction:



Mass action law:

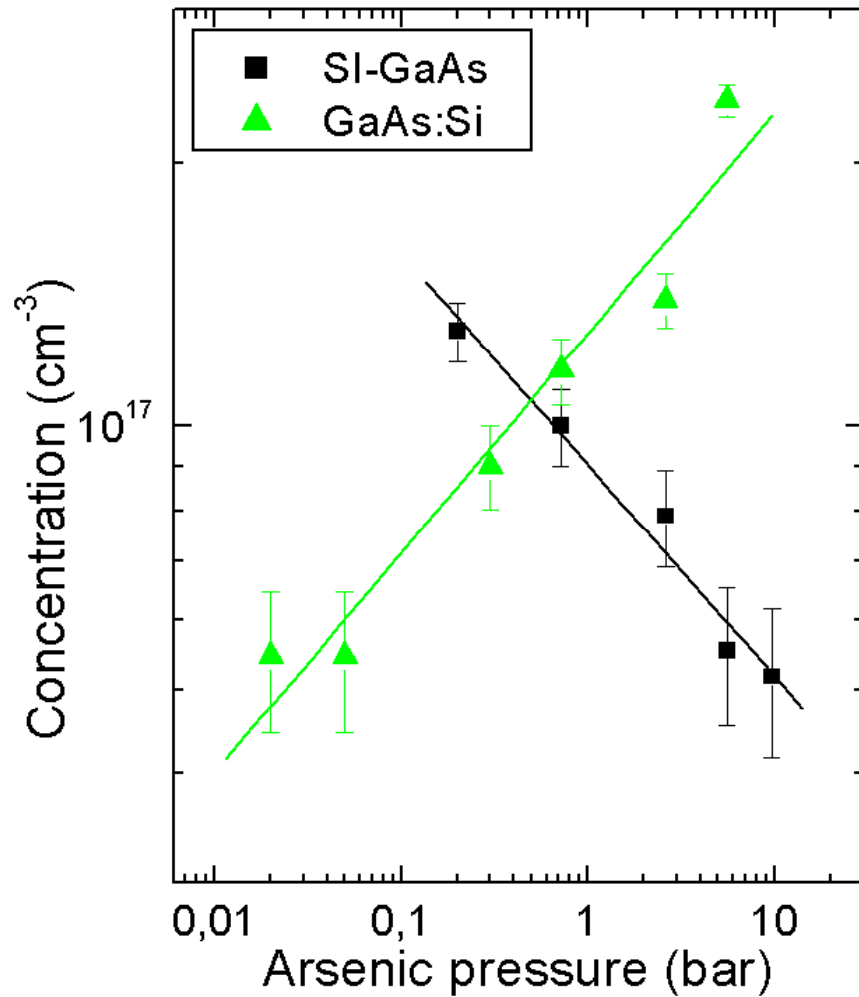
$$[\text{V}_{\text{Ga}}] = K_{\text{VG}} \times p_{\text{As}}^{1/4}$$

J. Gebauer et al.,
Physica B 273-274, 705 (1999)

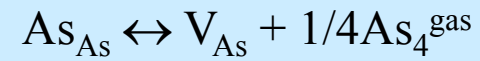
Fit: $[\text{V}_{\text{Ga}}-\text{Dopant}] \sim p_{\text{As}}^n$

$$n = 1/4$$

Comparison of doped and undoped GaAs



Thermodynamic reaction:



Mass action law:

$$[\text{V}_{\text{As}}] = K_{\text{VAs}} \times p_{\text{As}}^{-1/4}$$

Fit: $[\text{V-complex}] \sim p_{\text{As}}^n$

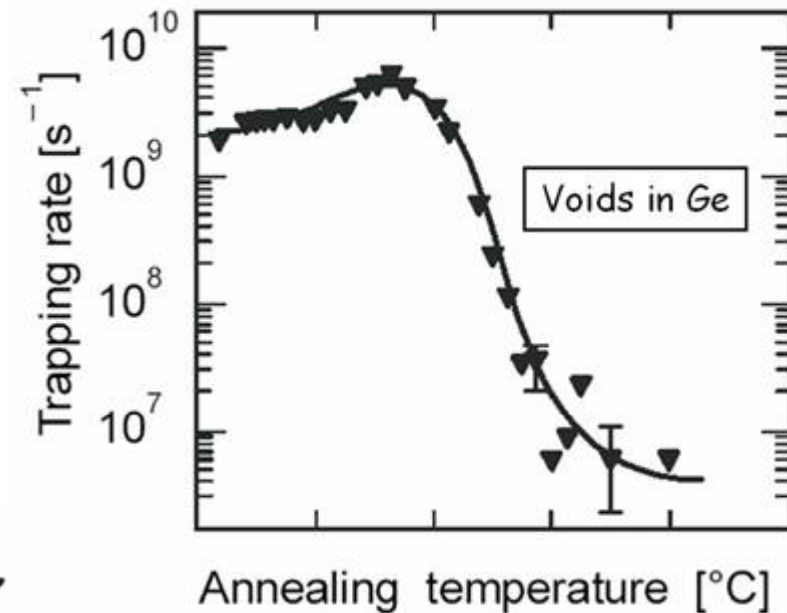
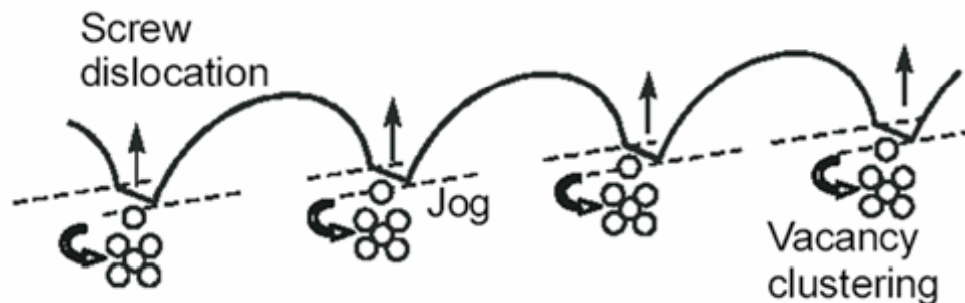
$$n = -1/4$$

undoped GaAs: As vacancy

7.3. Vacancy clusters in semiconductors

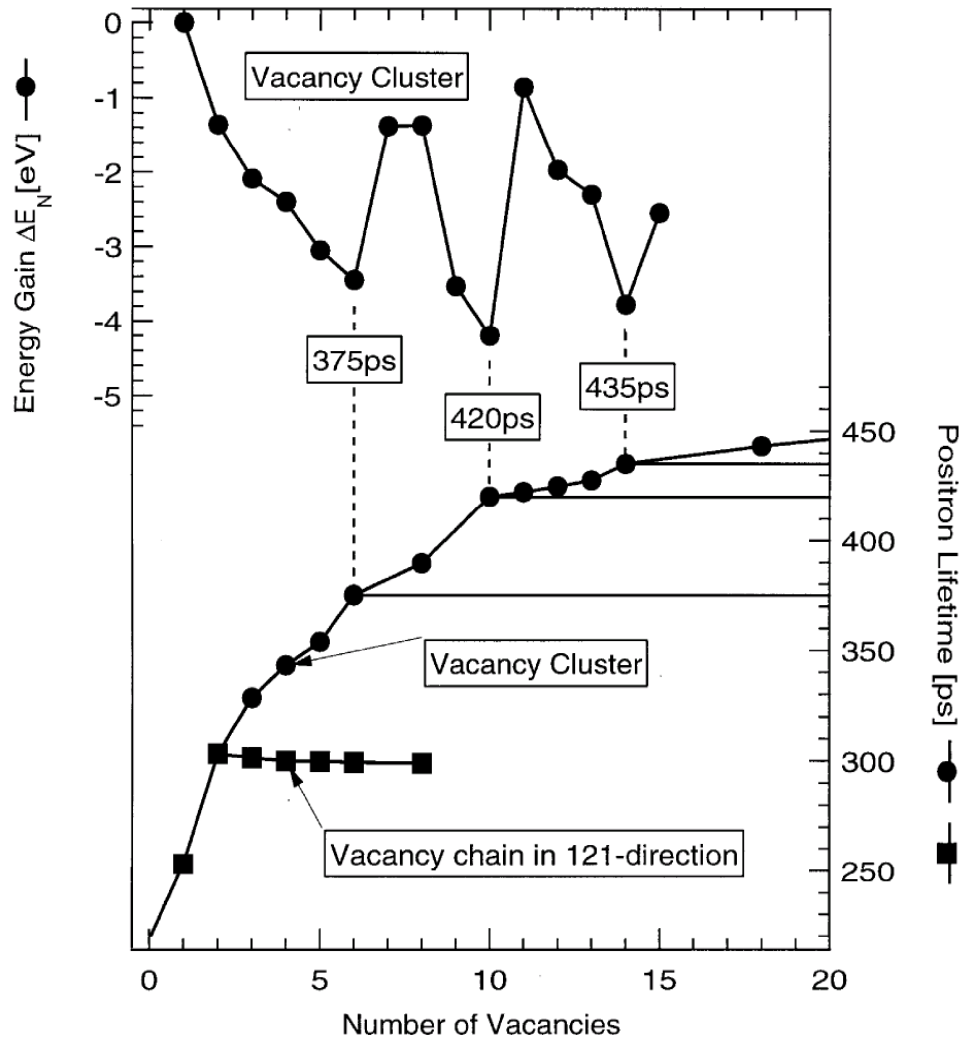
- vacancy clusters were observed after neutron irradiation, ion implantation and plastic deformation
- due to large open volume (low electron density) -> positron lifetime increases distinctly

- example: high-temperature plastically deformed Ge
- lifetime: $\tau_{\text{void}} = 525 \text{ ps}$
- reason for void formation: jog dragging mechanism
- trapping rate of voids disappears during annealing experiment



Krause-Rehberg et al., 1993

Theoretical calculation of vacancy clusters in Si



- there are cluster configurations with a large energy gain
- „**Magic Numbers**“ with 6, 10 und 14 vacancies
- positron lifetime increases distinctly with cluster size
- for $n > 10$ saturation effect, i.e. size cannot be determined any more

Theoretical calculation of vacancy clusters in GaAs

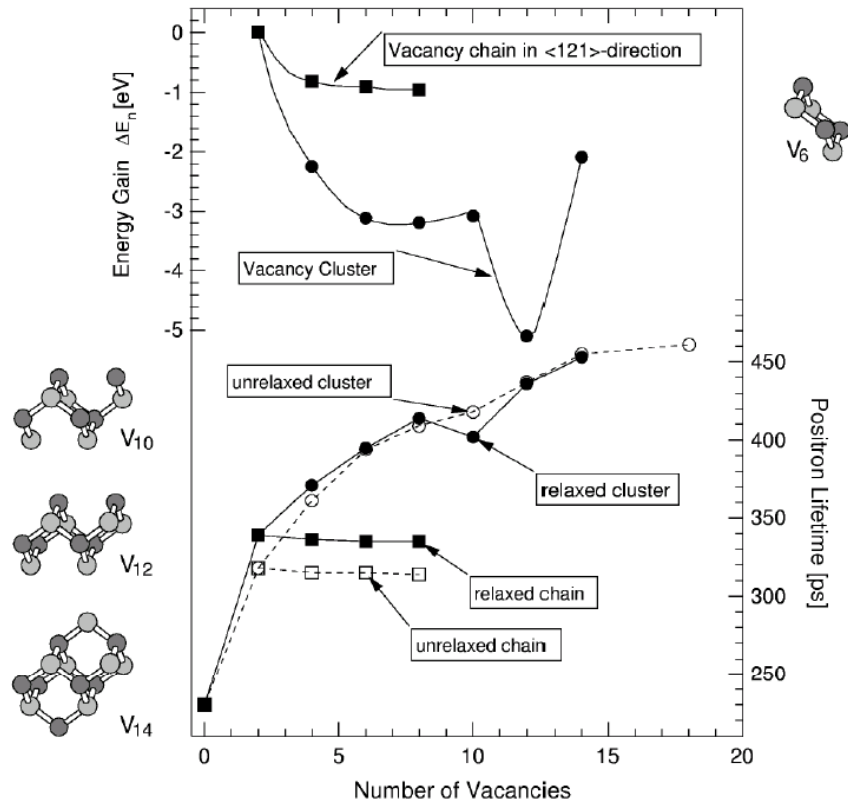


FIG. 2. Energy gained by adding a divacancy to an aggregate of $(n - 2)$ vacancies (upper part) and the corresponding positron lifetime (lower part). Structures of some V_n are shown beside the graphic (As atoms, dark gray; Ga atoms, light gray).

„Magic Number“ with 12 vacancies

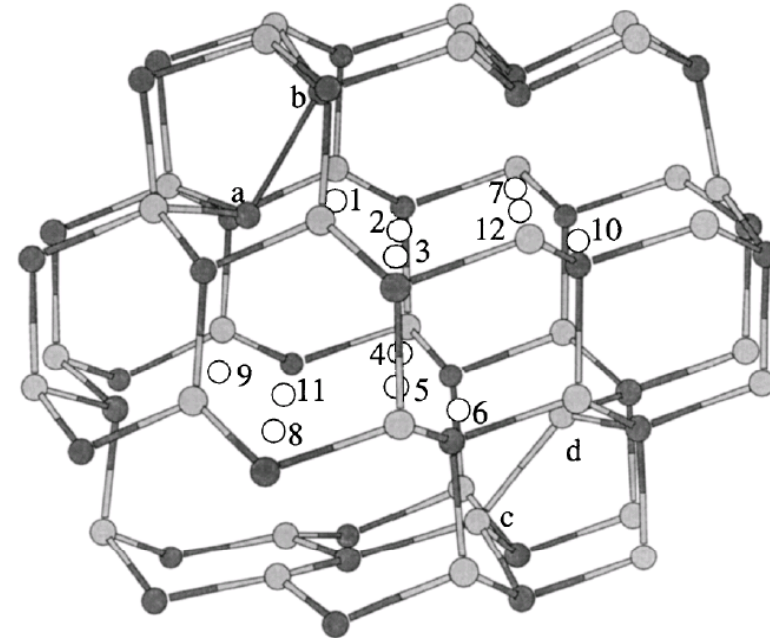
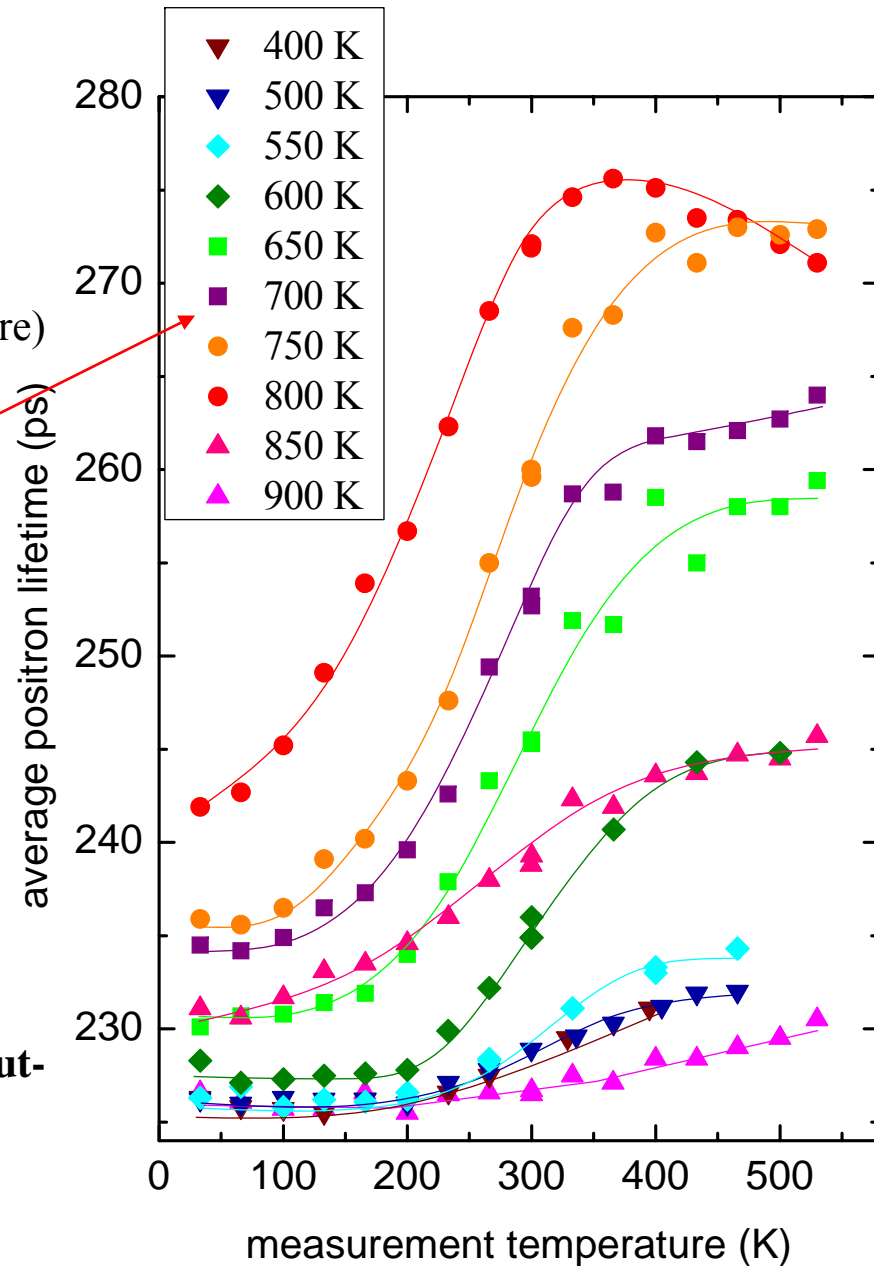


FIG. 3. Structure consisting of 12 vacancies. Dark gray balls denote As and light gray balls denote Ga atoms. The white spheres are the vacancies. The numbers give the order in which the atoms have been removed, starting from V_2 to V_{12} . Atoms a and d are removed to get V_{14} .

7.4. Defect generation during diffusion of Cu in GaAs

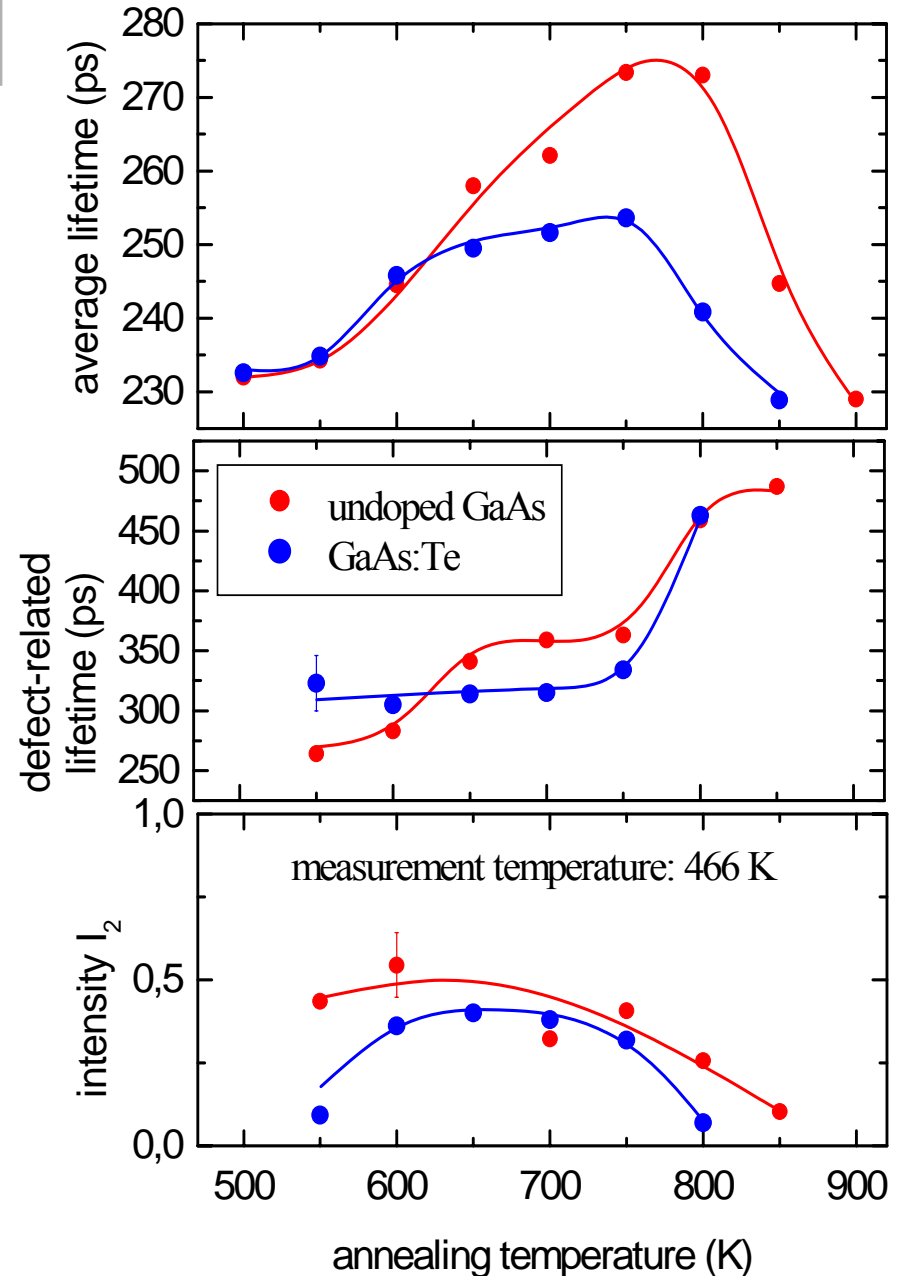
Positron experiment:

- 30 nm Cu-layer deposited by evaporation on GaAs surface
 - Annealing at 1100°C (under defined As-pressure) for Cu in-diffusion
 - Quenching to RT
 - then annealing with growing temperature
 - Positron lifetime measurement
 - no defects found – bulk properties
-
- Cu is completely solved at 1100°C
 - But it is oversaturated at RT
 - Precipitation starts very slowly (slow diffusion)
 - However: at elevated temperatures – diffusion becomes faster: out-diffusion process
 - Result: formation of vacancy-type defects when **out-diffusion** starts
 - Effect is not compatible with current diffusion models



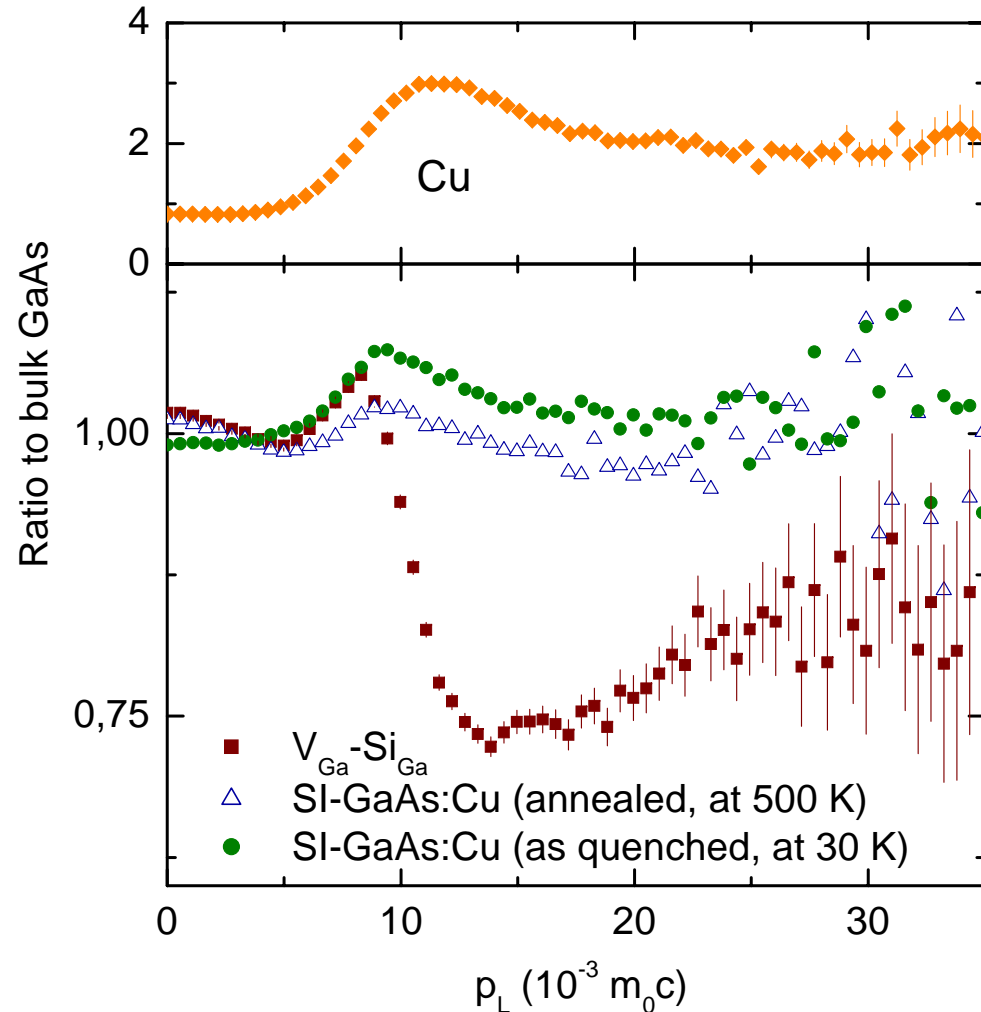
Determination of Defect Type

- Formation of these clusters is almost independent of doping / conduction type
- Identical behavior in undoped GaAs
- In beginning of defect formation: defect-related lifetime is about 250 ps – a monovacancy
- In course of annealing: lifetime growth to 320-350 ps corresponding to a divacancy
- at 800 K: $\tau_2 > 450$ ps: rather large vacancy clusters ($n > 10$)



Coincidence-Doppler Spectroscopy at GaAs:Cu

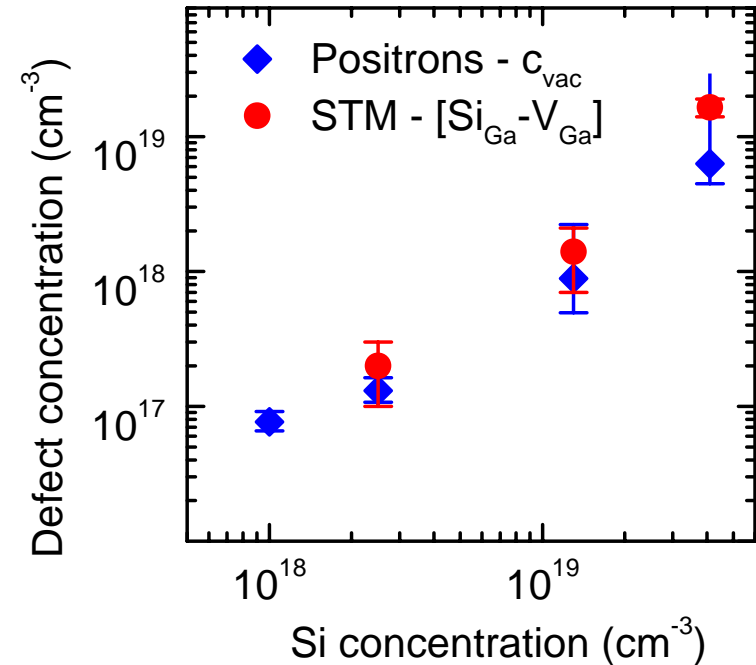
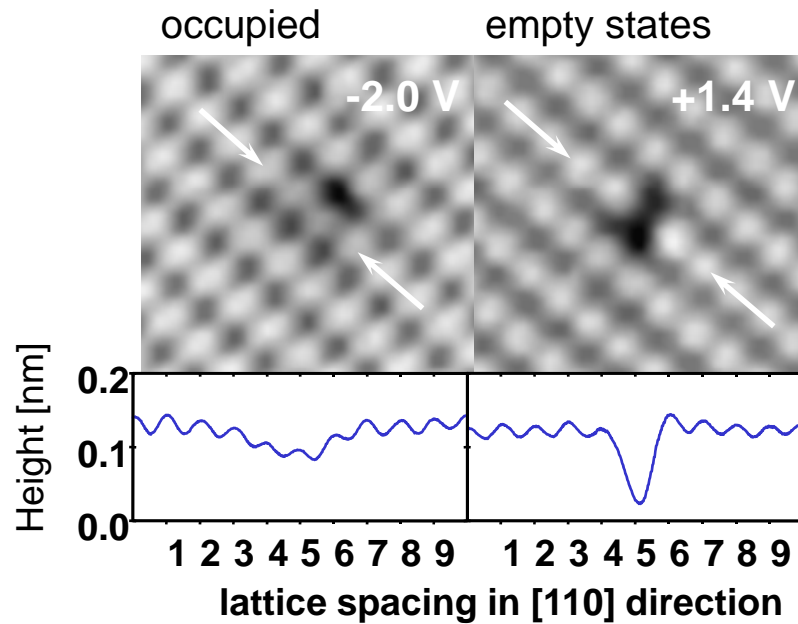
- In high-momentum region ($>10^{-2} m_0c$) annihilation with Core-electrons dominate
- Electron momentum distribution of core electrons almost not changed compared to individual atoms
- Relatively easy to calculate
- In example: the detected vacancies have Cu atoms in closest vicinity
- Vacancies are obviously stabilized by Cu



V. Bondarenko, et al., Physica B 308-310 (2001)792-795



7.5. Identification of V_{Ga} - Si_{Ga} -Complexes in GaAs:Si



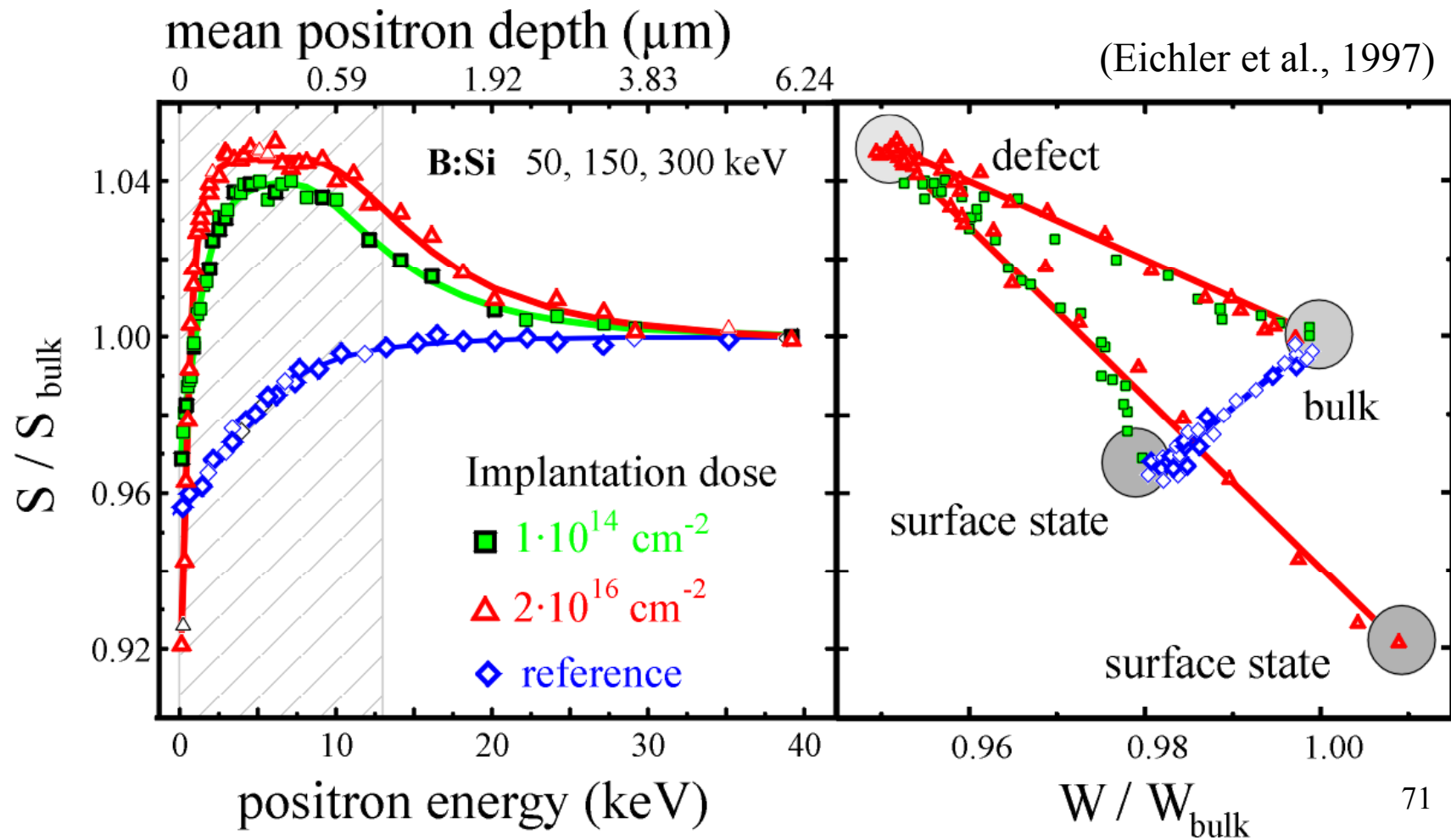
- Scanning tunneling microscopy at GaAs (110)-cleavages planes (by Ph. Ebert, Jülich/Germany)
- Defect complex identified as V_{Ga} - Si_{Ga}

- Quantification - Agreement

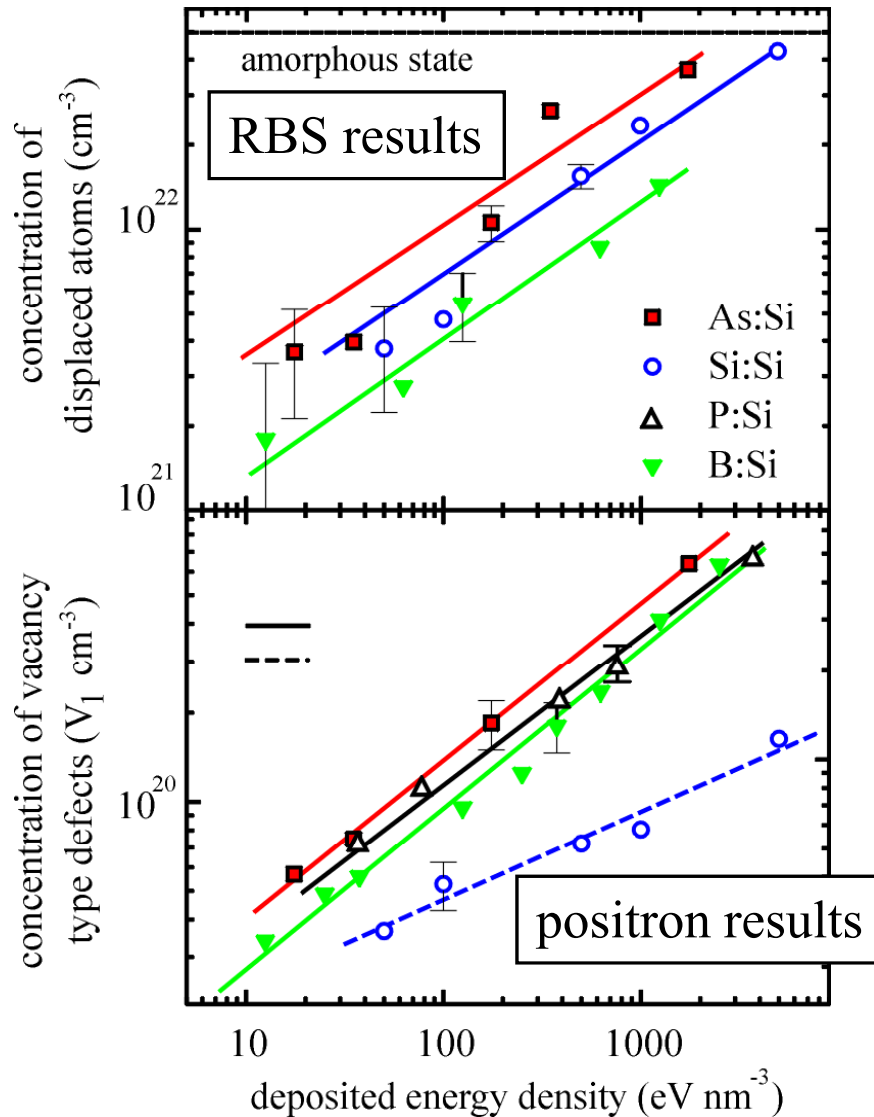
Mono-Vacancies in GaAs:Si are V_{Ga} - Si_{Ga} complexes

7.6. Defects in Si induced by Ion Implantation

- ion implantation is most important doping technique in planar technology
- main problem: generation of defects - positron beam measurements



Defect density as function of deposited ion energy



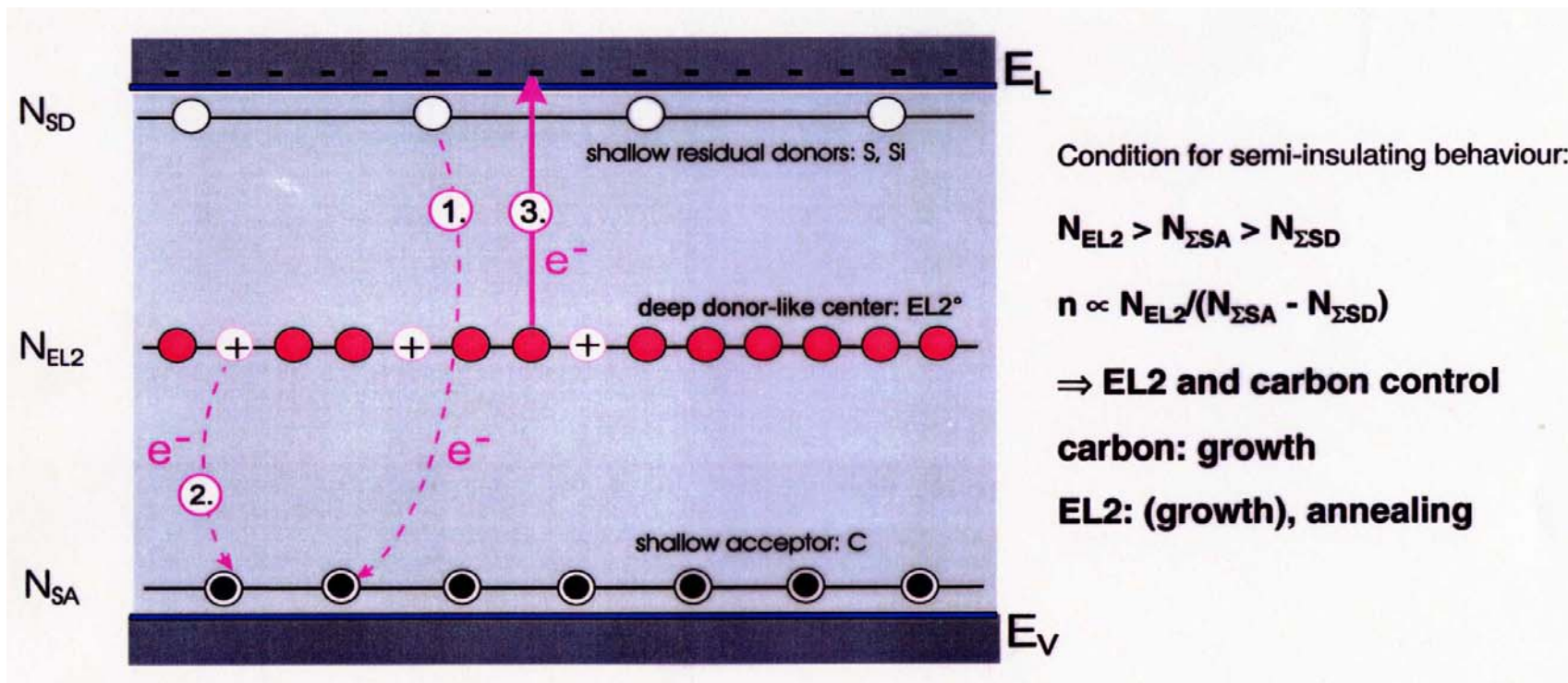
- Defect generation follows Chadderton's model of homogenous nucleation:

L.T. Chadderton, Rad. Eff. 8 (1971) 1

- $[\text{defect}] \sim \text{dose}^{0.5}$
- valid for RBS- and positron data
- only exception: Si self-implantation
- can be explained: extra Si atoms are interstitials and kill vacancies that are seen by positrons but not by RBS

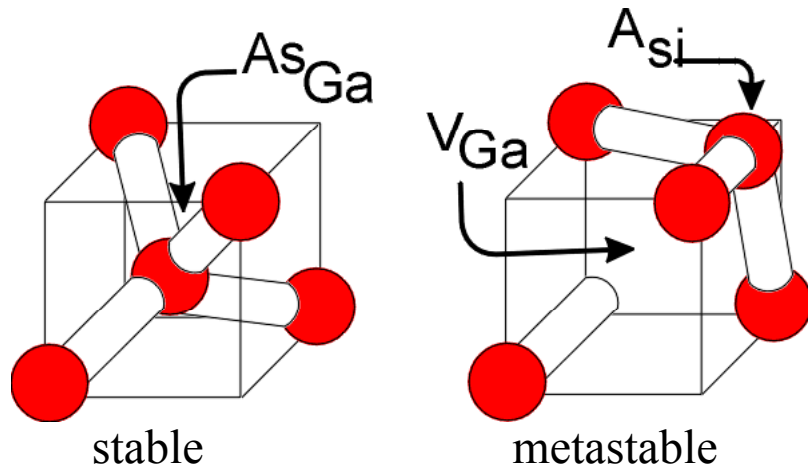
7.7. Compensation mechanism of semi-insulating GaAs

- GaAs often needed as high-resistive wafer material
- Dopant (impurity) level is about 10^{14} cm^{-3} - not low enough - but self-compensation was observed
- self-compensation works only when $[\text{EL2}] > [\text{shallow acceptors}] > [\text{shallow donors}]$
- (1) residual donors are compensated by shallow acceptors (carbon brought in by intension)
- (2) remaining acceptors are compensated by deep donor – EL2-defect
- (3) would need too high temperature, thus all carriers are compensated at “normal” temperatures
- Required conditions can be fulfilled in pure semi-insulating GaAs by “doping” with C



Positron Study: The nature of the EL2 defect in GaAs

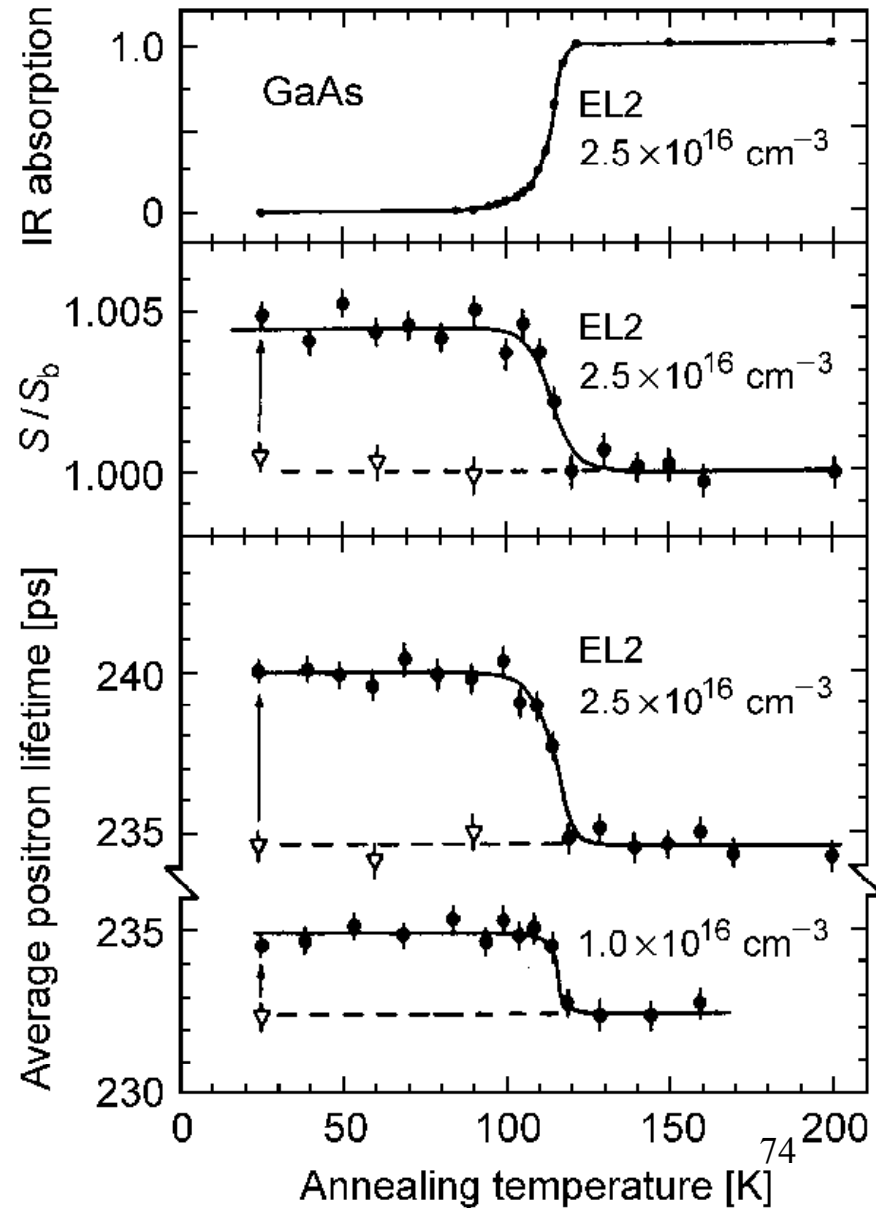
- one of mostly investigated defects
- exhibiting metastability at low T under light illumination



(Dabrowski 1988, Chadi 1988)

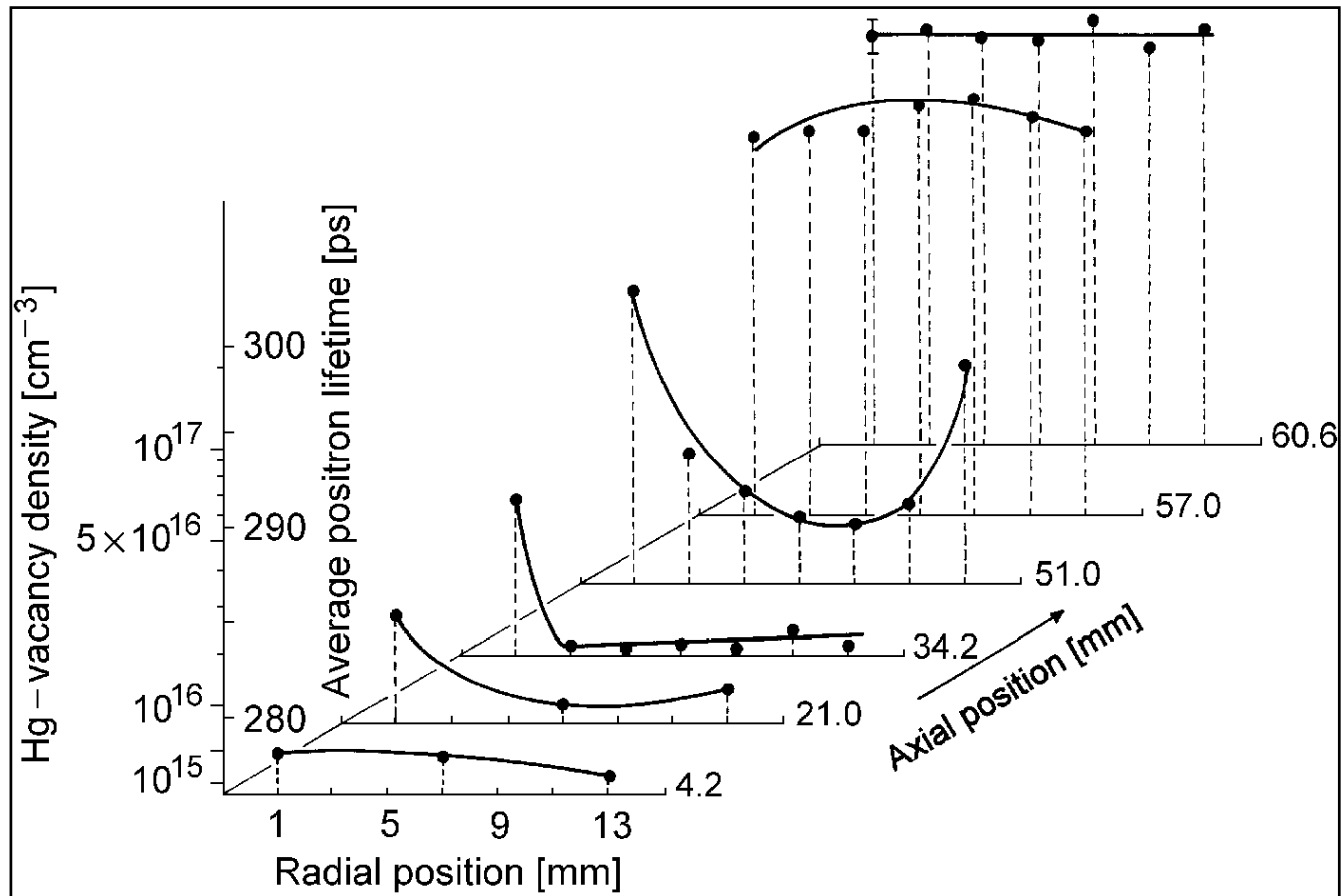
- there were several structural models of EL2
- the above shown model was proven by positron annihilation

(Krause et al., 1990)



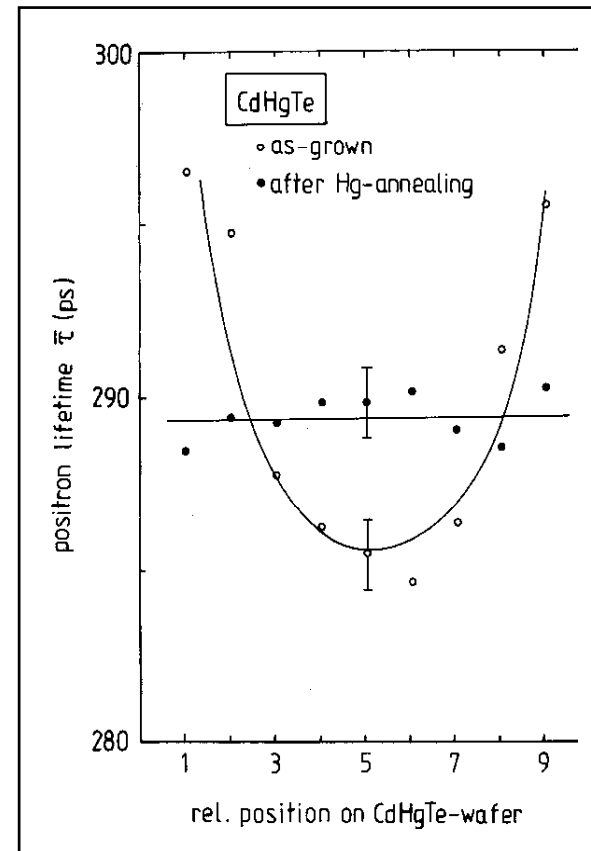
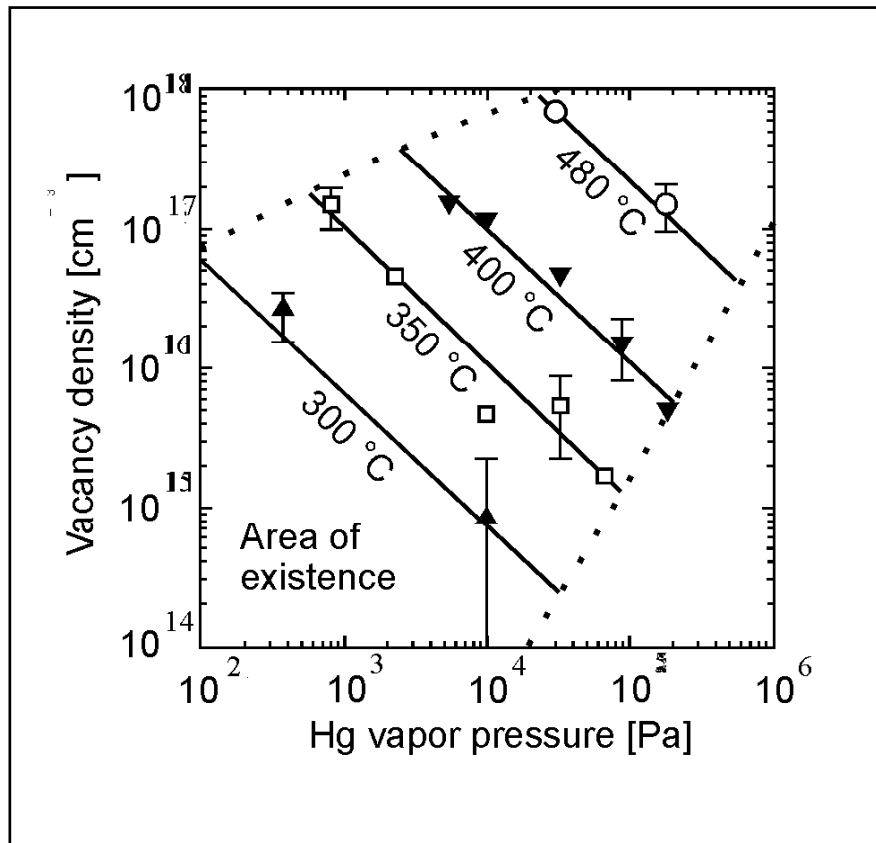
7.8. Defect engineering in II-VI compounds: Hg Vacancies in Hg_xCd_{1-x}Te

- material for infrared detectors (has small band gap)
- Hg diffuses very easily, high vapor pressure of Hg at relatively low temperatures
- V_{Hg} is acceptor and dominates electrical and optical behavior
- experimental finding: strong changes of [V_{Hg}] in THM-grown crystals



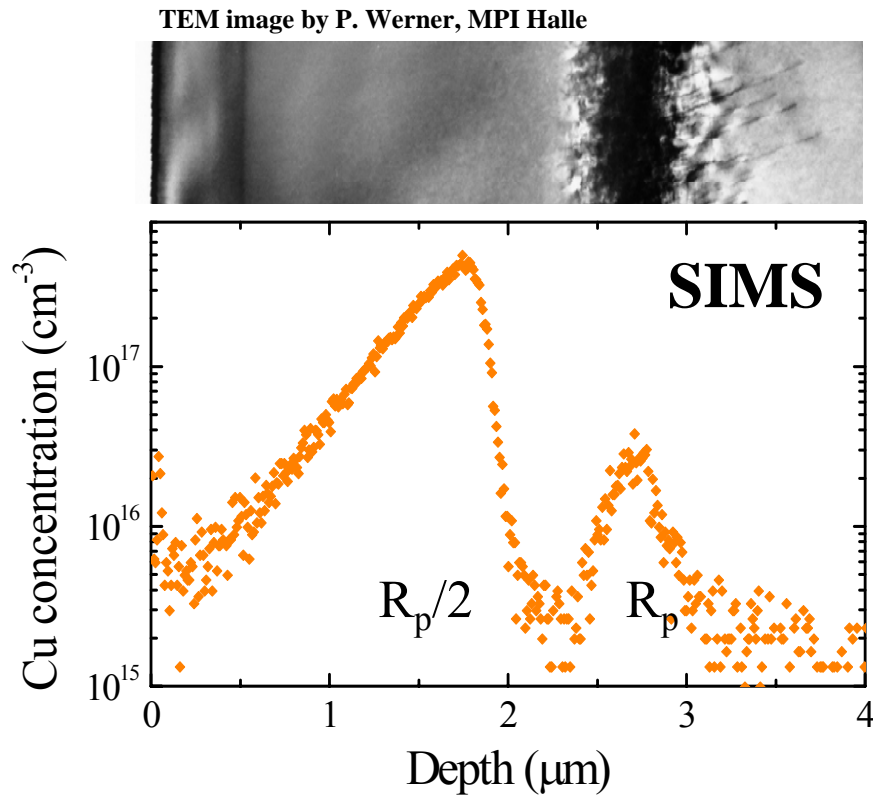
Control of V_{Hg} concentration

- Concentration of Hg vacancies can be controlled by annealing under defined vapor pressure of Hg
- all technological steps must be performed under Hg vapor pressure



7.9. Defects in high-energy self-implanted Si: The $R_p/2$ effect

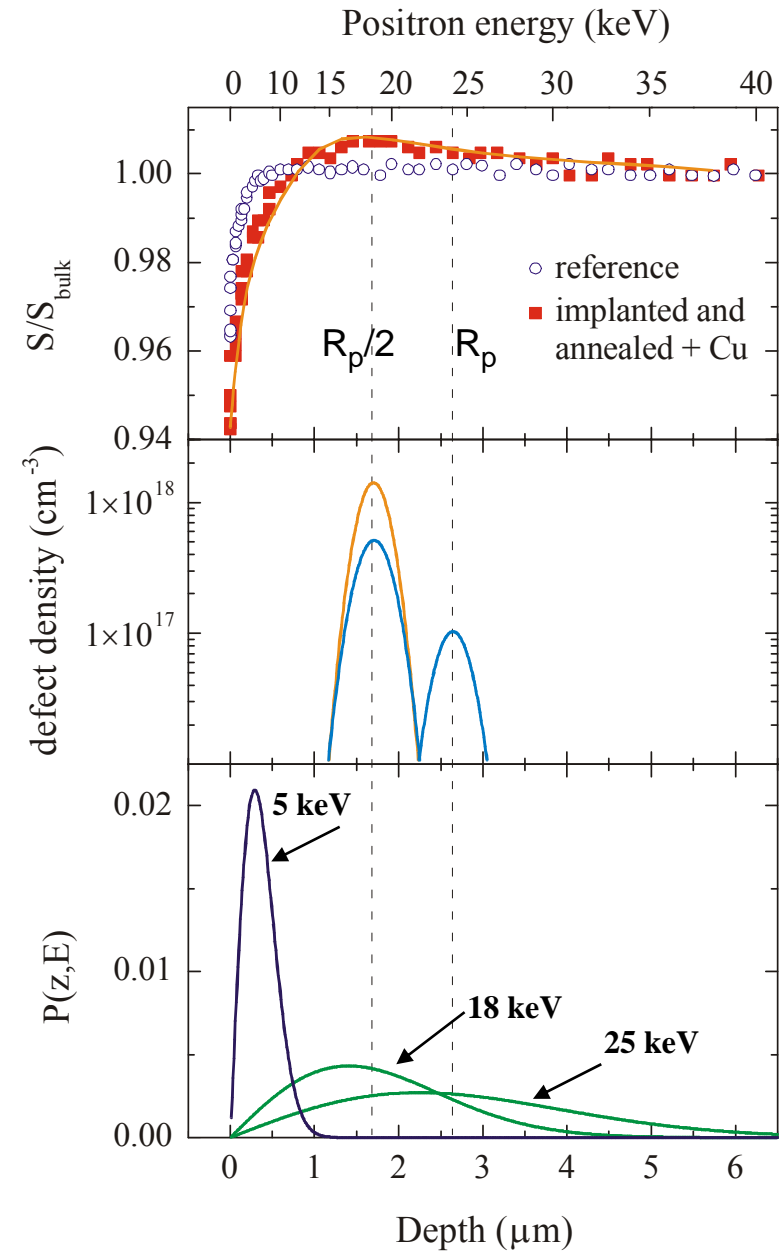
- after high-energy (3.5 MeV) self-implantation of Si ($5 \times 10^{15} \text{ cm}^{-2}$) and RTA annealing (900°C , 30s): two new gettering zones appear at R_p and $R_p/2$ (R_p = projected range of Si^+)
- visible by SIMS profiling after intentional Cu contamination



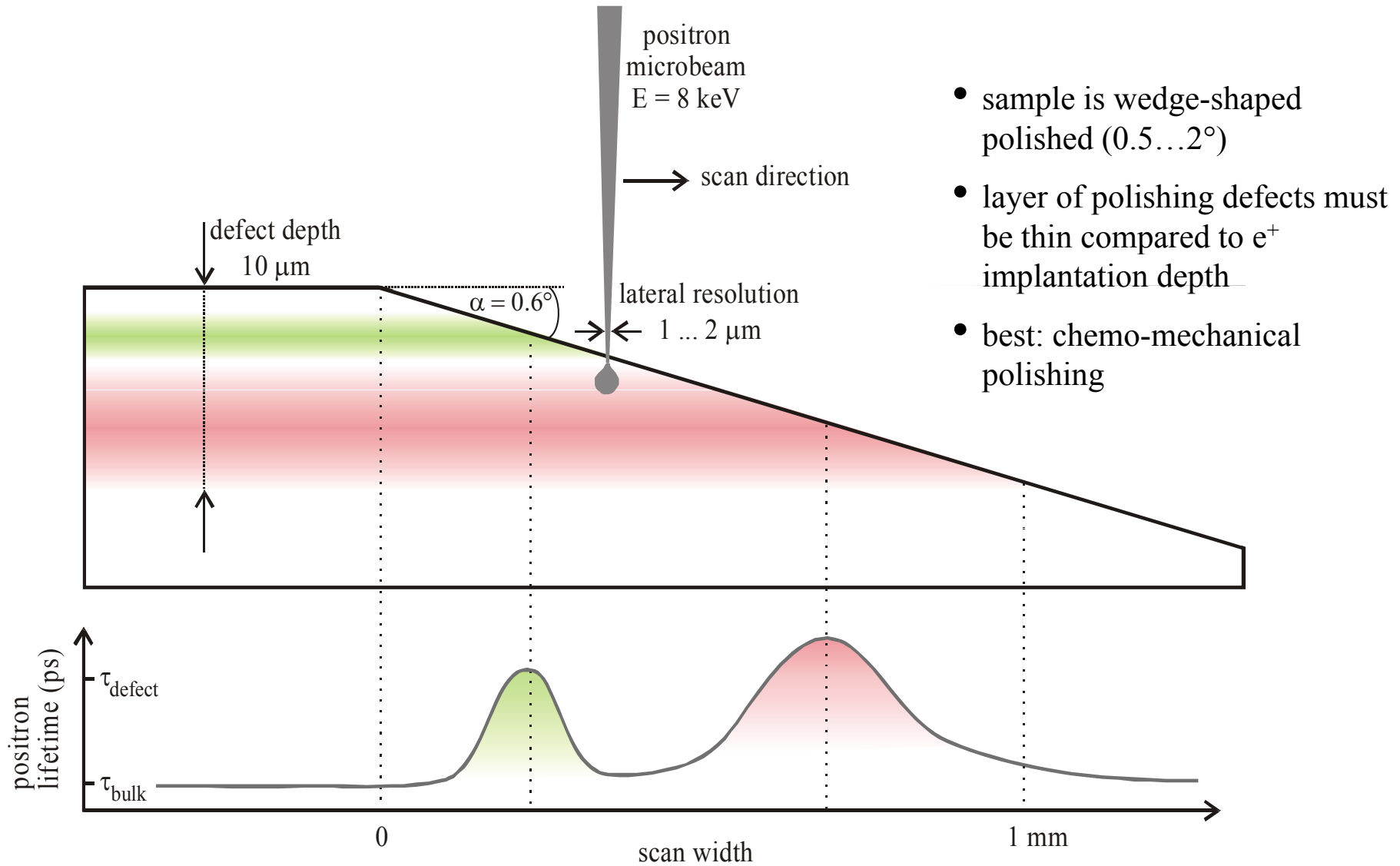
- at R_p : gettering by interstitial-type dislocation loops (formed by excess interstitials during RTA)
- no defects visible by TEM at $R_p/2$
- What type are these defects?

Investigation of the $R_p/2$ effect by conventional VEPAS

- the defect layers are expected in a depth of 1.7 μm and 2.8 μm corresponding to $E^+ = 18$ and 25 keV
- implantation profile too broad to discriminate between the two zones
- simulation of $S(E)$ curve gives the same result for assumed blue and yellow defect profile (solid line in upper panel)
- furthermore: small effect only
- no conclusions about origin of $R_p/2$ effect possible

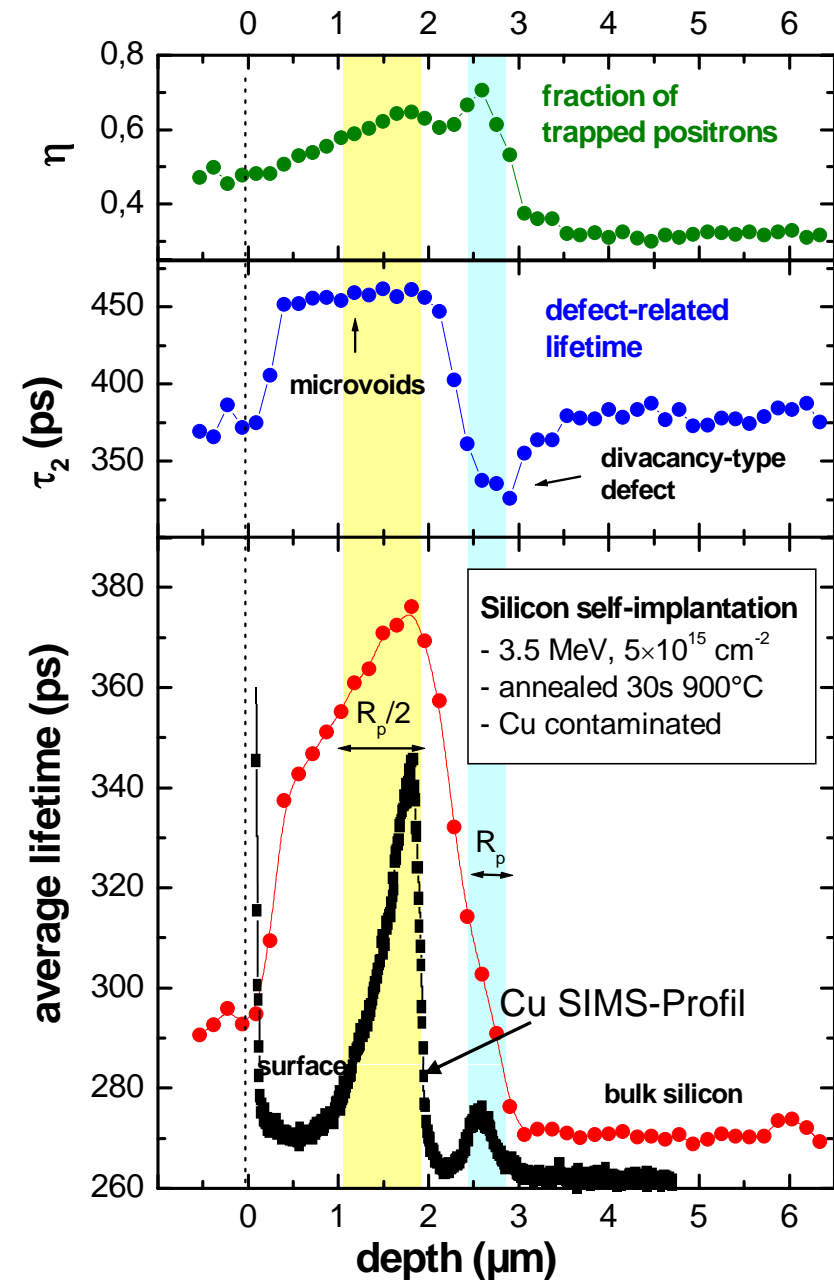


Enhanced depth resolution by using the Positron Microscope



First defect depth profile using Positron Microscopy

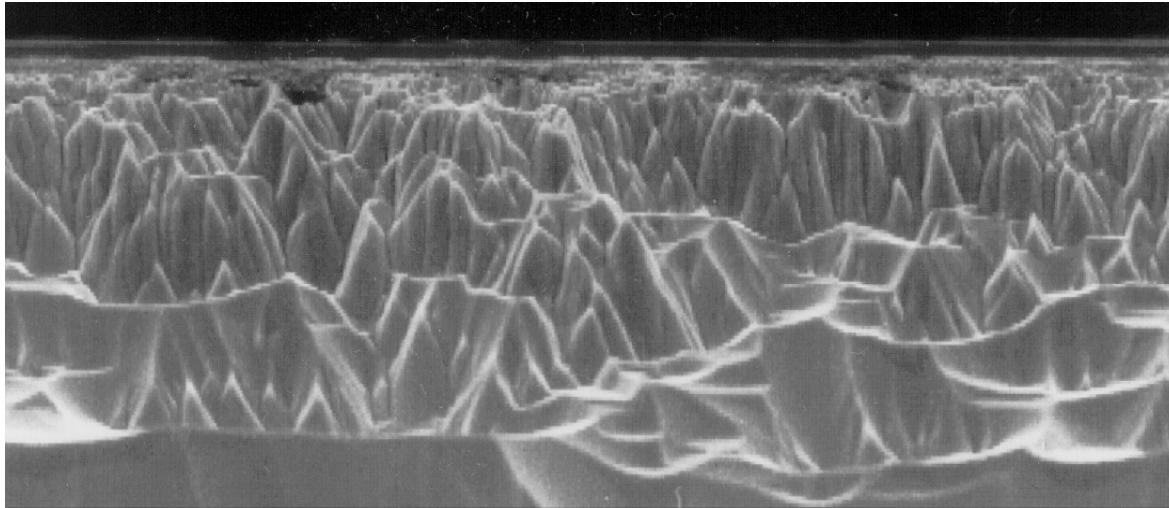
- 45 lifetime spectra: scan along wedge
- separation of 11 μm between two measurements corresponds to depth difference of 155 nm ($\alpha = 0.81^\circ$)
- beam energy of 8 keV: mean penetration depth is about 400 nm; represents optimum depth resolution
- no further improvement possible due to positron diffusion: $L_+(\text{Si @ } 300\text{K}) \gg 230 \text{ nm}$
- both regions well visible:
 - vacancy clusters with increasing density down to 2 μm ($R_p/2$ region)
 - in R_p region: lifetime $\tau_2 = 330 \text{ ps}$; corresponds to open volume of a divacancy; must be stabilized or being part of interstitial-type dislocation loops
- excellent agreement with gettered Cu profile



R. Krause-Rehberg et al., Appl. Phys. Lett. 77 (2000) 3932



7.10. Defects in GaAs introduced by wafer cutting

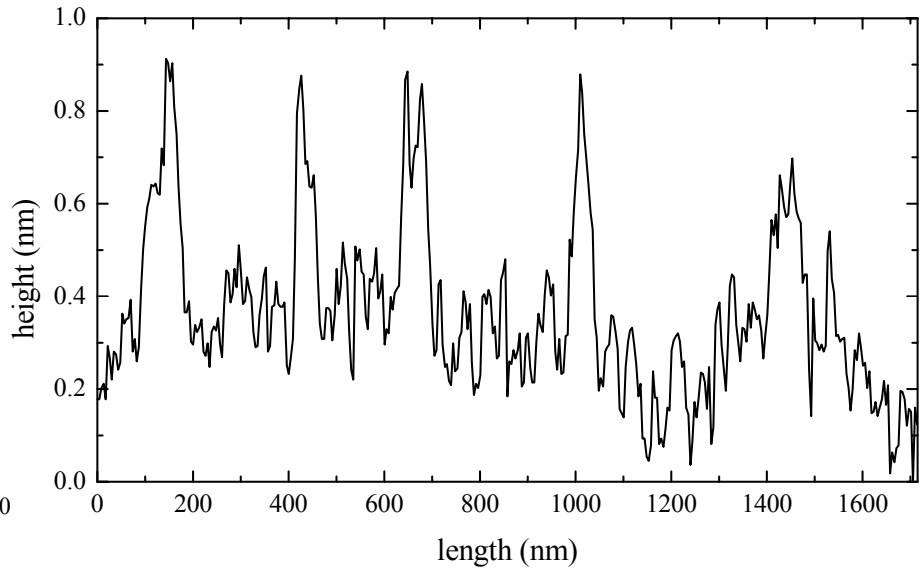
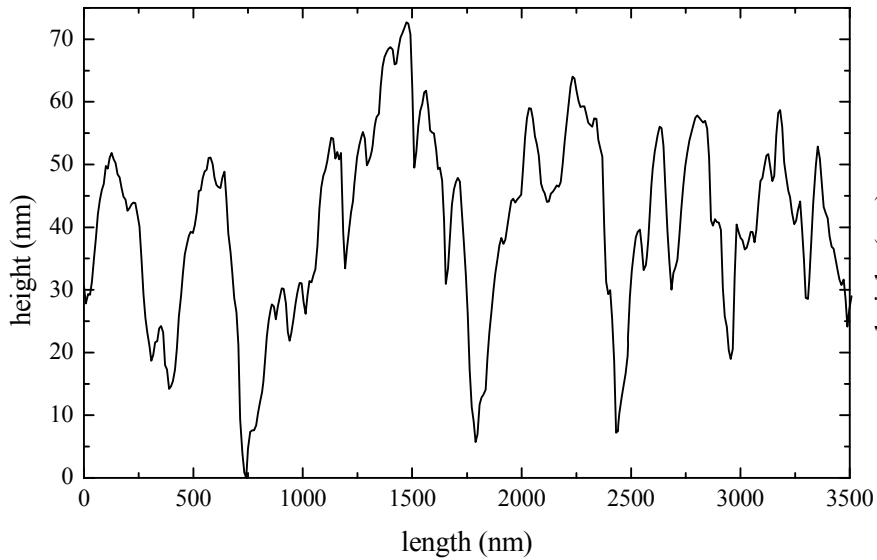
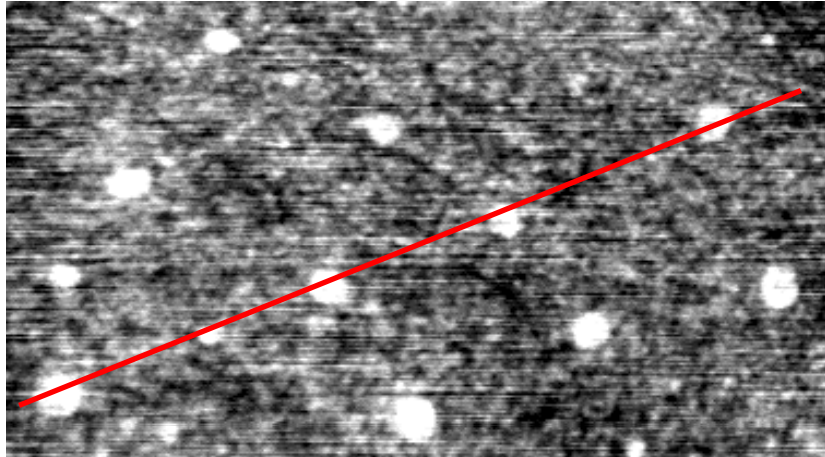
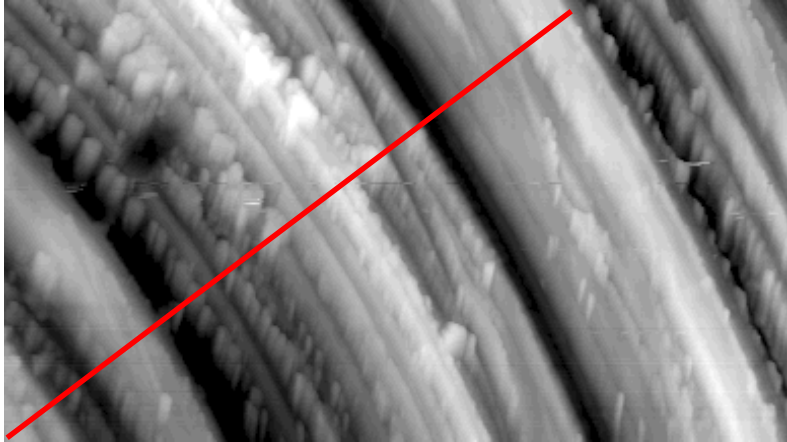


50 μm

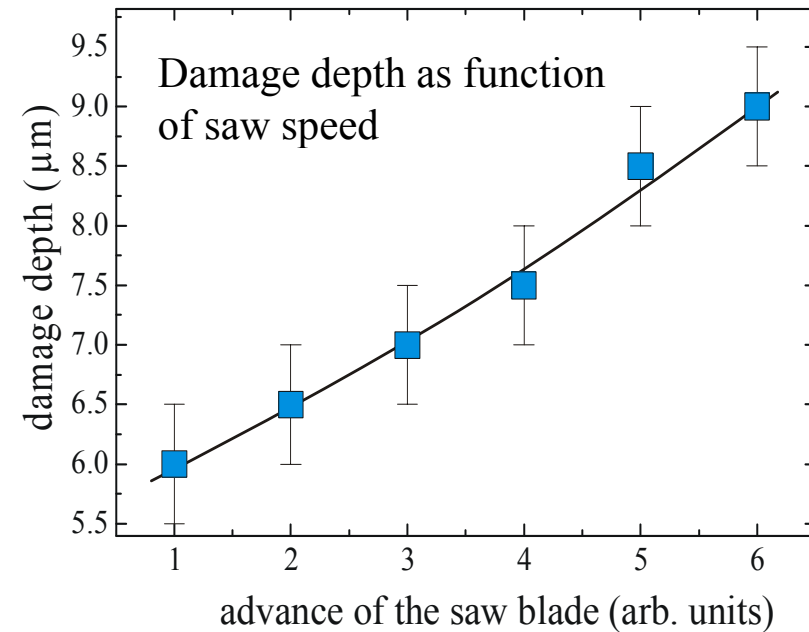
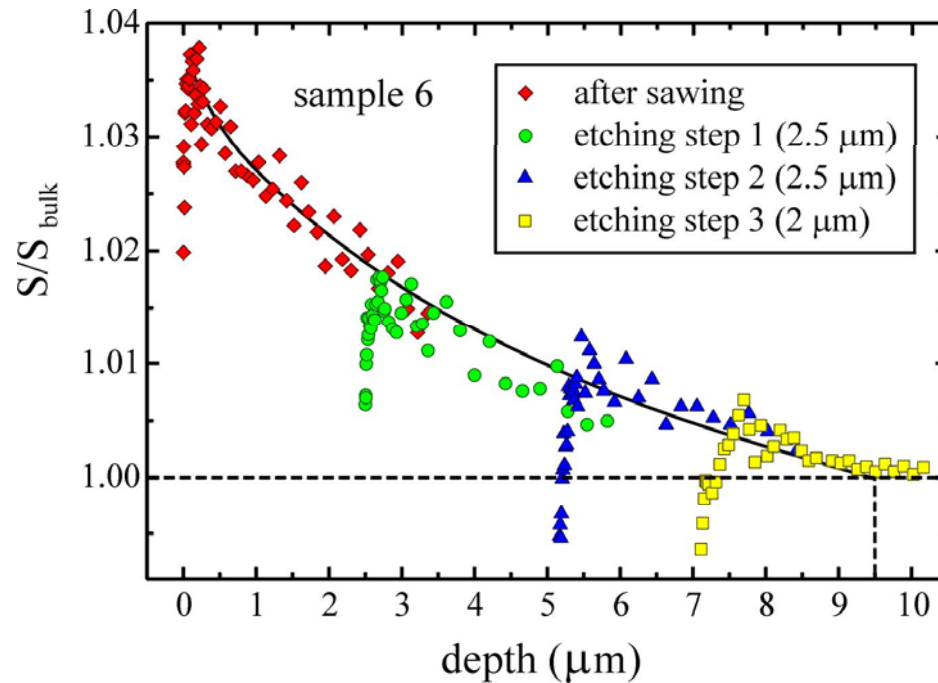
- cutting of wafer with diamond-saw (by wire and blade saws)
- after cutting: surface destroyed, defects several μm deep
- defect profile reaches far into the interior of the wafer
- Point defects can be studied e.g. by positron annihilation
- careful etching and polishing necessary
- Demand of technology: wafer roughness must be $< 1 \mu\text{m}$ for a complete 6" wafer

Cutting defects in GaAs: polishing

Atomic force microscopy before/after polishing and etching



Positron Study of Damage of Wafer Surface by a Diamond Saw



- maximum positron energy 40 keV: mean implantation depth = 3.3 μm
- step-wise etching (about 2...3 μm per step) of surface by ($\text{H}_2\text{O}_2\text{-NH}_3$)
- repeated positron beam measurement
- superimpose of different profiles

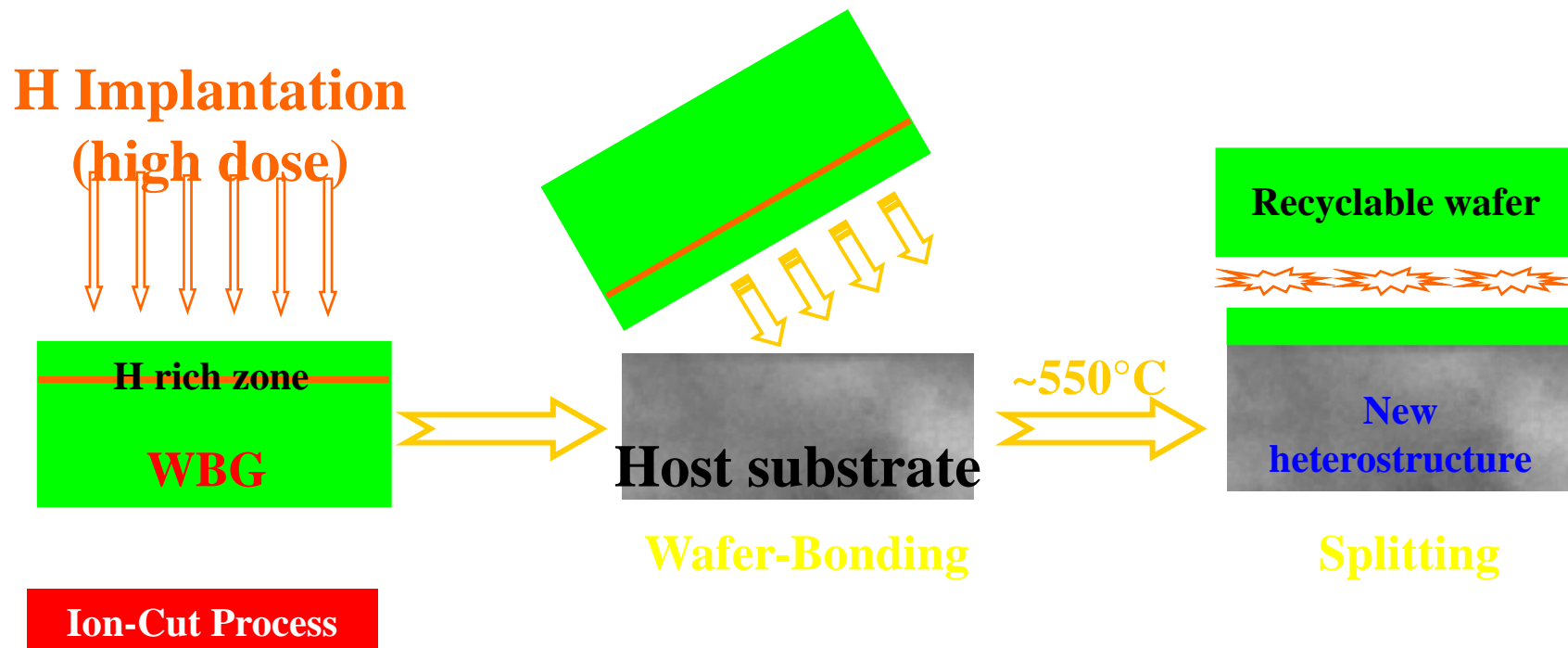
F. Börner et al., J. Appl. Phys. 84 (4), 2255-2262 (1998)



7.10. Smart-Cut process of GaN

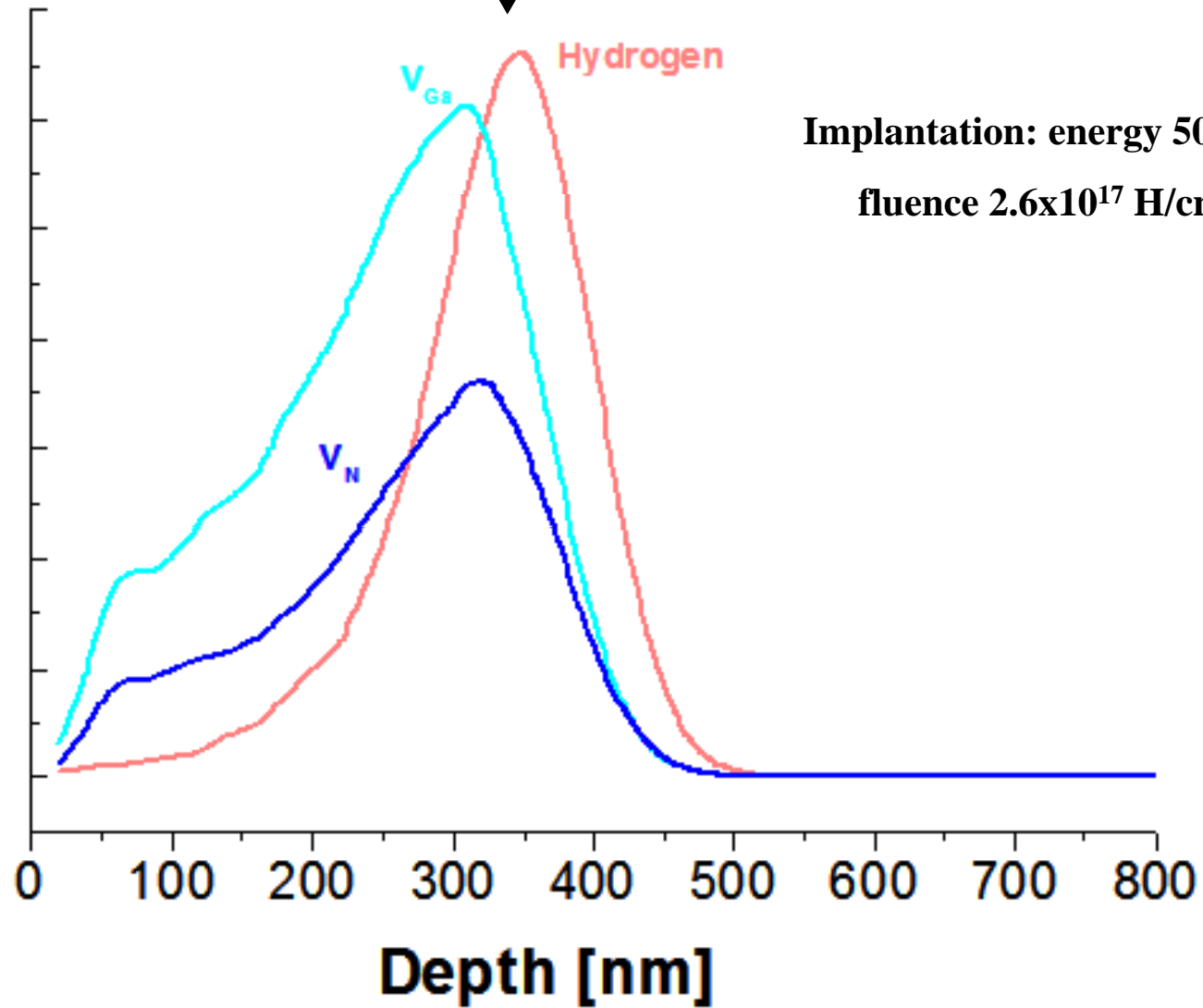
Technological context: Hetero-epitaxial growth of WBG materials on foreign substrates leads unavoidably to the formation of growth-related defects such as dislocations, stacking faults and twins that occur to relax the strain which significantly limits the quality of the grown structures with undesirable impact on devices performance.

What to do? Direct wafer bonding in combination with hydrogen ion-cutting is a promising stratagem to integrate bulk quality thin layers onto various host materials achieving a wide variety of heterostructures sometimes inconceivable by epitaxy. Having bulk properties, these new materials are very promising for a low cost fabrication of WBG-based devices such as phosphorous-free white LED and high performance laser diodes.

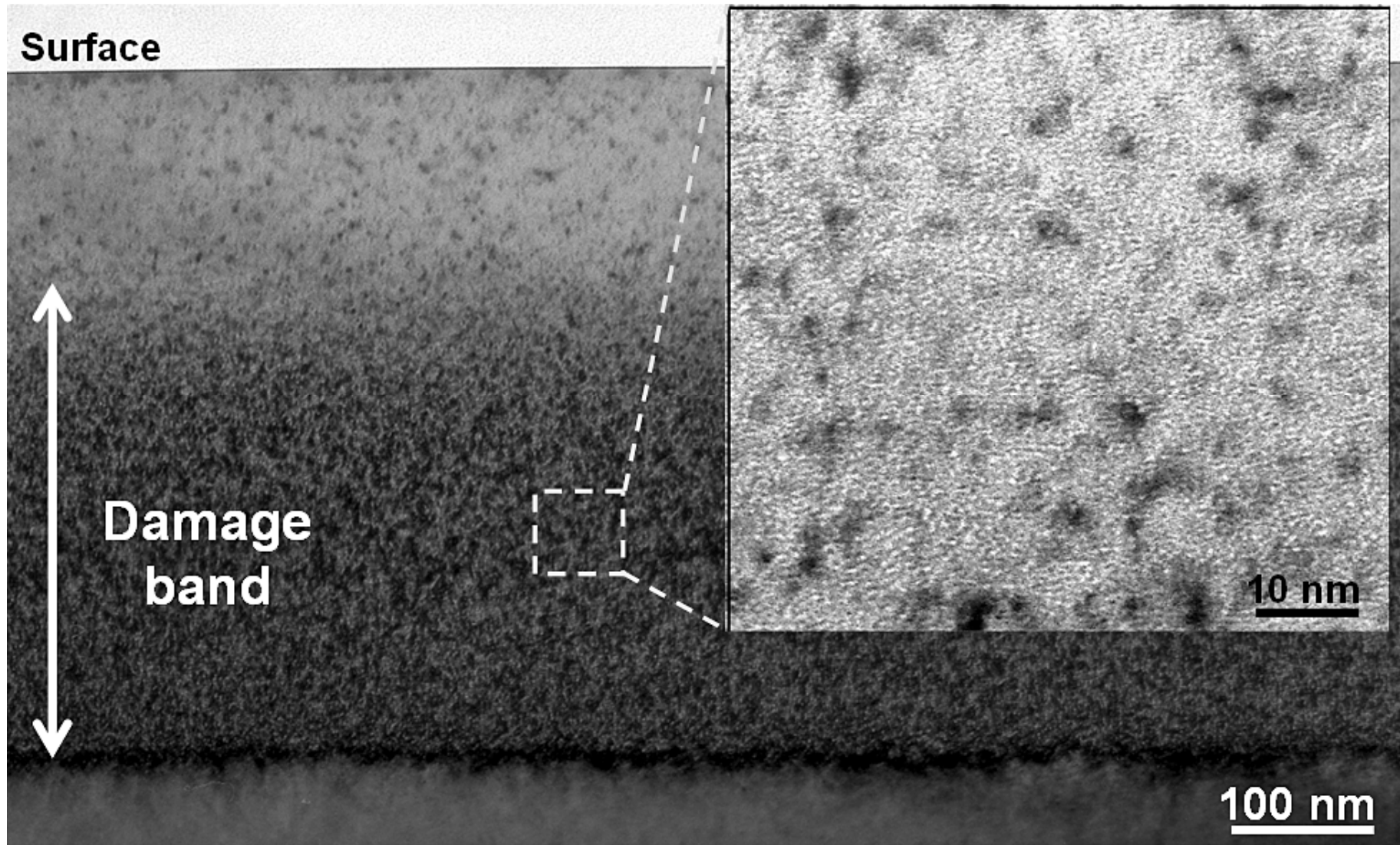


SRIM Simulations

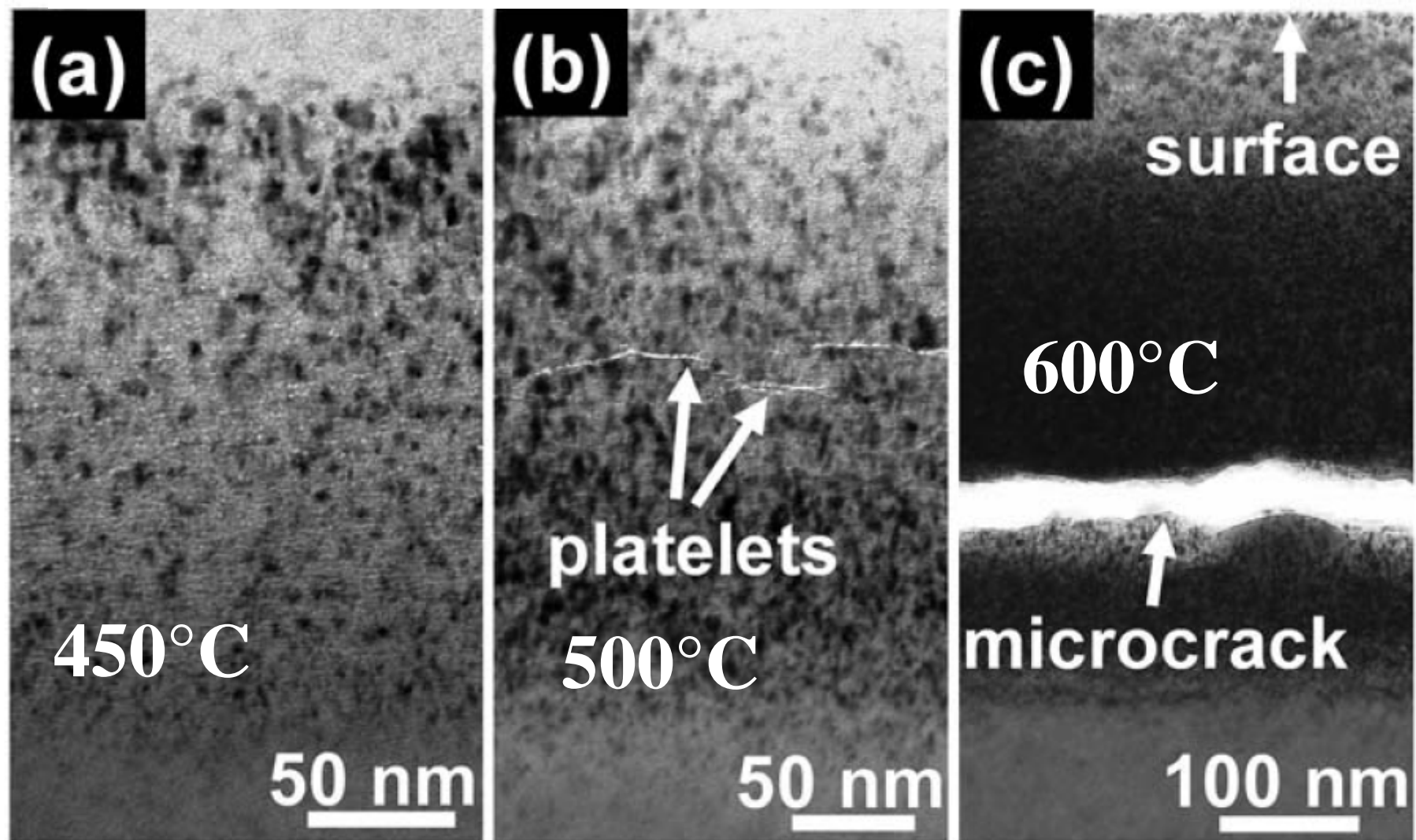
defect layer at about 350 nm



During implantation: nanobubbles 1-2 nm are formed

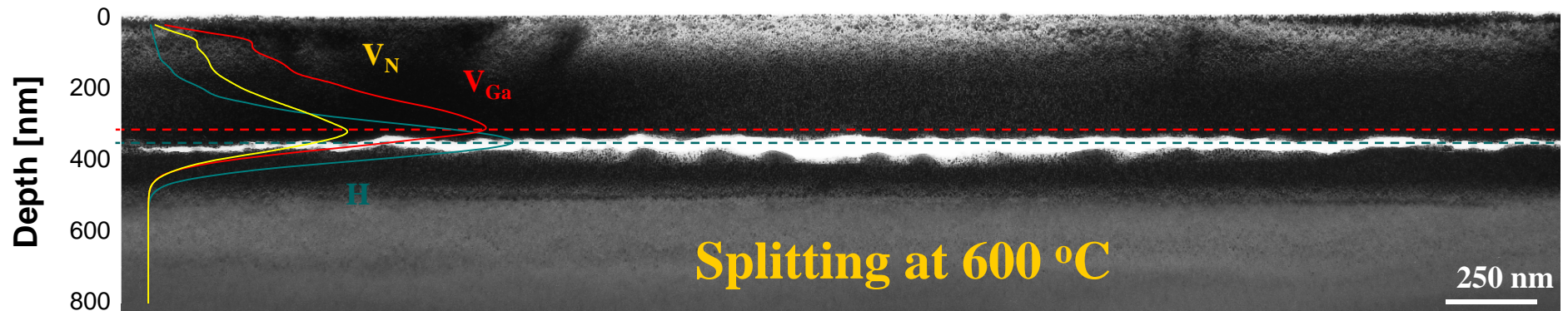


XTEM micrographs of H-implanted GaN annealed at different temperatures: 450 °C (a), 500 °C (b), and 600 °C (c).



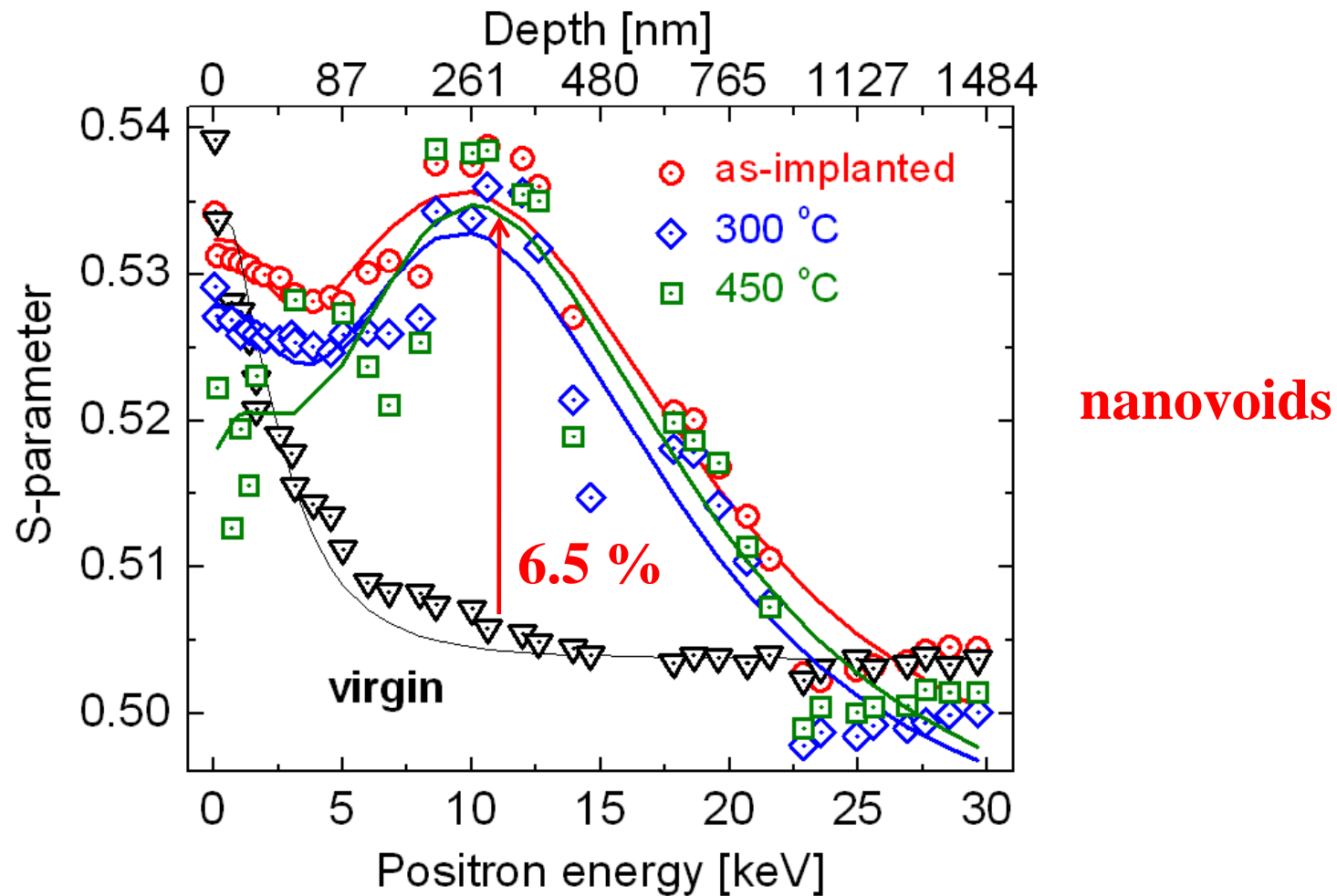
Understanding basic mechanisms of ion-cut process

- In order to draw a precise mechanistic picture of H-induced splitting of WBG materials a deep investigation thermal evolution of H-defect complexes is required
- Simulated defect concentration fits to position of platelets

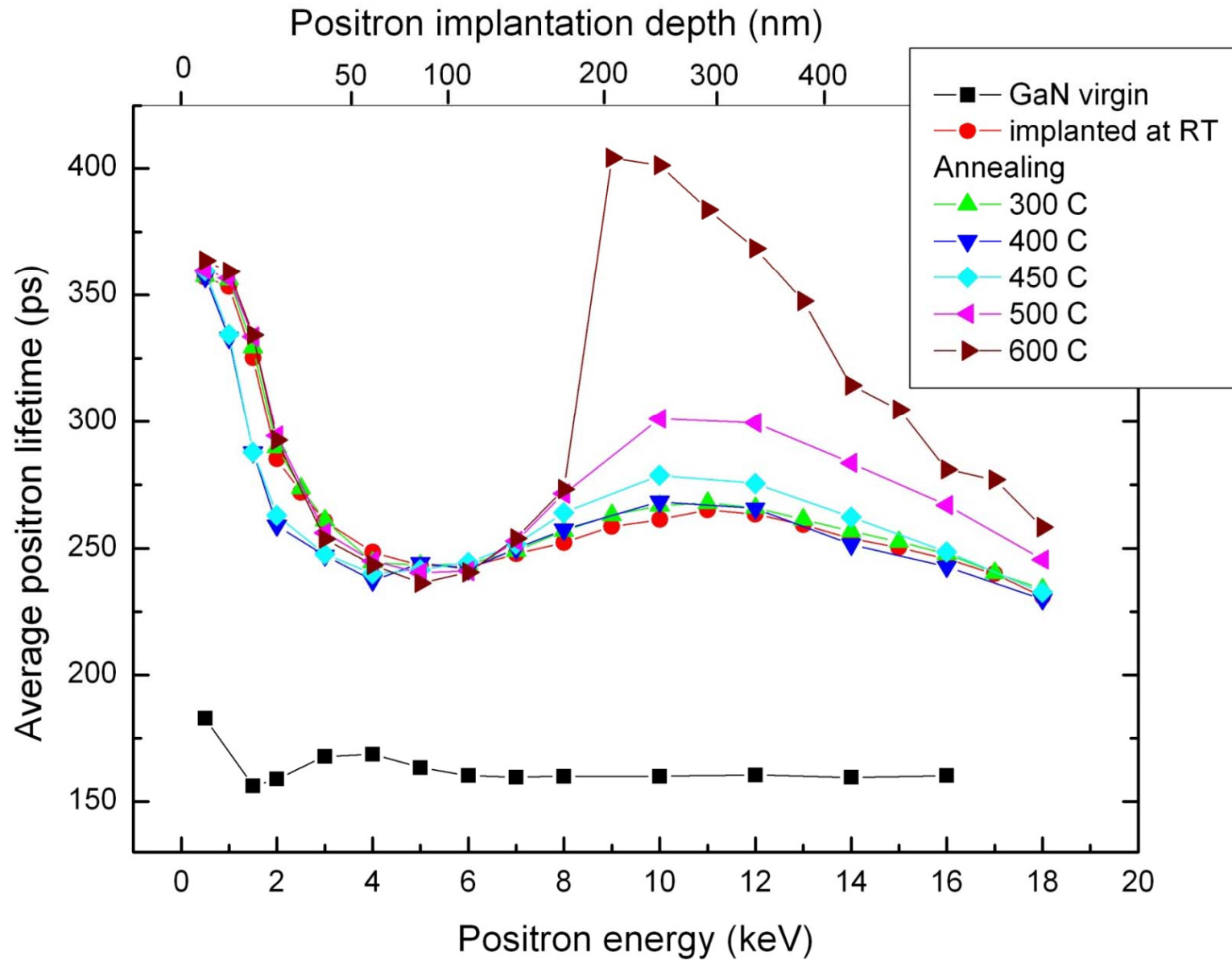


Doppler Broadening Measurements

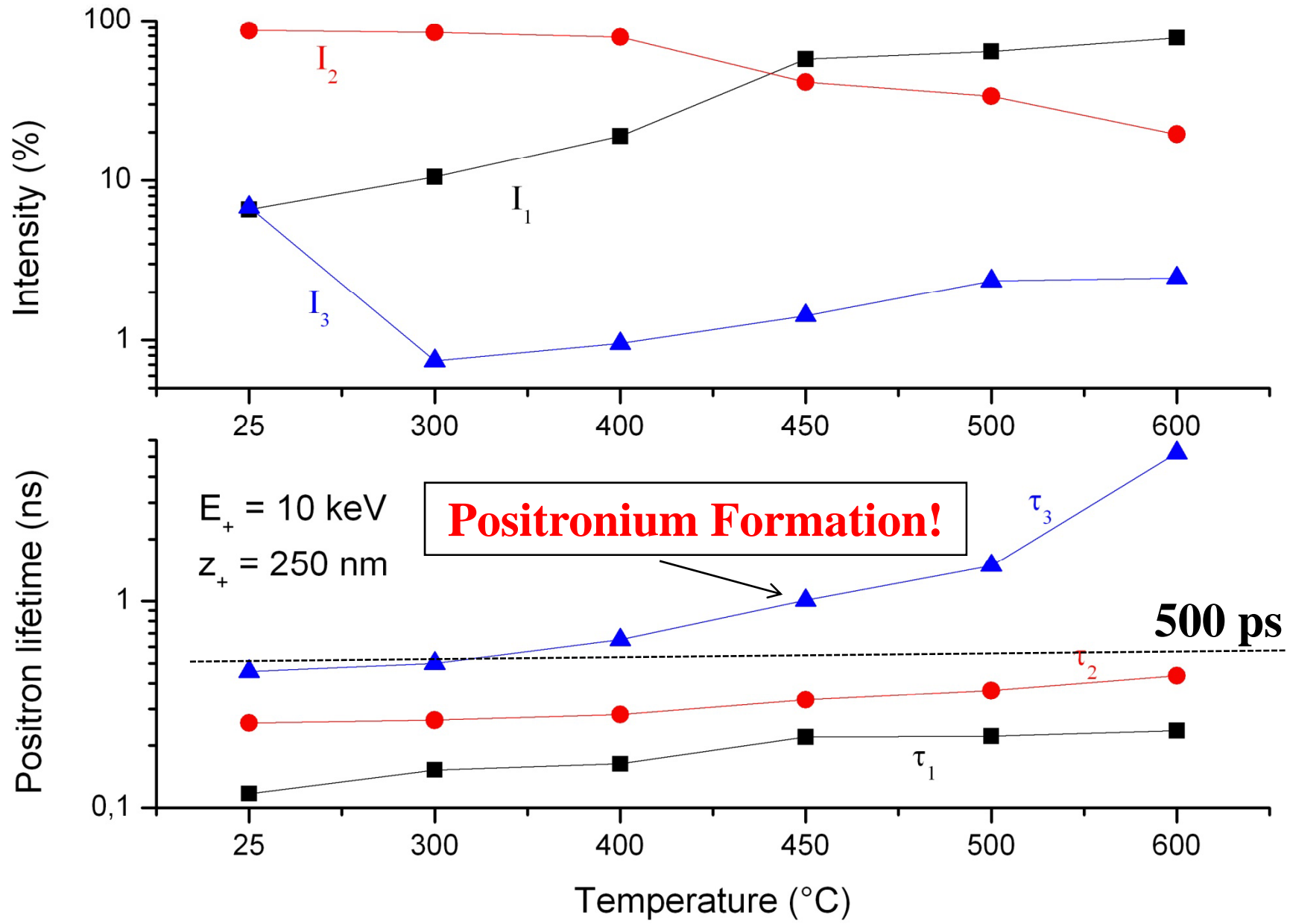
- Slow positron DOBS of implanted GaN sample: results show strong defect signal
- 50 keV protons and 2.6×10^{17} H/cm²



Positron Lifetime Experiments at PLEPS @ FRM-II



3-component decomposition of lifetime spectra



8. Conclusions

- Positrons Annihilation Spectroscopy is a unique tool for studying nanoscopic open-volume defects, such as vacancies, vacancy clusters, dislocations, nano-precipitates, nano-porosity, grain boundaries of nano-grains, acceptors (in semiconductors)
- high sensitivity starts at $5 \times 10^{14} \text{ cm}^{-3}$ (is about 10^{-7})
- defect type and density may be determined
- Coincidence Doppler Broadening – chemical information on surrounding of defect
- in semiconductors: sensitivity for charge state of defects
- different methods allow investigation of thin layers ($< 1 \text{ } \mu\text{m}$) up to cm thick samples
- positron micro-beams have about $2 \text{ } \mu\text{m}$ lateral resolution
- user-dedicated positron sources with high-intensity sources now available

9. Literature

- R. Krause-Rehberg, H.S. Leipner „Positron Annihilation in Semiconductors“; Springer 1998
- P. Coleman „Positron Beams and their applications“; World Scientific 2000
- M. Charlton, J.W. Humbertson „Positron Physics“; Cambridge University Press 2001
- New book project „Positron Annihilation“:
http://positron.physik.uni-halle.de/book_project

